2023-07-01

Functional Analysis Of The Gamma-Aminobutyric Acid Type A Receptor Subunit Alpha-1 (gabra1) Gene During Zebrafish Development.

Nayeli Gabriela Reyes-Nava
University of Texas at El Paso

FUNCTIONAL ANALYSIS OF THE *GAMMA-AMINOBUTYRIC ACID TYPE A RECEPTOR SUBUNIT ALPHA-1 (GABRA1*) GENE DURING ZEBRAFISH DEVELOPMENT.

NAYELI GABRIELA REYES-NAVA

Doctoral Program in Biosciences

APPROVED:

Anita M. Quintana, Ph.D., Chair

Rosa A. Maldonado, Ph.D.

Kyung-An Han, Ph.D.

Laura E. O'Dell, Ph.D.

Jeffrey T. Olimpo, Ph.D.

Stephen L. Crites, Jr., Ph.D.
Dean of the Graduate School

Dedication

A mi familia,

Roberto, Lety, Salma, Chelita, Don Felix, y Chabelita,

you, to whom my heart belongs,

and to The One that has called me by name.

FUNCTIONAL ANALYSIS OF THE *GAMMA-AMINOBUTYRIC ACID TYPE A RECEPTOR SUBUNIT ALPHA-1 (GABRA1*) GENE DURING ZEBRAFISH DEVELOPMENT.

by

Nayeli Gabriela Reyes-Nava, B.Sc.

DISSERTATION

Presented to the Faculty of the Graduate School of

The University of Texas at El Paso

in Partial Fulfillment

of the Requirements

for the Degree of

DOCTOR OF PHILOSOPHY

Department of Biological Sciences

THE UNIVERSITY OF TEXAS AT EL PASO

August 2023

Acknowledgements

For the opportunity of working in her laboratory, mentorship, opportunities, and learning lessons, I would like to express my gratitude to Dr. Quintana. To my Quintana lab colleagues, past and present, especially David Paz, Valeria Virrueta, and Isaiah Perez, you are the best lab mates ever.

Special thank you to my dissertation committee, Dr. Maldonado, Dr. Han, Dr. Olimpo, and Dr. O'Dell, for their support throughout my academic journey. Thank you also to the members of the BBRC core facilities, especially to Dr. Varela, Ana Betancourt, and Igor Estevao. Many thanks to Dr. Maldonado, Dr. Lannutti, Dr. Aguilera, Dr. Walsh, Dr. Keelung Hong, and Dr. Llano. The Bridges to the Baccalaureate program, the RISE fellowship, the Keelung Hong Fellowship, and the College of Science Graduate Student Research Fellowship provided invaluable resources for my success.

Thank you to my friends and colleagues, for the coffee breaks and your invaluable support, for looking after me and staying with me throughout this journey. Special thanks to Dr. Enriquez, my RISE fellow, dancing partner, and dearest friend. To Jesse Marie, for enlightening my days. Thanks to Juan Carlos Silva, Diana Prospero, Dr. Sayo, Dr. Grajeda, the G-RISE community and to my supportive and patient friends (KM, BT, MV).

To my family for their constant support, love, and patience. To my partner in life, for the insightful conversations about life, for supporting and nurturing my passion for science, and for being willing to continue this journey with me. Mom, Dad, Sal, Roberto, thank you for believing in me even when I did not.

Thank you, God, for the life you have blessed me with.

Abstract

The *GABRA1* gene encodes for the alpha-1 (α1) subunit of the Gamma-Aminobutyric acid type A receptor ($GABA_AR$), which are the primary modulators of synaptic inhibition in the central nervous system (CNS). Alpha-1 subunits are essential for maintaining the normal function of native receptors and contribute to over 60% of all $GABA_ARs$ in the CNS. Remarkably, a broad spectrum of neurodevelopmental and epilepsy-associated disorders have been linked with mutations in the *GABRA1* gene. However, the developmental, behavioral, and molecular mechanisms underlying *GABRA1*-associated epileptic disorders remain to be fully understood. Hence, the overarching goal of this dissertation is to investigate the behavioral and molecular mechanisms associated with *GABRA1* deficiency during brain development. Two independent experimental approaches were taken using zebrafish as a model system to address this goal. Our first study describes the identification of a *de novo* missense variant of *GABRA1* and the *in vivo* functional analysis of *gabra1* using morpholino-mediated knockdown. We developed a behavioral paradigm using the Zebrabox technology to investigate the behavioral consequences of *gabra1* loss of function. Interestingly, transient knockdown of *gabra1* resulted in hypomotility at early larval stages. This hypomotile phenotype was correlated with altered expression of genes that encode for other $GABA_AR$ subunits. Mainly we show downregulation of the β2 and γ2 transcripts, which are the primary assembly partners of α1, and upregulation of the homologous α6b subunit. Despite these molecular defects in the expression of major $GABA_AR$ subunits, morphant larvae exhibited a positive response to a potent $GABA_AR$ antagonist, pentylenetetrazol (PTZ), indicating the presence of an active receptor despite the deficient expression of *gabra1.* Our findings contrast with those described in a zebrafish germline mutant of *gabra1* generated previously. The distinct behavioral phenotypes between knockdown and germline mutation of *gabra1* prompted us to

characterize an additional *gabra1* germline mutant. Therefore, our second unpublished study describes the behavioral and molecular analysis of an uncharacterized nonsense mutant of *gabra1* (sa43718 allele) generated by the Wellcome Sanger Institute as part of the zebrafish mutation project in 2016. Behavioral analysis of this allele resulted in light-induced hyperactive locomotion resembling generalized seizures. Targeted mRNA analysis revealed that this behavioral phenotype was associated with reduced expression *of gabra1* and upregulation of *gabra4*, which encodes the a4 subunit. Mutant larvae were treated with PTZ to examine whether *gabra1* mutants had an active receptor. Notably, mutant larvae exhibited reduced response compared to controls, suggesting that a $GABA_AR$ with reduced functionality is present. Subsequent proteomic analysis of *gabra1* mutants revealed abnormal expression of proteins essential for synaptic vesicle transport, mitochondrial function, and potassium and sodium homeostasis regulation. Collectively, we highlight the essential role of *gabra1* in early development and epileptic phenotypes.

Table of Contents

List of Tables

List of Figures

Chapter 1: Introduction

The Gamma-Aminobutyric Acid type A receptor ($GABA_AR$) subunit Alpha-1 (*GABRA1*) encodes the alpha-1 subunit of the $GABA_AR$. $GABA_ARs$ are hetero-pentameric ion channels that mediate fast synaptic inhibitory responses of the central nervous system (1,2). The *GABRA1* gene is located on the long arm of chromosome 5 at position 5q34 in humans and is highly expressed in the central nervous system (1). Multiple transcript variants encoding the same protein have been identified for this gene and the main isoform consists of 456 peptides (ENST00000023897.10) (3). The *GABRA1* gene is conserved with 184 orthologs across species, including chimpanzees, rhesus monkeys, dogs, cows, mice, rats, chickens, zebrafish, and frogs. Notably, the alpha-1 subunit contributes to over 60% of all $GABA_AR$ (4,5) corresponding to the most abundant subunit in the mammalian brain.

I. Gamma-Aminobutyric Acid Type A Receptors ($GABA_AR$)

$GABA_ARs$ mediate the major inhibitory signals in the brain upon binding of GABA, an inhibitory neurotransmitter (Figure 1.1). $GABA_ARs$ play critical roles in controlling neuronal activity. Deficits in $GABA_AR$ and GABAergic inhibition have been associated with multiple neurological and psychiatric disorders, including epilepsy.

$GABA_AR$ Structure and Function

$GABA_AR$ are chloride ion channels that belong to the Cys-loop ligand-gated ion receptors superfamily (6). Receptors of this superfamily mediate fast synaptic transmission in the central nervous system. Specifically, $GABA_ARs$ mediate inhibitory

neurotransmission (7) (Figure 1.1). Activation of the $GABA_AR$ regulates the flow of chloride ions' across the plasma membrane, inducing hyperpolarization of the membrane potential and decreasing cellular excitability (1). $GABA_ARs$ are found in both postsynaptic and extra-synaptic membranes. Post-synaptically they mediate neuronal inhibition occurring at the millisecond range (also known as phasic inhibition). While extra-synaptically, they respond to ambient GABA, conferring long-term inhibition, also known as tonic inhibition (1).

$GABA_ARs$ are hetero-pentameric proteins assembled from a variety of subunits similar in structure and all encoded by different genes (Figure 1.2). The genes coding for the $GABA_AR$ subunits in humans are organized into four main clusters on chromosomes 4, 5, 15, and X (1). To date, 19 different $GABA_AR$ subunits have been identified (1,2). These subunits are categorized into eight classes based on amino acid sequence homology with each type having multiple members. In humans, there are six α subunits, three β subunits, three γ, three ρ subunits, and one ε, δ, θ, and π subunit (Figure 1.2A). $GABA_AR$ can occur various combinations of subunits, but the major $GABA_AR$ isoform is composed by 2α1, 2β2, and 1γ2 subunits (Figure 1.1A) (1,4,6,7). Each subunit structure contains a large N-terminal extracellular domain that corresponds to the GABA binding site, and four hydrophobic transmembrane domains (TMs) with a large intracellular domain between TM3 and TM4 (1) (Figure 1.2B). Together, TM2 of each subunit line the ion channel (1).

II. PHENOTYPIC SPECTRUM OF *GABRA1* MUTATION

GABRA1 mutations are associated with epilepsy, a brain disorder that results in recurrent seizures. The statistics are concerning, as epilepsy affects roughly 1% of the global population (8), with 4-10 out of every 1000 individuals experiencing active epilepsy (9). It is estimated that approximately 5 million people are diagnosed with epilepsy every year, highlighting its widespread impact as a significant neurological disorder worldwide.

Etiologically, epilepsy is a heterogeneous disorder. According to the international league against Epilepsy (ILAE), the underlying causes of epilepsy can be structural, metabolic, infectious, immune, genetic, or unknown (10). To date, many epilepsy cases remain without a clear etiology. However, it is hypothesized that genetic factors may contribute to their etiology. This is because over 30% of epilepsy cases have a defined/established underlying genetic origin (11,12). As genetic screening tools become more accessible, this percentage continues to rise, increasing the number of patients undergoing genetic analysis.

Mutations in *GABRA1* are known to contribute to the genetic etiology of both benign and severe epilepsy syndromes. According to the Online Mendelian Inheritance in Man (OMIM)[1], the primary phenotypes related to the mutation of *GABRA1* include idiopathic generalized epilepsy and developmental epileptic encephalopathies. Yet, the literature shows that the phenotypic spectrum associated with mutations in *GABRA1* is

[1] OMIM is a catalog of human Mendelian traits and disorders that focuses on the relationship between genotype and phenotype.

highly heterogeneous, including idiopathic generalized epilepsy (IGE), juvenile myoclonic epilepsy (JMC), myoclonic-astatic epilepsy (MAE), childhood absence epilepsy (CAE), Dravet syndrome and developmental-epileptic encephalopathies (13–17).

Clinical phenotypes of each epileptic syndrome are highly variable (Table S1.1). For instance, individuals with JME have only afebrile seizures with an onset during adolescence and myoclonic jerks (13). In contrast, individuals with CAE typically present with early onset epilepsy syndrome (3 months of age) with absence seizures, which involve brief and sudden lapses in attention (8). *GABRA1* mutations are associated with a large spectrum of phenotypes. Nonetheless, there is still no clear genotype-phenotype correlation between the many different variants in *GABRA1* and a particular/specific epileptic syndrome.

III. GENETICS, ALLELIC VARIANTS, AND *GABRA1*-ASSOCIATED EPILEPSY

Human genetic approaches have rapidly become an invaluable tool in human genetics and clinical diagnostics allowing the identification of novel genetic variations associated with human disease. Mutations in *GABRA1* were first identified using linkage analysis and candidate gene sequencing in large familial groups suffering from epilepsy in the early 2000s (13,14). Since then, high throughput and targeted next-generation sequencing (NGS) have led to the identification of numerous *GABRA1* variants associated with a spectrum of epileptic phenotypes (18,19) (Table 1.2).

Clinical and Molecular Descriptions of Patients with *GABRA1* Mutations

Cossette et al. (2002) reported the first pathogenic variant in the *GABRA1* gene. This variant was identified in a four generation French Canadian family with juvenile myoclonic epilepsy (JME) (13). The study was conducted in 14 family members, DNA was collected and analyzed from affected (n=8) and unaffected (n=6) members. Affected individuals presented generalized tonic-clonic seizures, myoclonus seizures, and an onset corresponding to juvenile myoclonic epilepsy (JME). Mutation screening identified a c.965C>A missense substitution in the *GABRA1*, which resulted in a single amino acid change (p.Ala322Asp) in all eight affected family members. This variant was absent in the unaffected family members.

After identifying the first epilepsy-associated mutation in *GABRA1*, further studies were conducted to investigate whether the mutated gene was associated with additional forms of epilepsy. Subsequently, a *de novo* heterozygous mutation (p.Ser326fs328*) was identified in a patient with childhood absence epilepsy (CAE) in 2006 (14). The study was conducted in a cohort of 98 unrelated individuals diagnosed with either JME, CAE, or epilepsy with grand-mal seizures. A single base pair deletion (c.975delC), predicted to result in a frameshift and a premature stop codon, was present in one of the 38 patients with CAE and was not present in any of the 292 healthy subjects. The pSer326fs328* and p.Ala322Asp variants were located within the transmembrane domain three (TM3) of GABRA1 (Figure 1.3).

To date, genetic screening technologies have led to the identification of over 500 clinical variants in *GABRA1.* These variants are located throughout multiple protein

domains of GABRA1, primarily the extracellular and transmembrane domains (Figure 1.2). According to the ClinVar[2] database, most variants are missense variants (225 variants), and additional variant types include 96 at UTR[3], eight nonsense, seven frameshift, and five splice site variants (20) (Table 1.1). Variants are heterozygous in most cases. Moreover, only a small fraction (~7%) of these variants are reported as clinically significant. All pathogenic variants are primarily missense or frameshift variants that arise from deletions (n=16), duplications (n=11), and single nucleotide changes (n=18). Overall, the vast majority of variants are missense and have been identified in association with different forms of epilepsy or epilepsy-related syndromes (Table 1.2).

Although there is a remarkable correlation between the mutation of *GABRA1* and different forms of epilepsy, there is still limited understanding of *GABRA1* function during brain development and epileptogenesis. Thus, functional analysis of *GABRA1* and its implications in brain development, behavior, and epileptogenesis is crucial.

---

[2] ClinVar aggregates information regarding sequence variation and its relationship to human health.

[3] Variants in both the 5 prime and 3 prime untranslated regions (UTR) have been reported. Specifically, 41 variants are reported in 5' UTR and about 55 variants in the 3' UTR. Importantly, none of these variants are reported as pathogenic according with the OMIM database.

IV. CURRENT MODELS OF *GABRA1*

In vitro functional analysis of *GABRA1*

Multiple efforts have been made to investigate the contribution of *GABRA1* to mammalian physiology. Initial *in vitro* functional analysis, using recombinant receptors expressing the epilepsy-associated p.Ala322Asp variant and electrophysiology, determined lower amplitude of GABA currents, independent of altered expression of the alpha-1 subunit, when compared to cells expressing wildtype receptors (13). Hence, suggesting the p.Ala322Asp variant affected receptor functionality, specifically its channel gating properties (13). Moreover, functional analysis of cells transfected with the p.Ser326fs328* variant showed no GABA-evoked currents and reduced surface expression of $GABA_AR$ expressing the mutated and truncated *GABRA1* (14,21). *In vitro* studies have focused on investigating the kinetic details of *GABRA1* mutation. Defective GABA-evoked currents have been used as direct evidence for abnormal GABA inhibition, thus neuronal overexcitation and consequently, epileptic phenotypes. However, different variants have been associated with normal and abnormal GABRA1 protein expression levels alongside abnormal GABA inhibition (GABA-evoked currents) without a clear molecular description of how mutation of *GABRA1* contributes to epileptic phenotypes.

Animal models of *GABRA1* deficiency: Mammalian Systems

Mouse (*Mus musculus)* is the traditional murine model for neuroscience research (5,22–24). Mice are small making them easy to house and maintain. Several generations can be studied relatively quickly due to their short life span and high fecundity (25).

Around 90% of mouse genes are conserved with human genes (26). Thus, mice have been used as a model system to understand neurological and psychiatric disorders such as anxiety, schizophrenia, and autism (24,27–30). In addition, many genetic and behavioral assays have been developed to study these disorders in the mouse model (5).

Studies using murine models have been developed to investigate the role of the alpha-1 subunit in $GABA_AR$ pharmacology, function, and behavior. Although homozygous knockout (KO) mice are physically normal, healthy, and viable, survival rates of Gabra1-KO are reduced (31). Moreover, murine models of *Gabra1* do not exhibit seizures but an essential tremor phenotype (5,31,32). Nonetheless, it has been shown in the literature that *Gabra1* deficient mice are susceptible to seizures (31). Specifically, after bicuculline administration, a $GABA_AR$ antagonist that induces clonic and tonic-clonic seizures, homozygous mice undergo seizures at a lower threshold compared to wild-type and heterozygous mice.

Furthermore, absence-like seizures[4] that evolve into myoclonic seizures[5] have been reported in additional murine models of *Gabra1* deficiency (35,36) and were observed upon deletion of Gabra1 (KO) or substitution with the p.Ala322Asp (KI) variant. Absence seizures are exhibited from post-natal day 35 to 120 (P35 and P120), while mice susceptibility to myoclonic seizures is only observed at P120 in heterozygous KO or KI (36). Analysis of homozygotes was limited due to premature death at P19.

---

[4] Absence seizures involve brief and sudden episodes of staring and loss-of-awareness (33).

[5] Myoclonic seizures are brief, sudden rapid jerks of a muscle or group of muscles (34).

Ye *et al.,* (2010) presented a phenotypic comparison between three independent murine *Gabra1* mutant lines in the context of anxiety and sleep behaviors (5). They reported a strong anxiety profile in *Gabra1* KO mice in several assays, including the platform and marble-burying assays. Additionally, KO mice exhibited abnormal sleeping behaviors (5). Their data suggested that the deletion of *Gabra1* had a sedative effect, potentially mediated by the upregulation of other $GABA_AR$ subunits.

Moreover, differential expression of $GABA_AR$ subunits has been reported in *Gabra1*-KO models (5,31,32,36–38). For instance, upregulation of the alpha-2 and alpha-3 subunits and downregulation of gamma-2 and beta-2/3 subunits are reported in alpha-1-depleted mice brains (31). Further, Gabra1 deletion and substitution with the p.Ala322Asp variant has been shown to alter cortical expression of $GABA_AR$, specifically by upregulation of the alpha-3 subunit, without altering the expression of gamma-2 and beta-2/3 subunits (36). Albeit, heterozygous substitution with the p.Ala322Asp variant significantly reduces the alpha-1 subunit expression, it does not altered the $GABA_AR$ synaptic clustering (36). Importantly, the knockout of *Gabra1* does result in the loss of over 50% of all $GABA_AR$ in the murine brains (31). Collectivelly, these data highlight the role of *GABRA1* expression for assembly and expression of primary $GABA_AR$, which are conformed by α1, β2, and γ2 subunits.

Together, the studies using *Gabra1*-KO mice have provided considerable insight into the physiological, pharmacological, and behavioral role of *Gabra1*. Nonetheless, these studies offer limited scope to the developmental component of the disease. First, deletion or mutation of *Gabra1* is associated with high mortality rates (31,35). Additionally,

phenotypes reported across murine models are highly heterogeneous and limited by sex and strain, where some behavioral and molecular phenotypes are observed in a sex or strain-specific manner (5,35). Moreover, regardless of the mutated domains (i.e. ligand binding or the transmembrane domains), these models primarily exhibit decreased locomotion and/or tremors (5,35,36), in contrast to the clinical manifestations (i.e., myoclonic, tonic-clonic seizures) observed in patients with *GABRA1* mutations. Importantly, murine models of *Gabra1* deficiency have increased mortality rates (35,36), indicating the crucial role of this gene in development. Therefore, alternative genetic models are needed to circumvent mammalian systems' limitations.

Zebrafish: A Model to Characterize *GABRA1* Function.

The zebrafish (*Danio rerio*) has become a primary model organism for vertebrate development and physiology research. Zebrafish are endemic to slow freshwater streams and East India and Burma rice paddies (39,40). Wild-type zebrafish are clear-colored, about an inch long, with black stripes running lengthwise down their body (Figure 1.4). Multiple features make zebrafish attractive for experimental manipulation. A single breeding pair can lay several clutches of around 100 eggs (40). Eggs are optically transparent and develop externally, making it possible to observe a zebrafish embryo develop in real time under a microscope (40). Zebrafish developmental processes are considerably rapid, where precursors to all major organs are developed in 36 hours (41) (Figure 1.4). Notably, the zebrafish genome is nearly 75% homologous to the human genome (42,43). Collectively, all these attributes led to the establishment of zebrafish as a model organism for modern biological investigation pioneered by George Streisinger

and colleagues (44).

More importantly, zebrafish are highly amenable to cost-effect genetic manipulation, which has led to the generation of thousands of mutations that have identified genes controlling vertebrate development (45–47). More recently, using CRISPR/Cas9 (48) technologies, stable germline mutations in the zebrafish genome have been generated. Furthermore, zebrafish can be manipulated transiently by microinjection with anti-sense morpholino oligonucleotides, plasmid DNA, or *in vitro* transcribed mRNA. The zebrafish genome has undergone genome duplication (49,50). Thus, many zebrafish orthologs have two genes for every human gene. This can help to circumvent embryonic lethality when creating germline mutants.

Advances in the behavioral neurosciences field have enabled the use of zebrafish as an emerging model to investigate behavioral paradigms. Zebrafish display complex behaviors as early as five days after fertilization (51) (Figure 1.5). For example, larvae display food-seeking and active avoidance behaviors within 2 to 3 days after hatching, allowing for the development of behavioral assays to study neurodevelopmental and psychiatric disorders. In that sense, zebrafish have become the future of behavioral neuroscience research.

ZebraBox, pioneering behavioral research in zebrafish.

The ZebraBox (ViewPoint) is a high-throughput monitoring system to analyze zebrafish behavior. It is a complete system designed for the high-throughput analysis of zebrafish larvae in multi-well plates and allows for total experimental control over the

environment (52). A single chamber can analyze up to 96 larvae, and multiple ZebraBox units can be installed in parallel, allowing for the efficient and automated tracking of over 96 larvae simultaneously. The ZebraBox system comprises innovative software (ZebraLab) for automated behavioral video tracking. This tracking software is adaptable and suitable for larval or adult monitoring since it can be connected to the ZebraBox or the ZebraCube, an adult-optimized system (43).

Furthermore, the ZebraBox has become an advantageous system for understanding developmental behavior. For example, larval behavior has been used to study the effect of cannabis-derived compounds on chemically and genetically induced seizures (53). Pentylenetetrazole (PTZ), a $GABA_AR$ antagonist, is a convulsant agent commonly used to cause seizures in larval zebrafish (54,55). To investigate the effect of cannabis-derived compounds in seizure amelioration, the antiseizure effect of these compounds was evaluated in PTZ and Dravet syndrome (DS) seizure models (53). DS syndrome is a genetic epilepsy syndrome characterized by febrile seizures, treatment resistance, abnormal development, and early onset. To test the anti-seizure effects of five different cannabis-derived compounds, a high-throughput assay was developed using ZebraBox. The ZebraBox was used to track and measure the total distance traveled to determine if the compounds reduced the seizure-like activity in the DS and PTZ seizure models. Overall, the ZebraBox identified an anticonvulsant effect in four out of five compounds in the DS model; in contrast, in the PTZ model, only two compounds decreased seizure activity. Together, these data demonstrate that larval zebrafish can be used to understand the behavioral phenotypes associated with seizure disorders of genetic origin.

The zebrafish utility has expanded as a popular model system to inform about the mechanisms underlying human disease. Behavioral analysis using zebrafish addresses functional effects of genetic alterations or specific mutations. Further, zebrafish provide numerous technical advantages, but most importantly, the development of fish organ systems is highly conserved. The latest technologies are increasing the power of zebrafish, allowing for cost-effective gene manipulation. Furthermore, cutting-edge advances in imaging and behavioral analysis will undoubtedly help investigate disease's molecular and cellular basis. Finally, zebrafish represent a growing model system to expand the current understanding and treatment of neurodevelopmental disorders.

Zebrafish GABRA1 loss of function model

The *GABRA1* gene is conserved in zebrafish; it is highly expressed throughout the zebrafish nervous system as early as 18 hours postfertilization (56–59). Using whole-mount in situ hybridization, expression analysis has shown strong expression of the *gabra1* transcript throughout the brain and spinal cord at 48hpf (56,57). The Gabra1 protein shows over 89% amino acid identity with the human protein (57). Specifically, the GABA binding site and the transmembrane domains have 95% and 88% identities, respectively, compared to the human protein (57).

Samarut *et al.,* (2018) developed the first zebrafish model of *GABRA1* deficiency. This fish line carries a frameshift mutation, leading to a premature stop codon at the extracellular GABA binding site. *gabra1* mRNA expression was significantly reduced by 50% in heterozygous mutants and close to 90% in homozygotes. Homozygous mutant fish prematurely died between seven at ten weeks post-fertilization. Importantly, *gabra1*

mutant fish exhibited fully penetrant, light-sensitive seizure-like behavior, characterized by involuntary and uncontrolled rapid movements, convulsions, and whirlpool swim behavior, at juvenile stages (5 weeks post-fertilization). Nonetheless, *gabra1* mutant larvae depicted light-induced increased swimming activity (startle response) as early as 4 days post fertilization.

Gabra1 induced seizure-like behavior was alleviated upon treatment with common antiepileptic drugs (i.e., clonazepam). Transcriptomic analysis of brain homogenates revealed differential expression of genes essential for brain development. Specifically, downregulation of genes involved in the brain's inhibitory network development and downregulation of genes encoding for $GABA_AR$ subunits (*gabra1*, *gabrg2*, *gabab1b,* and *gabab2).* In addition to abnormal expression of molecules essential for axon guidance, including genes encoding for protocadherins, ephrins, and semaphorins (57).

Samarut *et al.* data described a novel aspect of epileptogenesis in vertebrates. Interestingly, homozygote fish exhibit seizure-like phenotypes associated with abnormal expression of $GABA_AR$ subunits, which has been previously observed in murine models. This work highlights the role of *gabra1* in the development of inhibitory networks, suggesting that GABRA1-associated epilepsy results from early neurodevelopmental defects. Furthermore, these data emphasize using larval and juvenile zebrafish to study non-chemical-induced seizures.

Although mutation of *GABRA1* is thought to cause epilepsy, the mechanisms underlying these phenotypes have not been completely elucidated. Given the developmental role of *GABRA1* and its suggested contribution to epileptogenesis,

functional characterization of this gene at earlier developmental stages is crucial. This dissertation will investigate the functional role of *gabra1* during brain development at early larval stages (5 days post fertilization). We will assess the behavioral and molecular effects of *gabra1* genetic loss-of-function. Specifically, because KO of the alpha-1 subunit has been associated with differential expression of $GABA_AR$ subunits, we will investigate whether transient knockdown and germline mutation of *gabra1* induces changes in $GABA_AR$ subunit expression associated with behavioral phenotypes. Lastly, we present proteomic analysis of a novel *gabra1* mutant that, alongside the transcriptomic analysis by Samarut et al. (2018), could pinpoint novel molecular mechanisms underlying *gabra1*-associated epilepsies.

V. CONCLUSIONS

Complex epilepsy and neurodevelopmental disorders have been associated with mutations of *GABRA1.* To date, over allelic 500 variants have been reported in patients suffering from epilepsy or epilepsy-associated syndromes. However, only a few of these variants have been identified as pathogenic and many remain without clear significance. Current models have contributed to understanding *GABRA1* gene function and contribution to mammalian physiology. Because *GABRA1* encodes a major subunit of $GABA_AR$, defective GABA signaling, and neuronal inhibition have been described as primary underlying mechanisms of *GABRA1*-associated epilepsy. Nonetheless, research has shown that *GABRA1* has been implicated with the abnormal development of inhibitory networks early in development. Therefore, research and complementary models that

further delve into the role of *GABRA1* on brain development, behavior, and disease are required.

Table 1.1: Summary of Human Clinical Variants of *GABRA1* from ClinVar.

Number of Variants*		588
Molecular Consequence	Frameshift	7
	Missense	225
	Non-sense[6]	8
	Splice	5
	UTR	96
Variation Type	Deletion	40
	Duplication	25
	InDel	3
	Insertion	14
	Single nucleotide	519
Clinical Significance	Conflicting interpretations	53
	Benign	58
	Likely benign	168
	Uncertain significance	238
	Likely pathogenic	36
	Pathogenic	45

*Last updated 4/21/2023

[6] In chapter 3, a non-sense mutant of the *gabra1* gene (sa43718 allele) is studied. Non-sense mutations in *GABRA1* are associated with developmental and epileptic encephalopathy and idiopathic generalized epilepsy.

Table 1.2: Summary of phenotypic spectrum of selected human *GABRA1* variants.

Variant	Variation type	Inheritance	Domain	Clinical Manifestation	Ref
p.Phe92Leu	Missense	De novo	Extracellular	GTCS, limb tremor, FS, ID.	(60)
p.Arg112Gln	Missense	De novo	Extracellular	EE, early onset, AE, GTCS, ID, FS, ASD	(16,61,62)
p.Tyr187Asp	Missense	NA	Extracellular	IGE	(63)
p.Arg214His	Missense	NA	Extracellular	EE and ID	(64)
p.Asp219Asp	Missense	Autosomal dominant	Extracellular	IGE and FS	(65)
p.Gly251Ser	Missense	De novo	Extracellular	DS	(61)
p.Met263Val	Missense	De novo	TM1	Early onset, myoclonic, tonic, and atonic seizures, ID, EIEE, EDEE	(60)
p.Val284Ala	Missense	De novo	TM2	Early onset, GTCS, EIEE, EDEE, ID, microcephaly, hypotonia, growth delay, premature death	(60)
p.Thre292Ile	Missense	De novo, autosomal dominant	TM2	IGE and EE.	(15,65)
p.Leu296Phe	Missense	De novo	TM2	No seizures. Drooling, bruxism, anxiety, growth delay.	(60)
p.Ala322Asp	Missense	Autosomal dominant	TM3	JME	(13)
p.Ser326fs328*	Frameshift/ Nonsense	De novo	TM3	AE, early onset.	(14)
p.Ala332Val	Missense	De novo	TM3	DEE.	(66)
p.Lys353delins18*	Nonsense	Autosomal dominant	Intracellular loop	Late-onset, afebrile seizures, GTCS, photosensitivity seizures.	(65)

GTCS: generalized tonic-clonic seizures, FS: Febrile Seizures ID: Intellectual Disability, EE: Epileptic Encephalopathy, AS: Absence Seizure, ASD: Autism Spectrum Disorder, IGE: Idiopathic Generalized Epilepsy, DS: Dravet Syndrome, EIEE: Early Infantile Epileptic Encephalopathy, EDEE: Developmental and Epileptic Encephalopathy, EDEE: Early Developmental and Epileptic Encephalopathy, JME: Juvenile Myoclonic Epilepsy.

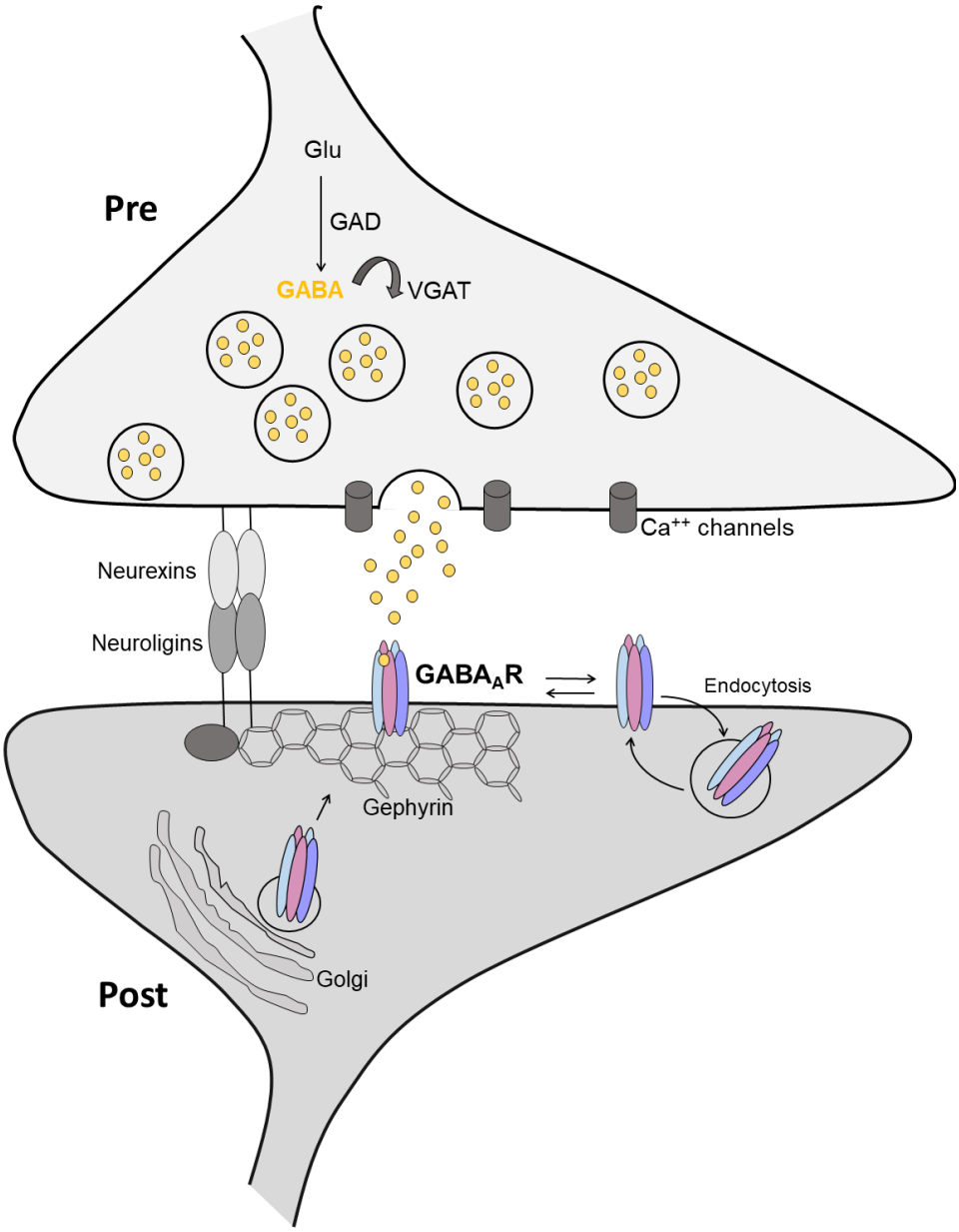

Figure 1.1. Schematic representation of GABAergic synapses.

$GABA_AR$s mediate inhibitory neurotransmission. Upon interaction with GABA (yellow), the major inhibitory neurotransmitter of the nervous system, $GABA_AR$ regulates chloride ions' flow across the plasma membrane, inducing hyperpolarization of the membrane potential and consequently decreasing cellular excitability. Illustration modified from Pizzarelli and Cherubini (2011).

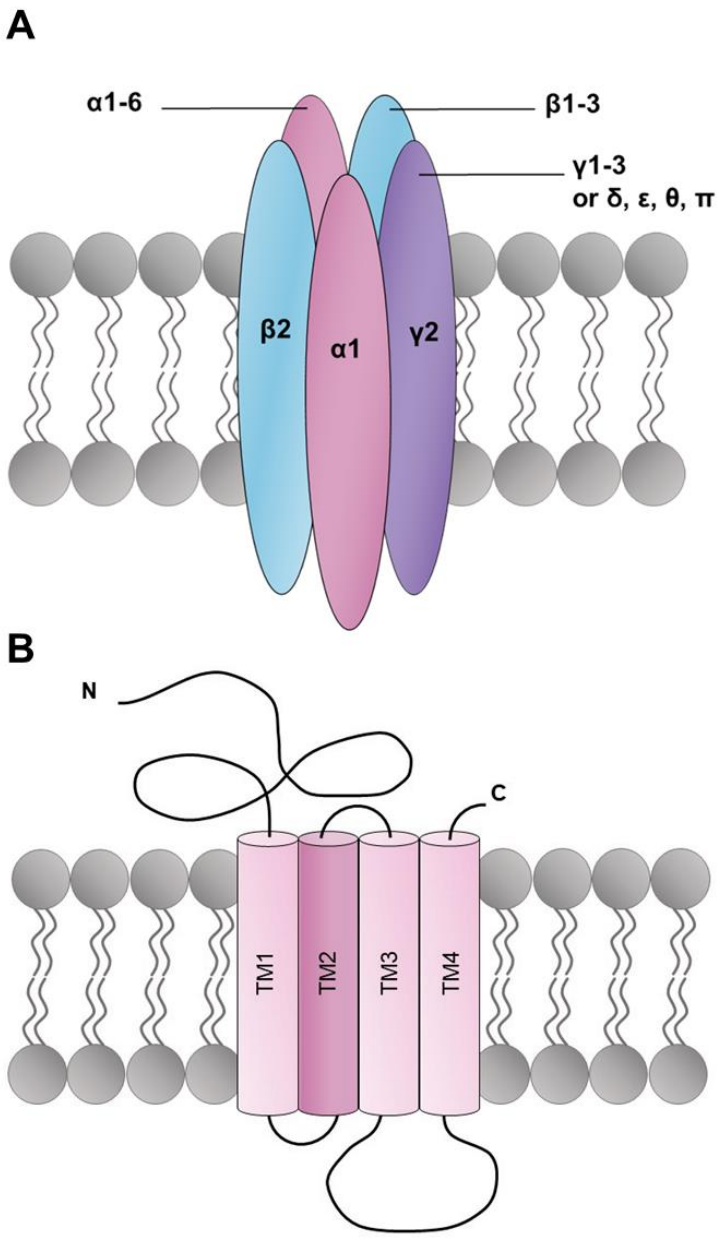

Figure 1.2. Schematic representation of $GABA_AR$ structure.

A) $GABA_AR$ are the major inhibitory neurotransmitter receptors in the mammalian brain. The activating ligand of these receptors is the gamma-aminobutyric acid (GABA). $GABA_AR$ are heteropentamers assembled by a combination of up to 19 different subunits (α1-6, β1-3, γ1-3, ρ1-3, and ε, δ, θ, and π). The primary $GABA_AR$ isoform comprises 2α1,

2β2, and 1γ2 subunits. B) Individual subunits comprise a large extracellular domain, four transmembrane domains (TM1-4), and a large intracellular loop within transmembrane domains three and four.

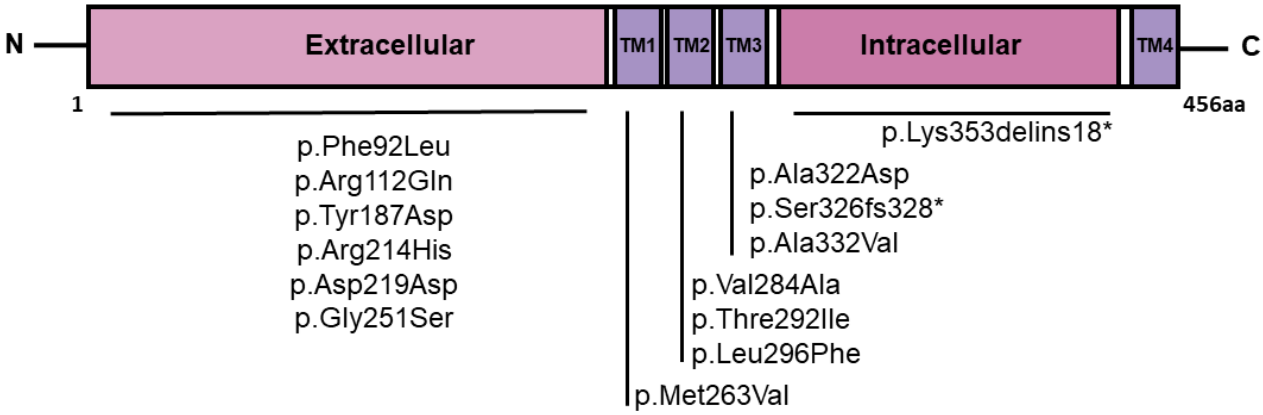

Figure 1.3. Schematic representation of clinical variants in GABRA1.

GABRA1 encodes the alpha-1 (α1) subunit of the $GABA_AR$. To date close to 600 variants have been identified in *GABRA1*. Of these only a small percentage are considered clinically pathological. This schematic represents the location of the selected pathogenic variants described in Table 1.1. Allelic variants of *GABRA1* are located across multiple domains of the α1 subunit, primarily extracellular and transmembrane domains. Most variants are heterozygous missense variants and are associated with various forms of epilepsy or epilepsy syndromes.

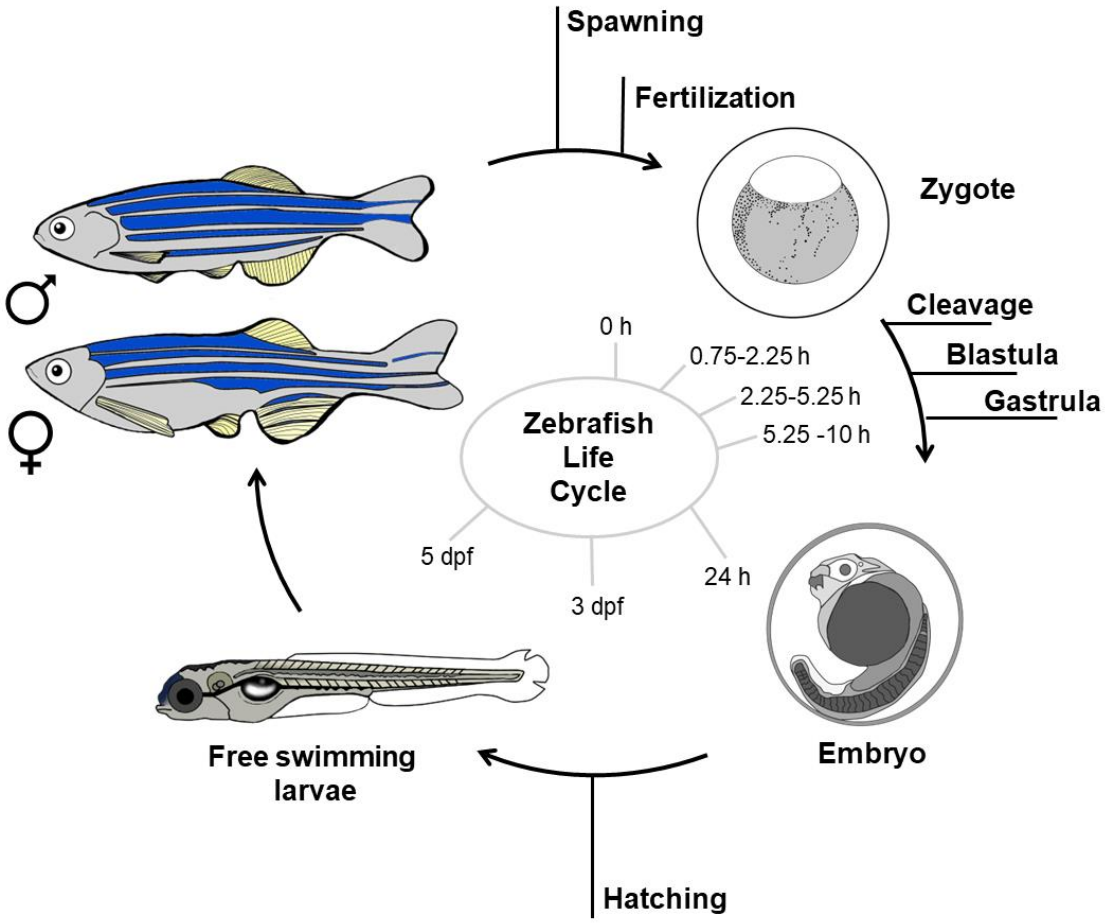

Figure 1.4. Schematic representation of the zebrafish life cycle.

A single female can produce clutches of several hundred eggs in a single spawning. Courtship behavior in zebrafish consists of a male chasing the female rapidly to stimulate oviposition and simultaneous sperm release. Once eggs are released, they become activated on contact with water and fertilized in the presence of sperm. Cleavage events occur synchronously around 40 minutes after fertilization. The blastula period is referred to as the period in which the developing embryo reaches 128-cells and begins to look like a ball. Onset of gastrulation occurs around five hours post fertilization (hpf). Gastrulation

events give rise to the primary germ layer and the embryonic axis. The onset of neurogenesis in the zebrafish occurs during late gastrulation. 24 hpf, the developing embryo has a heartbeat and a mature brain with functional regions, and pigmentation starts to appear. Hatching takes place between 48- and 72-hours post fertilization. By 72 hpf most neuronal cell types and circuits are formed. At 5 dpf zebrafish larvae have a fully inflated swim bladder that allows them to be free-swimming.

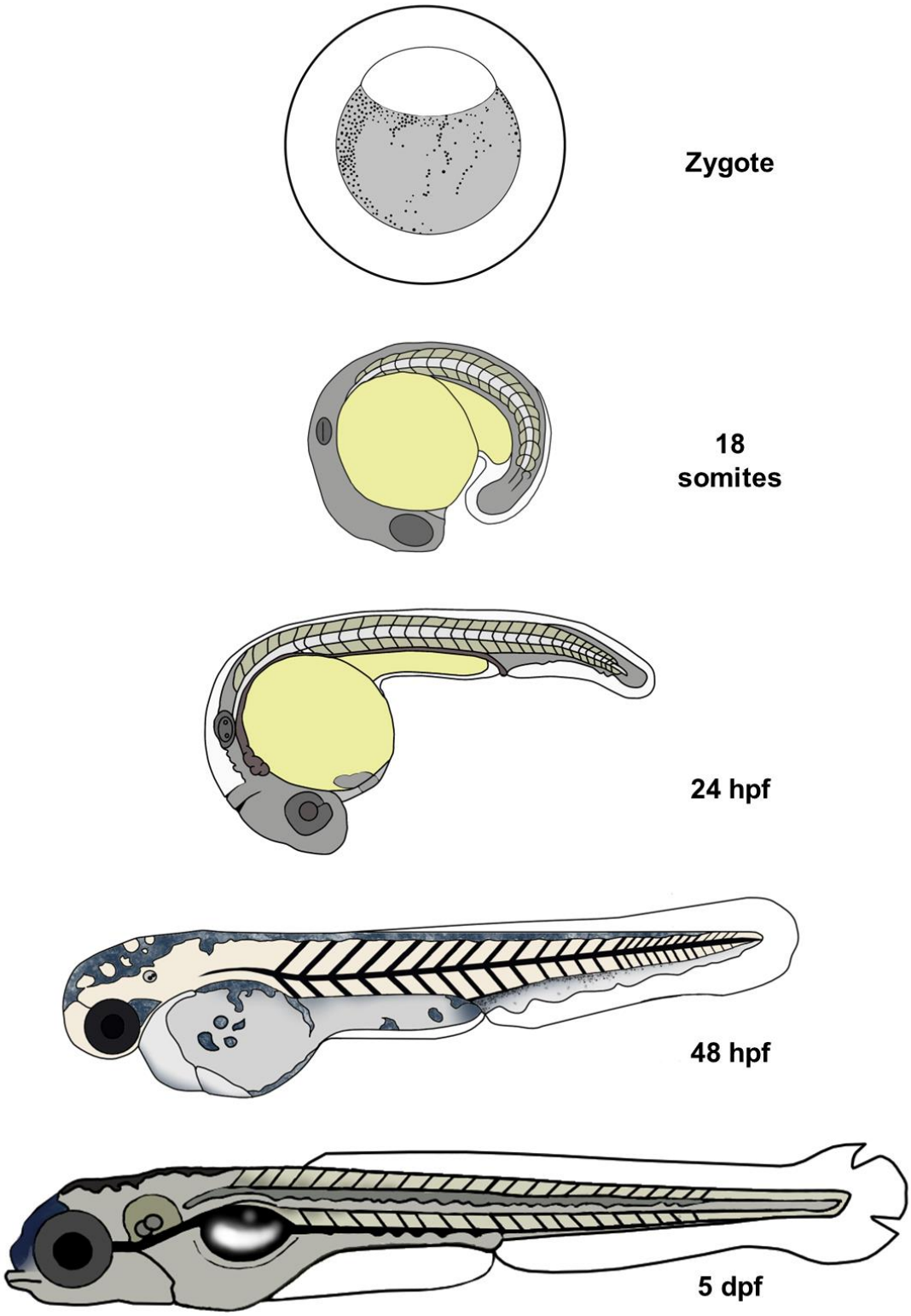

Figure 1.5. Schematic representation of the zebrafish developmental stages.

A fertilized egg (one-cell stage) stays in the zygote period until the first cleavage occurs. The zygote is about 0.7mm in diameter. After 18 hours post fertilization, at 28°C, 18 somites are present. Somites are precursor populations of cells/segmental axial structures from which vertebrate column, skeletal muscles, and subcutaneous tissue are derived. Importantly, by this stage, neural migration occurs, and the first post mitotic neurons are observed. At this stage the developing embryo is about 0.9 mm in length. By 24 hpf, the embryo is around 1.9 mm long, and a mature brain with functional regions is formed. During the first 5 days all major organ systems develop and begin functioning. By 5 days post fertilization the early larva, 3.9 mm in length, starts to display complex swimming behaviors, including pray chasing. This schematic is to scale in reference to the 5 dpf larvae.

Chapter 2: Abnormal Expression of $GABA_AA$ receptor subunits and hypomotility upon loss of *GABRA1* in zebrafish

This chapter presents a research manuscript written, submitted, and published in Biology Open on April 13th, 2020 (DOI:10.1242/bio.051367). In this manuscript we identified a heterozygous missense mutation in GABRA*1* and performed functional analysis using knockdown in zebrafish. The male pediatric subject presented with severe epileptic disorder alongside metabolic defects, intellectual disability, vision loss, and non-verbal speech. A p.Thr292Ile variant was identified and is located within the second transmembrane (TM) domain of GABRA1. Notably, this variant was previously reported by the Epi4k consortium in a patient with infantile spasms and other overlapping phenotypes, strongly suggesting that the p.Thr292Ile variant causes complex epilepsy-associated syndromes.

To better understand the role of *GABRA1* during neurodevelopment and behavior, we developed zebrafish model of *gabra1* deficiency. Our results demonstrated that morpholino mediated knockdown of *gabra1* results in hypomotility and altered gene expression of other $GABA_AR$ subunits. Specifically, we observed downregulation of *gabrab2* and *gabrg2,* and upregulation of *gabra6b,* which encodes for the alpha-6 subunit of the $GABA_AR$. Moreover, *gabra1* morphants were responsive to a GABA antagonist, suggesting that a functional $GABA_AR$ is being synthesized. Collectively, this study demonstrated a role for the zebrafish *gabra1* gene in motility and gene expression of unique $GABA_AR$ subunits during development.

AUTHOR CONTRIBUTIONS

The following manuscript discusses the findings and observations of collaborative efforts of multiple individuals: Nayeli G. Reyes-Nava (N.R.-N), Hung-Chun Yu (H.-C.Y.), Curtis R. Coughlin II (C.R.C), Tamim H. Shaikh (T.H.S.) and Anita M. Quintana (A.M.Q). NR performed behavioral and molecular experiments, *in situ* hybridization, and all morpholino injections. HY performed bioinformatics analysis and wrote portions of the manuscript. THS and CC supervised and managed patient IRB, genetic counseling, contributed to writing the manuscript, and provided patient assessment expertise. AMQ synthesized the hypothesis, performed data management and analysis, and wrote the manuscript.

Title: Abnormal expression of $GABA_A$ receptor sub-units and hypomotility upon loss of *gabra1* in zebrafish.

Running title: *gabra1* function in development.

Authors:

Nayeli Reyes-Nava*, Hung-Chun Yu†, Curtis R. Coughlin II†, Tamim H. Shaikh†, and Anita M. Quintana*

Author Affiliations:

*University of Texas El Paso, Department of Biological Sciences, Border Biomedical Research Center, El Paso TX 79968
† University of Colorado School of Medicine, Department of Pediatrics, Section of Genetics, Aurora, CO 80045

Emails:

ngreyesnava2@miners.utep.edu;
Tamim.shaikh@ucdenver.edu;
Hung-Chun.Yu@ucdenver.edu;
Curtis.Coughlin@ucdenver.edu;
Aquintana8@utep.edu

Animal Protocol Number: 811689-5
IRB Protocol Number: COMIRB #07-0386

Keywords: development, zebrafish, genetics, GABRA1, locomotion

Corresponding Author:

Anita M. Quintana PhD.
Department of Biological Sciences
The University of Texas El Paso
El Paso TX 79968
t:915-747-8988
email:aquintana8@utep.edu

SUMMARY STATEMENT

We report that heterozygous mutation of the *GABRA1* gene is associated with severe seizure phenotypes in a patient with a multiple congenital anomaly syndrome. Subsequent *in vivo* functional analysis revealed a role for the zebrafish *gabra1* gene in motility and the developmental gene expression of unique sub-units of the $GABA_A$ receptor.

ABSTRACT

We used whole exome sequencing (WES) to determine the genetic etiology of a patient with a multi-system disorder characterized by a seizure phenotype. WES identified a heterozygous *de novo* missense mutation in the *GABRA1* gene (c.875C>T). *GABRA*1 encodes the alpha subunit of the Gamma-Aminobutyric Acid receptor A ($GABA_AR$). The $GABA_AR$ is a ligand gated ion channel that mediates the fast inhibitory signals of the nervous system and mutations in the sub-units that compose the $GABA_AR$ have been previously associated with human disease. To understand the mechanisms by which *GABRA1* regulates brain development, we developed a zebrafish model of *gabra1* deficiency. *gabra1* expression is restricted to the nervous system and behavioral analysis of morpholino injected larvae suggests that the knockdown of *gabra1* results in hypoactivity and defects in the expression of other sub-units of the $GABA_AR$. Expression of the human GABRA1 protein in morphants partially restored the hypomotility phenotype. In contrast, the expression of the c.875C>T variant did not restore these behavioral deficits. Collectively, these results represent a functional approach to understand the mechanisms by which loss of function alleles cause disease.

INTRODUCTION

Rare disorders affect 4-8% of the global population (67) and approximately 80% of these disorders are predicted to have a genetic etiology (68). In recent years, whole exome sequencing (WES) emerged as a diagnostic tool for patients with rare disorders of unknown origin (69,70). The success of WES has provided a unique window of opportunity to identify disease related genes in humans and it is predicted that gene identification of rare disorders has the potential to contribute to our knowledge of other, more complex genetic disorders (71,72). Most importantly, studies of rare disorders have demonstrated that WES can be successful with very few subjects and/or using a trio based approach (73,74).

In 2013, the Undiagnosed Disease Network (UDN) was founded and includes seven clinical sites across the nation, a coordinating center, two DNA sequencing centers, a model organism screening center, a metabolomics core, and a central biorepository (75). Within the first 4 years of the UDN, the sequencing centers identified 956 genes associated with human disease, 375 of them have not previously been associated with disease (76). This is a staggering number, as it suggests that nearly 1/3 of the genes identified are of unknown function. These data strongly support the need for *in vivo* functional analysis of gene function.

Here we describe the identification of a putative disease variant and perform *in vivo* functional analysis of gene function using genetic loss of function. We describe a patient who was presented with a severe seizure disorder, intellectual disability, cardiac arrhythmia, and non-verbal speech. We identified a heterozygous *de novo* missense

mutation in the *GABRA1* gene (c.875C>T), which resulted in a single amino acid substitution in one of the three known transmembrane domains (p.Thr292Ile). *GABRA1* is located on chromosome 5 and encodes the alpha (α) sub-unit of the multi-sub-unit gamma-aminobutyric acid receptor ($GABA_AR$). The $GABA_AR$ is the primary inhibitory receptor of the central nervous system and the c.875C>T variant was previously associated with epileptic phenotypes in the Epi4K consortium (77). Although mutations in *GABRA1* have been associated with disease, the molecular and cellular mechanisms by which *GABRA1* regulates neural development are not completely understood. Consequently, we performed functional analysis in the developing zebrafish embryo.

Zebrafish are a cost-effective model organism and nearly 75% of their genome is conserved with humans (43,78). Additionally, they are highly amenable to genetic manipulation. To ascertain the function of *GABRA1* during development and behavior, we performed morpholino mediated knockdown of the zebrafish ortholog of *GABRA1*. We analyzed the behavioral and molecular consequences associated with knockdown of *gabra1*. Morphants exhibited hypomotility as indicated by swim speed and total distance swam. This hypomotility was accompanied by distinct changes in the expression of the major sub-units of the $GABA_AR$, including decreased expression of β2 and γ2 transcripts. Despite this decrease in the expression of unique $GABA_AR$ sub-units, morphants continued to respond to treatment with pentylenetetrazol (PTZ), a potent antagonist of the $GABA_AR$, indicating that morphants continue to produce an active $GABA_AR$ even in the absence of adequate *gabra1* expression.

RESULTS

Subject

The subject initially presented for care at three months of age with infantile spasms that evolved into Lennox-Gastaut syndrome. Seizure activity included a light-sensitive myoclonic epilepsy and generalized tonic clonic seizures. The seizures were treated with adrenocorticotropic hormone (ACTH), multiple antiepileptic medications, and ketogenic diet, although seizure activity continued to occur daily.

His clinical course was also marked for hypotonia, visual impairment, developmental delay and bilateral neuromuscular hip dysplasia. He had a Torsades de pointes cardiac arrest during an acute illness, with normal cardiac function outside of the acute event. Laboratory findings included lactic acidosis (peak serum lactate 4.18, ref range 0.5-2.0 mM) and metabolic acidosis. Multiple diagnoses were suggested based on his clinical history including a channelopathy and primary mitochondrial dysfunction. In previous clinical testing, the patient was negative for mutations in a panel of genes including *ADSL, ALDH7A1, ARX, ATP6AP2, CDKL5, CLN3, CLN5, CLN6, CLN8, CNTNAP2, CTSD, FOXG1, GABRG2, GAMT, KCNQ2, KCNQ3, MECP2, MFSD8, NRXN1, PCDH19, PNKP, PNPO, POLG, PPT1, SCN1A, SCN1B, SCN2A, SLC25A22, SLC2A1, SLC9A6, SPTAN1, STXBP1, TCF4, TPP1, TSC1, TSC2, UBE3A,* and *ZEB2.* In order to investigate the underlying genetic etiology for his complex medical history, the subject and his parents were enrolled into a research protocol approved by the Colorado Multiple Institutional Review Board (COMIRB #07-0386).

Whole-Exome Sequencing

WES was performed on a male subject and his unaffected parents to obtain over 70X coverage of targeted exons in each sample (Table S2.1). A large number of variants (106,737 variants) were detected in the patient after applying appropriate quality measures as described in Table S2.2. Our downstream analyses focused on nonsynonymous coding variants, coding InDels (insertions/deletions <50 bp), and variants affecting splice-sites as they are more likely to have a functional impact on the gene product and hence more likely to be pathogenic (9,631 variants). Common variants with minor allele frequency (MAF) greater than 1% in dbSNP137 were filtered out. Our analysis identified 1,846 rare variants in the patient and these were considered for further analysis. Parental WES data was used to detect the pathogenic variant under various inheritance models including dominant (*de novo* mutations) and recessive (compound heterozygous, homozygous, and X-linked hemizygous mutations) models. This resulted in identification of seven candidate genes (Table S2.2). These included *de novo* variants in *CACNA1C, GABRA1,* and compound heterozygous variants in *SCNN1B*, *FNIP1, TTN*, *OTOG*, and *FAT4.*

Additional evaluation of each candidate gene according to the criteria described in MATERIAL AND METHODS section identified 2 top priority candidate genes, including the *de novo* variant in *GABRA1* under a dominant model and compound heterozygous variants in *TTN* under a recessive model (Table S2.2). *TTN* encodes Titin, a sarcomeric protein involved in the assembly of cardiac and skeletal muscle. The second candidate gene, *GABRA1* has been associated with early infantile epileptic encephalopathy

(EIEE19; MIM: 615744) and juvenile myoclonic epilepsy (EJM4, EJM5; MIM: 611136) and therefore, became the primary putative candidate gene based on clinical phenotype. Both parents had normal alleles but the subject had a heterozygous missense variant in *GABRA1* (NM_000806.5:c.875C>T, NP_000797.2:p.Thr292Ile) that results in a change in protein sequence (Figure 2.1A). Sanger sequencing also confirmed that the variant is *de novo* (Figure 2.1B) and mostly likely the result of a germline mutation. Amino acid Thr292 is highly conserved evolutionarily between multiple vertebral species (Figure 2.1C) according to several conservation algorithms (PhyloP: 7.66; PhastCons: 1; GERP: 5.8). Notably, multiple mutation prediction algorithms predict this variant to be deleterious (CADD: 33; PolyPhen2 = probably damaging (1); PROVEAN = deleterious (-5.34); SIFT = damaging (0); MutationTaster: disease causing (0.99999)). Amino acids from position 279 to 300 of GABRA1 form a functionally important transmembrane helix domain (TM2) that is critical for overall functionality (Figure 2.1D). The significance of p.The292Ile variant in the subject is further supported by previous studies, which have established that *de novo* mutations in the first three transmembrane domains (TM1, TM2, and TM3) are associated with neurological and epileptic conditions (62). Most importantly, the c.875C>T heterozygous variant has been reported by the Epi4K consortium (77). Collectively, these data provide strong evidence that the heterozygous c.875C>T missense variant in *GABRA1* is likely pathogenic.

Expression patterns of the zebrafish ortholog of *GABRA1*.

In order to understand the mechanisms by which *GABRA1* regulates development, we used the zebrafish (*Danio rerio*) as a model organism. We first confirmed the spatial

and temporal expression patterns of zebrafish *gabra1* using whole-mount *in situ* hybridization (WISH). We performed WISH at 1, 2, and 3 days post fertilization (DPF). *gabra1* expression was localized to the developing nervous system at each time point with the broadest expression at 1 DPF (Figure 2.2). Over the course of development the expression of *gabra1* became more restricted to the midbrain-hindbrain regions (Figure 2.2) consistent with previously published work (79,80).

Gabra1 regulates zebrafish larval motility.

Mutations in *GABRA1* have been associated with epileptic phenotypes (13,81,65,62,82,83) and behavioral assays to monitor seizure like behaviors in zebrafish have emerged (43,54). Consequently, we developed a protocol using the Zebrabox behavioral unit to monitor swim speed and total distance swam in larvae injected with anti-sense morpholinos that inhibit either the translation of *gabra1* or mRNA splicing. Embryos were injected at the single cell stage with randomized control morpholinos (RC), translational targeting morpholinos (tbMO), or mRNA disrupting morpholinos (sMO) and raised to 5 DPF. Larvae were monitored according to the protocol described in the materials and methods for swim speed and total distance swam. As shown in Figure 2.3, the tbMO was associated with a statistically significant ($p<0.001$) reduction in total swim speed (Figure 2.3A) and decreased total distance swam (Figure 2.3B) consistent with a hypomotility phenotype. The decrease in speed and distance was observed in both light and dark conditions at 5 DPF (Figure S2.1). Importantly, injection of an equivalent concentration of sMO induced a hypomotility phenotype (Figure S2.2B,C; $p=0.0263$). These results are consistent with the phenotype present in morphants injected with the

translational blocking morpholino. Importantly, we validated the effects of injection of sMO on mRNA splicing using RT-PCR. As shown in Figure S2.2A, injection of the *gabra1* targeting sMO induced abnormal alternative splicing relative to injection with RC morpholinos (note double band observed using RT-PCR). RT PCR analysis confirmed a near 50% reduction in wildtype *gabra1* (Figure S2.2A).

Next, we sought to restore the hypomotility phenotype in morphants (tbMO) by co-injection of *GABRA1* encoding mRNA. Embryos were injected at the single cell stage with RC morpholinos, tbMO morpholinos, *GABRA1* mRNA, or a combination of *GABRA1* mRNA with RC or tbMO morpholinos. Injection of the tbMO caused a statistically significant decrease in the total distance swam ($p= 0.000161$) and the overall swim speed ($p=0.036384$) (Figure 2.4A,B; tbMO relative to RC). Injection of *GABRA1* encoding mRNA had no significant effect on speed or distance at a concentration of 1000pg/embryo (Figure 2.4A,B; mRNA and RC+). The co-injection of the tbMO and *GABRA1* encoding mRNA at 1000pg/embryo restored the total distance swam to normal levels ($p= 0.003010689$), but was not sufficient to restore the deficits in overall speed to control levels (Figure 2.4A,B). Thus, co-injection of 1000pg of *GABRA1* encoding mRNA with the tbMO produced a partial rescue of the observed phenotype. Injection of *GABRA1* mRNA at higher concentrations was accompanied by some degree of toxicity (cardiac edema and death) and therefore, additional rescue experiments with higher concentrations could not be attempted.

The c.875C>T *GABRA1* variant does not restore the hypomotility phenotype in morphants.

The functional consequences of the c.875C>T variant are currently unknown. Therefore, we asked whether expression of the c.875C>T variant was sufficient to restore the hypomotility induced by knockdown of *gabra1*. Embryos were injected at the single cell stage with RC morpholinos, tbMO morpholinos, *GABRA1* c.875C>T mRNA (SDM), or a combination of SDM mRNA with tbMO morpholinos. Consistent with previous experiments, injection of the tbMO morpholino caused a significant reduction ($p=0.0153$) in the total distance swam relative to embryos injected with the RC (Figure 2.4C). Interestingly, the co-injection of the mRNA encoding the c.875C>T (SDM) and the tbMO was unable to restore the total distance traveled to control levels (Figure 2.4C). Importantly, the injection of the *GABRA1* c.875C>T variant (SDM) at 1000pg/embryo had no significant effects on the total distance swam (Figure 2.4C).

The expression of *gabrb2* and *gabrg2* are decreased in *gabra1* morphants.

Previous studies suggest that approximately 60% of all $GABA_AR$s consist of two α1, two β2, and one γ2 subunit (1). We hypothesized that the knockdown of *gabra1*, which encodes the α1 sub-unit would alter the sub-unit composition of the $GABA_AR$. To begin to test this, we analyzed the expression of the genes that encode the β2 and γ2 sub-units. As shown in Figure 2.5A, knockdown of *gabra1* caused a decrease in the expression of *gabrb2* (β2) and *gabrg2* (γ2). We next measured the expression of other alpha sub-units in *gabra1* morphants. As shown in Figure 2.5A, injection of the tbMO was associated with increased expression of *gabra6a* and *gabra6b*, but only *gabra6b* was statistically

significant across biological triplicates. A similar expression pattern of *gabra6a* and *gabra6b* was observed upon injection of the sMO (Figure S2.2D), with both genes demonstrating a statistically significant increase in expression. We did not detect a statistical change in the expression of any other α sub-unit across either the tbMO or the sMO (Figs 2.5A, S2.2D).

We sought to build upon these data by determining whether morphant larvae had an intact receptor capable of responding to pentylenetetrazol (PTZ), an antagonist of the $GABA_AR$. Non-injected wildtype embryos treated with 10mM PTZ exhibit short convulsions and a whirlpool swimming behavior with a 2-fold increase in swim speed (p= 6.74E-06) and an approximate 6-fold increase in total distance swam (p= 2.14E-05) (Figure 2.5B,C). These phenotypes were consistently observed in larvae injected with RC morpholinos as the RC morpholino had no effect on larval behavior or their response to PTZ. Interestingly, *gabra1* morphants (tbMO) responded normally to PTZ according to both distance and speed measurements (Figure 2.5B,C). Collectively, these data demonstrate that knockdown of *gabra1* alters the expression of unique $GABA_AR$ subunits, although, morphants continue to respond to PTZ treatment.

DISCUSSION

We have identified an individual presenting with multi-system disorder carrying a *de novo* missense variant in the *GABRA1* gene (NM_000806.5:c.875C>T, NP_000797.2:p.Thr292Ile). The *GABRA1* gene encodes the α1 sub-unit of the $GABA_AR$, which mediates the fast inhibitory synapses of the nervous system. $GABA_ARs$ are pentameric and can be composed of different combinations of the following components:

six α subunits, three β subunits, three γ subunits, three ρ subunits, one ε, δ, θ, or π subunits. Of these sub-units, mutations in *GABRA1* (12,13,62,84), *GABRA6* (85), *GABRB2* (12), *GABRB3* (84,86), *GABRG2* (84), and *GABRD* (12) have been associated with epileptic phenotypes (reviewed in (87)). Most importantly, in a recent international collaboration (Epi4K Consortium), the heterozygous *de novo* p.Thr292Ile variant we describe here was identified in a male patient diagnosed with infantile spasms (77). The individual studied in the Epi4K study had febrile seizures at the age of 1-month and at 15-months of age, his electroencephalogram (EEG) showed bursts of generalized spike and wave (GSW) at 2.5 Hz with multiple foci of epileptiform activity. He presented with features of generalized tonic clonic (GTC) and myoclonic seizures. He was developmentally delayed, hypotonic, and did not speak at 18-months of age with additional features that include esotropia, poor vision, abnormal electroretinogram, and a head circumference at 5th percentile. The subject reported here was diagnosed with seizure disorder, intellectual disability, vision loss, and was non-verbal; phenotypes consistent with the previously identified case. Additionally, the p.Thr292Ile variant is present in one of the 3 transmembrane domains of the GABRA1 protein and these domains have been associated with epileptic phenotypes (62). Collectively, these data strongly suggest that the heterozygous mutation p.Thr292Ile causes a complex disorder characterized by a severe seizures. This is supported by the fact that there are at least two subjects with overlapping phenotypes harboring this variant.

It is not yet known how mutations in the GABRA1 transmembrane domain result in seizure like phenotypes. Genetic knockout mice have been developed to understand how mutations in *Gabra1* (mouse) affect $GABA_AR$ function, but the results have been

difficult to interpret, as the deletion of *Gabra1* (mouse) causes strain and sex specific phenotypes (88). Due to these strain differences, additional systems have been developed including a zebrafish harboring a mutation in the *gabra1* gene. Interestingly, mouse models of *Gabra1* deletion are viable, but the homozygous deletion of *gabra1* in fish is lethal (80). Despite this lethality, mutant zebrafish survive to several weeks post fertilization, which has allowed for the characterization of *gabra1* function in fish at 7-10 weeks post fertilization (80).

In this report, we demonstrate that morpholino mediated knockdown of *gabra1* in zebrafish leads to hypomotility in the presence and absence of light. We perform our studies at 5 DPF, during the larval stage, prior to the onset of feeding or sexual dimorphism, but after swim bladder formation. *gabra1* morphants consistently demonstrated with reduced swim speed and reduced overall distance travelled relative to control. These data are consistent with Samarut et. al., who demonstrated that mutation of *gabra1* results in hypomotility, albeit at a later stage in development that would be equivalent to a juvenile onset (80). In contrast to Samarut et. al., we did not observe overt indications of myoclonic seizures at any time point in our protocol. For example, within the first minute of light exposure, Samarut and colleagues observed intense seizures characterized by convulsions, uncontrolled movements, and whirlpool swim behavior. This phenotype was not observed in morphant animals (data not shown). This can likely be attributed to the fact that our study is performed using a knockdown of *gabra1*, which maybe more consistent with the heterozygous phenotypes reported by Samarut and colleagues at 4 DPF. To address the function of the c.875C>T *GABRA1* variant, we performed restoration experiments in which this variant was co-injected with *gabra1*

targeting morpholinos. Co-injection of mRNA encoding the c.875C>T variant did not restore the hypomotility phenotype present in morphants, whereas co-injection of wildtype *GABRA1* restored the total distance travels to control levels. These data suggest that the c.875C>T variant is a loss of function allele, however, future studies characterizing the function of this variant are warranted. Should this allele be a loss of function allele, morpholino mediated knockdown is an alternative approach towards understanding the mechanisms by which the c.875C>T allele causes disease.

We further demonstrate that knockdown of *gabra1* causes abnormal expression of other sub-units of the $GABA_AR$. Despite changes in the expression of various $GABA_AR$ sub-units, morphant animals continue to respond to PTZ stimulus. PTZ is a potent antagonist of the $GABA_AR$ and treatment of wildtype larvae with PTZ induces a myoclonic seizure (54,55) because PTZ binds directly to the $GABA_AR$ resulting in disinhibition (89). The continued response of morphants to PTZ, suggests that these embryos maintain the ability to produce some form of the $GABA_AR$. Consistent with this hypothesis, we observed increased expression of *gabra6a and gabra6b* mRNA, which encode the two zebrafish α6 sub-units of the $GABA_AR$. Other sub-units did not demonstrate consistent changes in expression across multiple morpholinos or biological replicates. Interestingly, mutations in *GABRA6*, which encodes the α6 sub-unit are associated with disease (85). Thus, it is unclear whether the hypomotility phenotype observed is the direct result of a lack of g*abra1* or the up-regulation of *gabra6*. Future studies analyzing the function of α6 and other alpha sub-units in *gabra1* mutant animals are needed.

The gene expression changes we observe are strongly supported by previous conclusions in mice with mutations in the *Gabra1* gene (90,91). Recent work in zebrafish has demonstrated that the homozygous nonsense mutation of *gabra1*, does not disrupt overall brain structure or the total number of GABAergic cells, but does influence the brain transcriptome (80). Collectively, these data raise the possibility that other alpha sub-units may compensate for the loss of *gabra1,* ultimately producing unique compositions of the $GABA_AR$. The function of these receptors is unknown. But it is conceivable that the production of $GABA_AR$ with unique sub-unit composition in incorrect regions of the brain might underlie the impaired synapse formation observed in zebrafish harboring germline mutations in the *gabra1* gene (80).

We provide strong evidence that heterozygous *de novo* mutation of *GABRA1* is associated with a multi-system disorder characterized by severe seizures. We further characterized the developmental and behavioral defects associated with knockdown of *gabra1* in zebrafish. Behaviorally, morphant animals present with hypomotility at 5 DPF measured by reduced swim speed and total distance traveled. These deficits coincide with significant changes in the expression of $GABA_AR$ sub-units and cannot be restored by the *de novo* c.875C>T allele. Although a zebrafish harboring a mutation in the *gabra1* gene has recently been created, detailed behavioral analysis was performed at the juvenile stage (weeks post fertilization). Here we complement previous studies using a morpholino mediated knockdown approach, as the homozygous deletion of *gabra1* was lethal (80). Our behavioral study is the first to our knowledge that comprehensively characterizes the phenotype of *gabra1* deletion during early development (DPF as opposed to weeks post fertilization). We observed hypomotility consistent with previous

studies in zebrafish and our study likely informs about specific types of mutations, those of which result in loss of function alleles. Importantly, our restoration experiments with the c.875C>T allele suggest that this allele is in fact a loss of function allele. Thus, morpholino mediated studies might provide insight into the mechanisms by which loss of function alleles cause disease.

MATERIALS AND METHODS

Animal Husbandry

For all experiments, embryos were obtained by crossing AB wildtype or Tupfel Long Fin wildtype. Fish were maintained at The University of Texas at El Paso according to the Institutional Animal Care and Use committee (IACUC) guidelines. They were maintained and bred in groups of two females and two to four males. The collected zebrafish embryos were kept in egg water consisting of 0.03% Instant Ocean (Aquaneering, San Diego, CA) in D.I. water at 28°C.

Whole-Exome Sequencing and Data Analysis

High quality, unamplified, and unfragmented genomic DNA (A260/A280 ≥ 1.8 and A260/A230 ≥ 1.9) was extracted from whole blood obtained from the subject and his parents using the Puregene Blood kit from Qiagen (Valencia, CA). Whole exome sequencing was performed using the service provided by Beijing Genomics Institute (Cambridge, MA). Details of data analysis were similar to the procedure as previously described (77). Approximately 78 to 168 million, 100 bp, paired-end reads (>70X) were obtained and mapped to the reference human genome (GRCh37/hg19) using Burrows-

Wheeler Aligner (BWA) (92) (summarized in Table S1). Variants were determined by the utilities in the SAMtools (93) and further annotated with SeattleSeq. Filtering and the test of inheritance model was performed using tools available in Galaxy (94). Variants were filtered against dbSNP build 137, 1000 Genomes (November 23, 2010 release version), Exome Variant Server (EVS, ESP6500SI-V2) and Exome Aggregation Consortium ExAC browser (version 0.3). Rare variants were identified as a variant with a minor allele frequency (MAF) less than 1% using dbSNP137. The sequence data from the family was then used to test for causal variants under different inheritance models, including dominant (*de novo* mutations) and recessive (compound heterozygous, homozygous, and X-linked hemizygous mutations) models. In the dominant model, variants found in any database (dbSNP, 1000 Genomes, EVS, ExAC) were removed from the top candidacy list. In the recessive model, autosomal variants which had homozygotes found in the databases, such as EVS and ExAC, (or variants on chrX or chrY with hemizygotes in databases) were deleted from the top candidacy list.

Sanger Sequencing Verification

Sanger sequencing was used to validate the variant described. Briefly, primers were used to amplify the PCR product (fwd 5'-GCTGTFATAGGGTGGAGGTG-3', rev 5'GCTATCAACGCCATTGTGAA-3') using 1X GoTaq Green (Promega, Madison, WI) with a final primer concentration of 0.2uM. Reaction parameters for PCR include an initial cycle at 95°C for 10 minutes, followed by 30 cycles of 95°C for 30 seconds, 60°C for 30 second, and 72°C for 1 minute, finishing with extension at 72°C for 5 minutes. Amplified

PCR products were sequenced using the PCR primers as sequencing primers. Variations detected in *GABRA1* were assigned using cDNA accession number NM_000806.5.

Whole mount *in situ* hybridization (WISH) and injections

WISH was performed as previously described (95). Embryos were harvested at 1, 2, and 3 DPF and fixed in in 4% paraformaldehyde (PFA) (Electron Microscopy Sciences, PA) for 1 hour at room temperature (RT). Embryos were dehydrated using a methanol: PBS gradient and stored in 100% methanol overnight in -20°C. Embryos were rehydrated using PBS: Methanol gradient, washed in PBS with 0.1% Tween 20 and permeabilized with proteinase K (10ug/ml) for the time indicated by Thisse and Thisse (95). Permeabilized embryos were prehybridized in hybridization buffer (HB) (50% deionized formamide (Fisher, Waltham, MA), 5X SSC (Fisher, Waltham, MA), 0.1% Tween 20 (Fisher, Waltham, MA), 50μg ml^{-1} heparin (Sigma, St. Louis, MO), 500μg ml^{-1} of RNase-free tRNA (Sigma, St. Louis, MO) , 1M citric acid (Fisher, Waltham, MA) (460μl for 50ml of HB) for 2-4 hours and then incubated overnight in fresh HB with probe (*gabra1* 100ng) at 70°C. Samples were washed according to protocol, blocked in 2% sheep serum (Sigma, St. Louis, MO), 2 mg ml^{-1} bovine serum albumin (BSA) (Sigma, St. Louis, MO) for 2-4 hours at RT, and incubated with anti-DIG Fab fragments (1:10,000) (Sigma, St. Louis, MO) overnight at 4°C. Samples were developed with BM purple AP substrate (Sigma, St. Louis, MO) and images were collected with a Zeiss Discovery Stereo Microscope fitted with Zen Software. The *gabra1* probe was created using primers specific to the endogenous cDNA sequence (*gabra1* ISH fwd 5'-TAAGCTGCGCTCTTCTCCTC-3', *gabra1* ISH rev 5'-GCAGAGTCCCTTCCTCTGTG-3').

For morpholino injections, a translational blocking morpholino (tbMO) (TCTTCCACCCCACATCATTCTCCGA) and a splice site inhibiting morpholino (sMO) (ACACGCTCTGTTGAAGCAAGAAATT) targeting *gabra1* were designed. The efficiency of knockdown for the sMO was performed with primers flanking the target site (Fwd: GACAGCCTCCTCGATGGTTA and Rev: GCAGAGTCCCTTCCTCTGTG). Each morpholino was injected independently at the single cell stage at a concentration of 1.6 ng/embryo. An equivalent concentration of randomized control morpholinos (25-N) was injected as a control. Final concentration of morpholino was determined empirically after an injection gradient was performed to determine optimal survival. For rescue experiments, the human *GABRA1* complete open reading frame was purchased from TransOMIC Technologies (Huntsville, AL). The c.875C>T *GABRA1* variant was created from the original vector obtained from TransOMIC Technologies using the QuikChange II Site-Directed Mutagenesis Kit (Fisher, Waltham, MA) with forward (TAACAACTGTGCTCATCATGACAACATTGAG) and reverse primers (GAGTTACAACAGTACGACTCGTGTCAACAAT). *In vitro* RNA was synthesized using the mMessage Machine kit (Fisher, Waltham, MA). The synthesized mRNA was injected at the single cell stage alone or in conjunction with tbMO at the indicated concentrations in the figure legends.

Quantitative Real Time PCR (QPCR)

Total RNA was isolated from brain homogenates obtained from embryos injected with random control morpholinos or tbMO at 5 DPF using Trizol (Fisher, Waltham, MA). Reverse transcription was performed using the Verso cDNA Synthesis Kit (Fisher,

Waltham, MA) and total RNA was normalized by concentration (ng) across all samples. PCR was performed in technical triplicates for each sample using an Applied Biosystems StepOne Plus machine with Applied Biosystems associated software. Sybr green (Fisher, Waltham, MA) based primer pairs for each gene analyzed are as follows: *gabra2a* fwd GATGGCTACGACAACAGGCT*, gabra2a* rev TGTCCATCGCTGTCGGAAAA, *gabra3* fwd GCTGAAGTTCGGGAGCTATG, *gabra3* rev GGAGCTGATGGTCTCTTTGC*, gabra4* fwd GACTGCGATGTACCCCACTT*, gabra4* rev ATCCAGGTCGGAGTCTGTTG, *gabra5* fwd CATGACAACACCCAACAAGC, *gabra5* rev CAGGGCCTTTTGTCCATTTA*, gabra6a* fwd TCGCGTACCCATCTTTCTTC, *gabra6a* rev CCCTGAGCTTTTCCAGAGTG*, gabra6b* fwd CGGAGGAGTGCTGAAGAAAC, *gabra6b* rev GGGAAAAGGATGCGTGAGTA, *gabrb2* fwd CCCGACACCTATTTCCTCAA*, gabrb2* rev TCTCGATCTCCAGTGTGCAG, *gabrg2* fwd ACACCCAATAGGATGCTTCG*, gabrg2* rev AGCTGCGCTTCCACTTGTAT. Analysis performed using $2^{\Delta\Delta ct}$. Statistical analysis of mRNA expression was performed using a T-test. All QPCR was performed in biological duplicate or triplicate using a pool of embryos (30-40) per time point.

Behavioral analysis and pentylenetetrazol treatment

Embryos injected with random control morpholinos, tbMO, sMO, *GABRA1* mRNA, *GABRA1* (c.875C>T), or a combination as indicated in the figure legends were raised to 5 DPF. Behavioral analysis was performed using the Zebrabox (ViewPoint Behavior Technology, Montréal, Canada). Larvae were individually tracked for swim speed and total distance swam in a 96 well plate. The behavioral protocol (adapted from (55)) was a total of 15 minutes divided into 5 minute intervals of dark/light/dark conditions. For light

exposure, the Zebrabox produces 8000 Lux of light at 550nM at max setting. We ran experiments at 100% light power for 5 minutes and then removed the light stimulus. All larvae were acclimated to the dish and housing conditions for 1 hour prior to analysis. A baseline measure of activity was performed for 5 minutes in the dark prior to the onset of light stimulus. An additional measure of activity was performed post-light stimulus for 5 minutes. Settings for the program include a threshold of 16 and integration period of 300 seconds. Data was measured as total distance traveled (mm) and total swim speed (mm/sec) (Swim Speed= {Total distance traveled in large and small movements) (Smldist+Lardist)}/{Total duration spent by the animal in small and large movements(smldur+lardur)}. Statistical significance was determined according to a T-test. All experiments were performed in biological triplicate. For PTZ treatment, PTZ (10mM) was added directly to the 96 well plate following acclimation period. Final concentration of PTZ was determined from previously published results (54,55,96,97).

ACKNOWLEDGEMENTS

These data could not have been completed without the patients involved in the study and without the support of Dr. Douglas Watts.

COMPETING INTERESTS STATEMENT

Authors report no conflict of interest.

FUNDING

This work was supported by NIH NINDS Grant no. 5K01NS099153-02, the Bridges to the Baccalaureate Program, Grant no. 2R25GM049011-16, the RISE program Grant no. R25GM069621-11, and the Border Biomedical Research Center Grant no. 2G12MD007592 from National Institute on Minority Health and Disparities

DATA AVAILABILITY

All reagents are available upon request from the corresponding author.

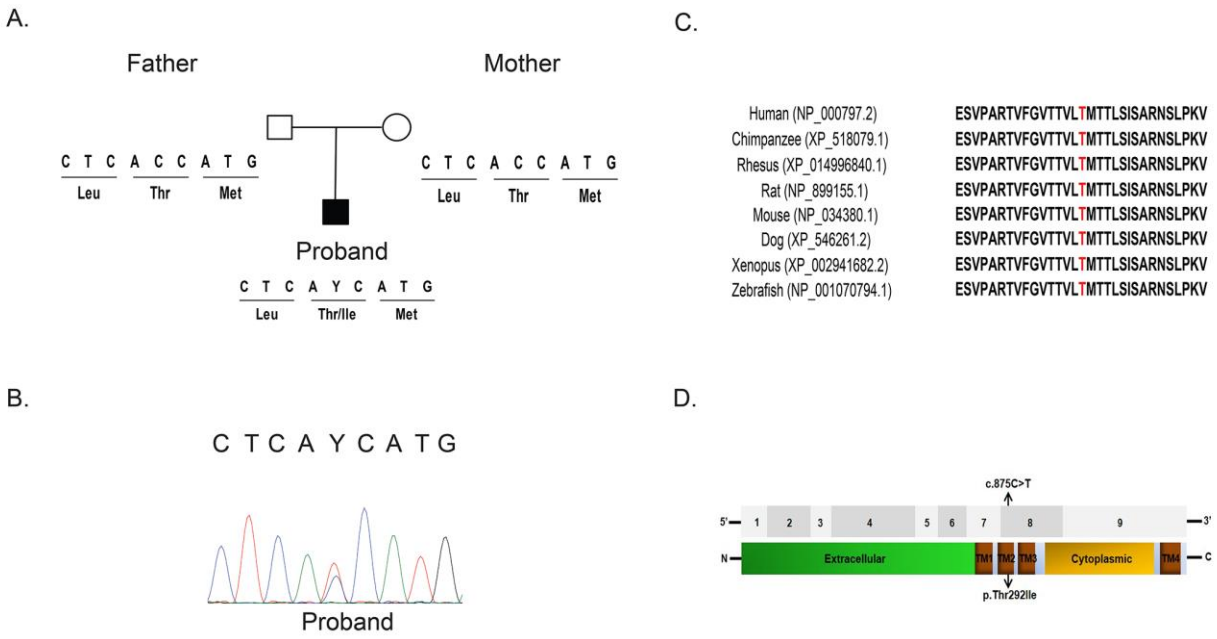

Figure 2.1. Identification of pathogenic variants in the *GABRA1* gene.

(A) Depiction of a de novo missense variant c.875C>T (p.Thr292Ile) in the patient and his unaffected parents. (B) Partial chromatograms demonstrating Sanger Sequencing validation in the Proband. (C) Comparative analysis of the GABRA1 protein from multiple species. Thr292 (highlighted in red) and its neighboring amino acids are evolutionarily conserved. Protein sequences were obtained from NCBI Protein database or Ensembl. (D) Top: annotation of the nine coding exons in the GABRA1 gene. Bottom: the GABRA1 protein includes an extracellular domain, a cytoplasmic domain and four transmembrane domains (TM1-4) (annotated by Universal Protein Resource, UniProt). Location of variant identified in the patient is indicated by arrows within TM2.

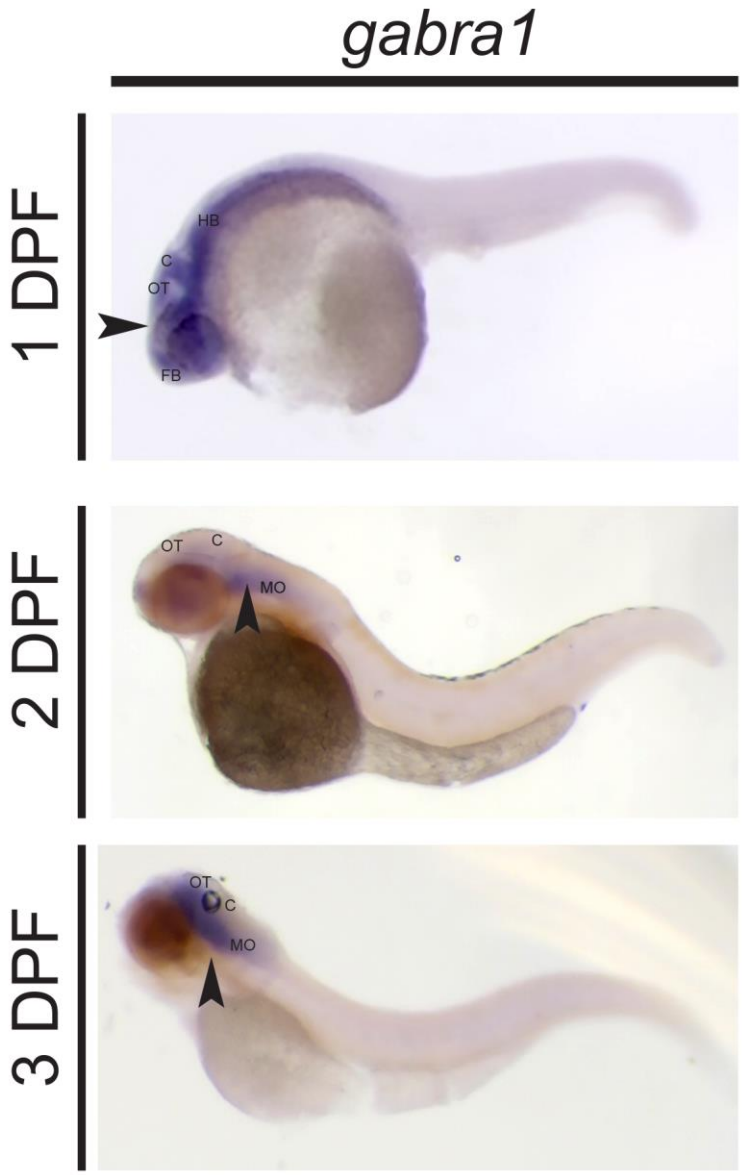

Figure 2.2. *gabra1* expression in the developing zebrafish.

WISH was performed at 1, 2 and 3 DPF with an anti-sense gabra1 probe. Arrows indicate the expression of gabra1 at each developmental stage. Minimum of ten larvae per group/biological replicate. Abbreviations: FB, forebrain; OT, optic tectum; C, cerebellum; HB, hindbrain; MO, medulla oblongata. Scale bars: 0.2 mm.

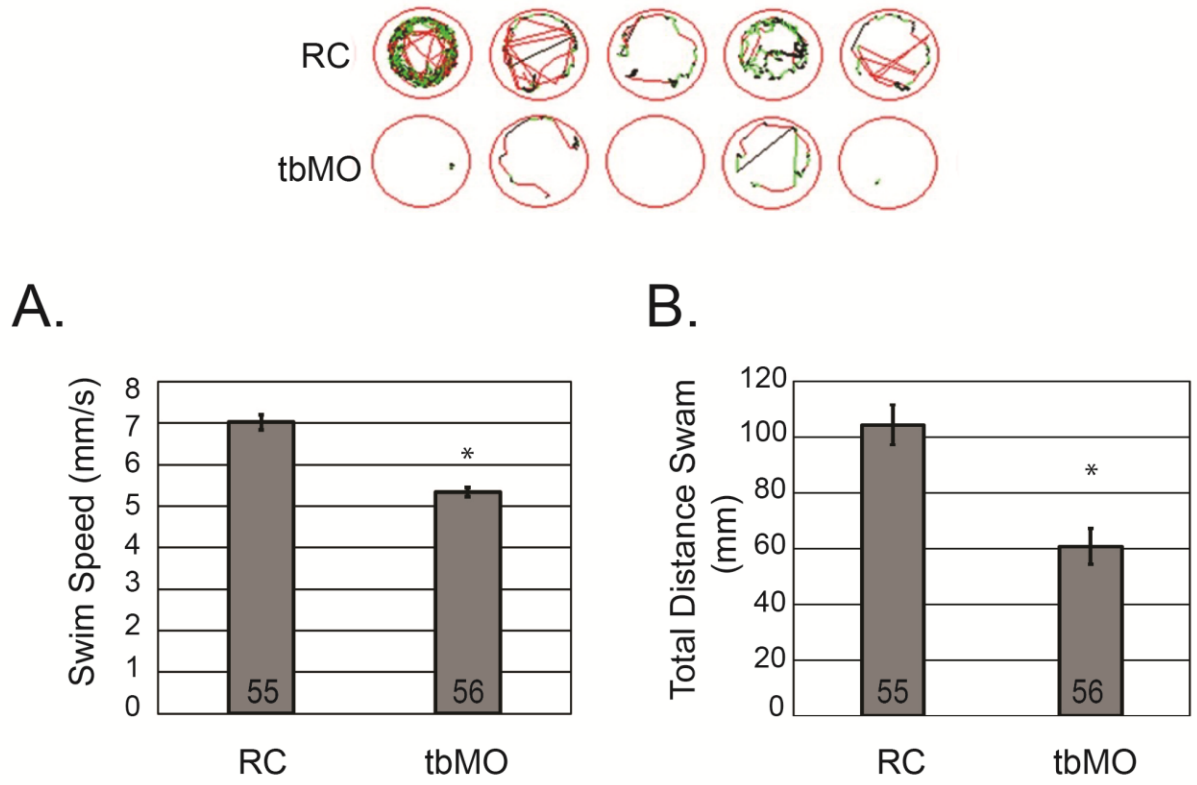

Figure 2.3. Knockdown of *gabra1* causes hypomotility.

(A) Total swim speed of larvae injected with RC morpholinos or tbMO morpholinos was determined using Zebrabox technology at 5 DPF. Total number of embryos analyzed per group is depicted in the graph. *P<0.001. (B) The total distance swam was assessed at 5 DPF using Zebrabox technology. *P<0.001. Representative images of larval swim patterns are depicted above panel A and B. All experiments were performed in biological duplicate or triplicate and statistical analysis was performed using a standard two-tailed test. Error bars represent standard error of the mean of independent experiments.

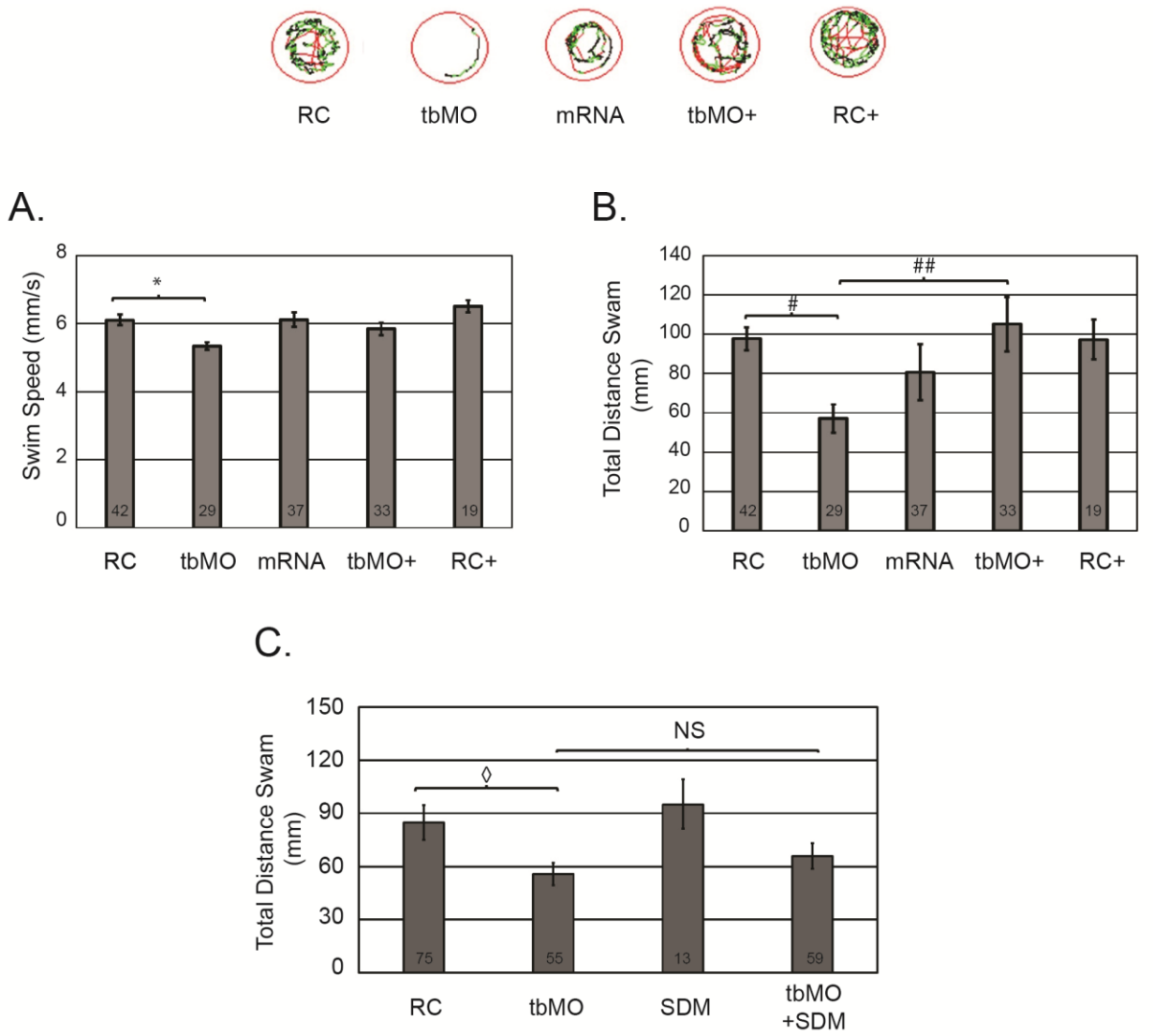

Figure 2.4. Ineffective restoration of hypomotility by co-injection of the c.875C>T variant.

(A) Total swim speed of larvae injected with RC morpholinos, tbMO morpholinos, GABRA1 encoding mRNA (1000 pg/embryo), RC with GABRA1 mRNA (RC+), or tbMO with GABRA1 mRNA (tbMO+) was determined using Zebrabox technology at 5 DPF. Total number of embryos analyzed per group is depicted in the graph. (B) The total distance swam was assessed at 5 DPF using Zebrabox technology for each of the conditions in A. *P=0.036384 and #P=0.000161 and ##P=0.003010689.

Representative images of larval swim patterns are depicted above panel A and B. (C) Total distance swam of larvae injected with RC, tbMO, GABRA1 c.875C>T (SDM) encoding mRNA, or tbMO with GABRA1 c.875C>T encoding mRNA (tbMO+SDM) was determined at 5 DPF. Total number of animals is indicated in the graph. ◊P=0.0153. All experiments were performed in biological triplicate and statistical analysis was performed using a standard two-tailed t-test. Error bars represent standard error of the mean of independent experiments.

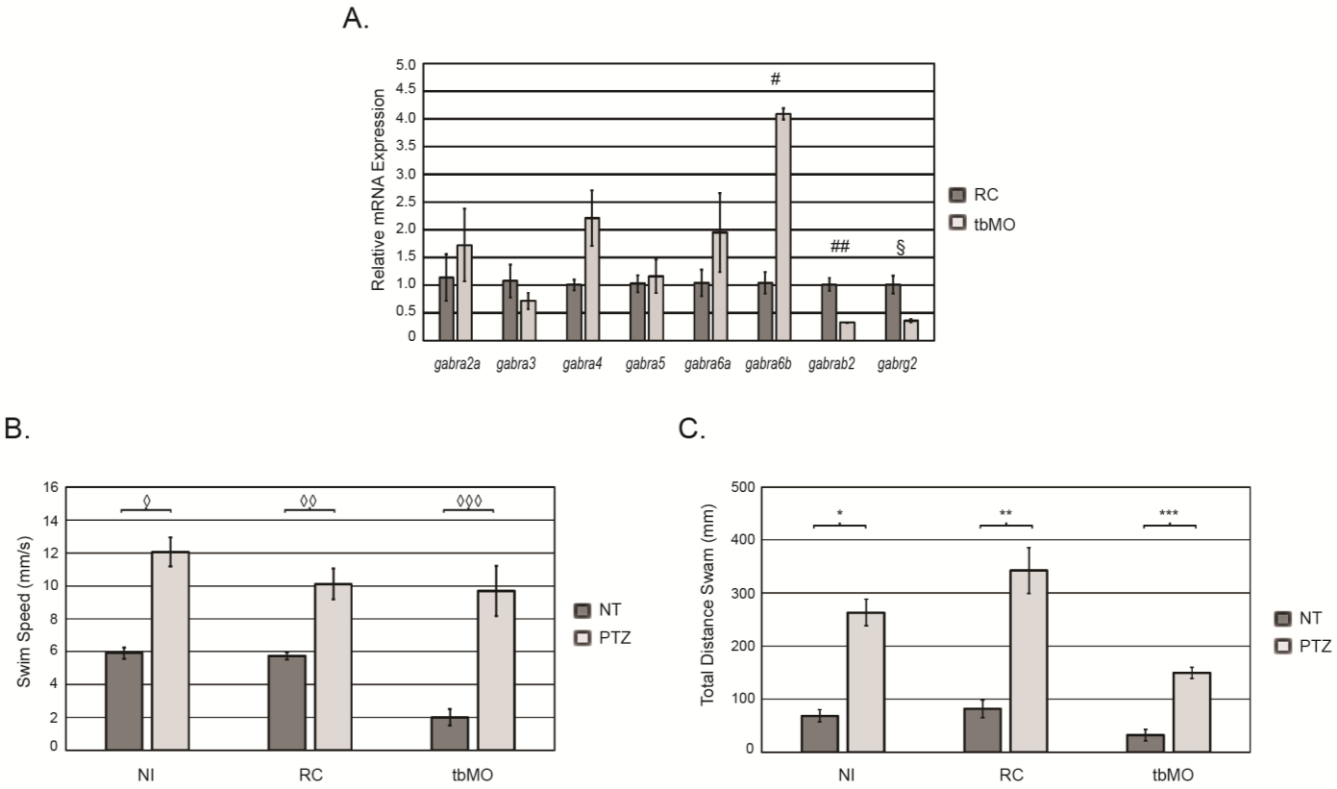

Figure 2.5. Molecular and behavioral responses of *gabra1* morphants.

(A) QPCR was performed at 5 DPF to measure the expression of each gene indicated. Total RNA was isolated from RC injected embryos or tbMO morpholinos. Error bars represent standard deviation of biological triplicates. #P=0.0016, ##P=0.003681, §P=0.009. (B) At 5 DPF, non-injected (NI) larvae, larvae injected with RC, or larvae injected with tbMO were treated with 10 µM PTZ or no treatment (NT) control and total swim speed was assessed using Zebrabox technology. ◊P=6.74E-06, ◊◊P=5.34E-07, ◊◊◊P=1.019E-05. (C) Total distance travelled was assessed at 5 DPF in each of the groups described in B. *2.14E-05. **P=3.92141E-05, ***P=0.0002636. All experiments in B and C were performed in biological triplicate and statistical analysis was performed using a standard two-tailed t-test. Error bars represent standard error of the mean of independent experiments. For B and C, N=12/group/biological replicate.

Supplemental information

Table S2.1. Summary of next generation sequencing statistics

	Proband	**Mother**	**Father**
	NGS statistics		
Raw reads	168,649,368	159,679,186	78,385,962
Reads mapped to hg19	165,308,012	156,265,642	76,698,260
Reads after duplicate removal	66,521,226	65,637,640	65,295,304
Mapped bases	6.65 Gb	6.56 Gb	6.53 Gb
Reads mapped to coding region	35,499,550	34,317,271	33,562,592
Average coverage of coding region	75.04 X	72.59 X	70.89 X

Table S2.2. Summary of exome variants and test of inheritance models.

	Proband			
Total variants	106,737			
Coding variants	18,693			
Nonsynonymous, splice-site, InDel variants	9,631			
Rare variants	1,846			
Test of inheritance model	Dominant model	Recessive models		
	de novo	Compound heterozygous	Homozygous	X-linked hemizygous
Candidate Genes	2 (*CACNA1C, GABRA1*)	5 (*SCNN1B, FNIP1, TTN, OTOG, FAT4*)	0	0
Top Candidates	1 (*GABRA1*)	1 (*TTN*)	0	0

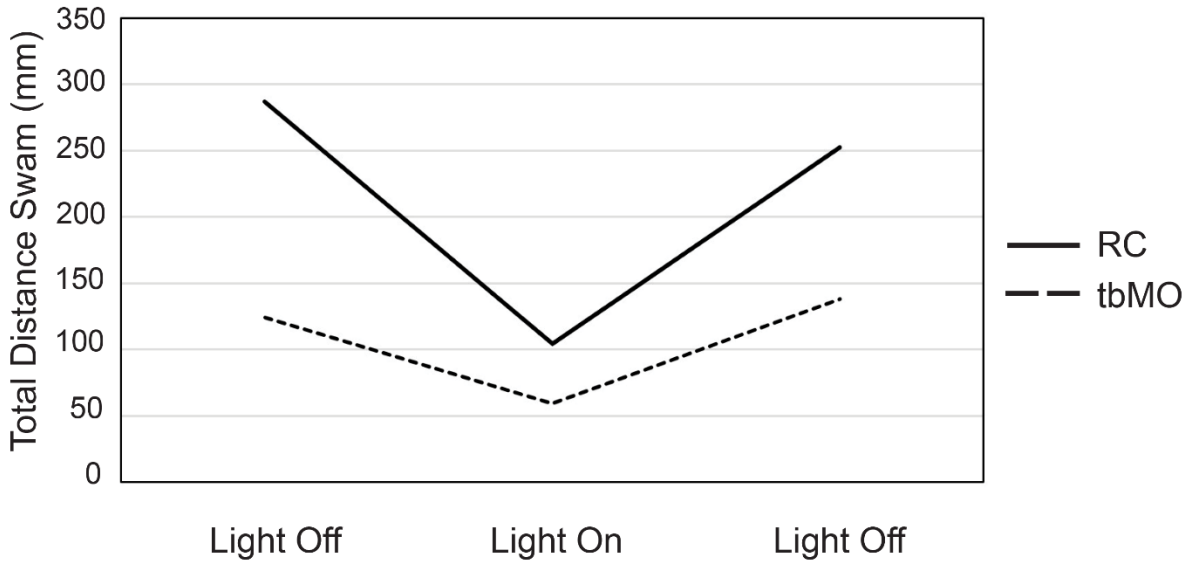

Figure S2.1. Hypomotility in *gabra1* morphants in alternating dark-light conditions. Total distance of larvae injected with random control morpholinos (RC) or translational targeting gabra1 morpholinos (tbMO) was determined using Zebrabox technology at 5 days post fertilization (DPF). Distance was calculated without light, after the onset of light for a 5 minute duration, and an additional period without light.

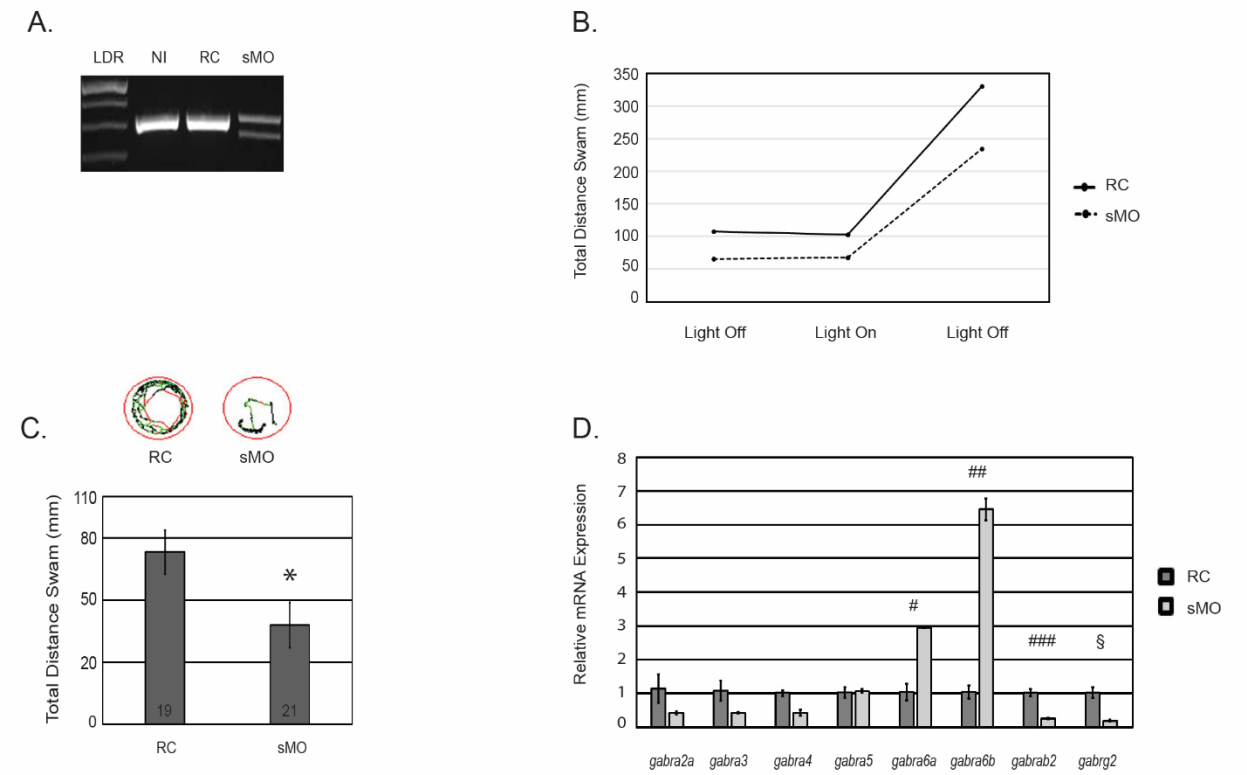

Figure S2.2. Knockdown of *gabra1* induces defects in splicing, hypomotility, and gene expression changes.

(A) PCR analysis of alternative splicing was performed on non-injected control embryos, embryos injected with random control morpholinos (RC), or morpholinos inhibiting gabra1 mRNA splicing (sMO). LDR is molecular weight ladder. (B) The total distance swam was assessed in gabra1 morphants (sMO) and random control (RC) injected larvae at 5 days post fertilization (DPF). Distance was calculated without light, after the onset of light for a 5 minute duration, and an additional period without light. (C) The total distance swam was assessed at 5 DPF using Zebrabox technology. *p<0.0263. Representative images of larval swim patterns are depicted above graph. (D) Quantitative real time PCR (QPCR) was performed at 5 DPF to measure the expression of each gene indicated. Total RNA was isolated from random control injected embryos (RC) or gabra1 targeting morpholinos

(sMO). Error bars represent standard deviation. Expression was measured in biological triplicate. #p=0.0087, ##p=0.0001, ###p=0.003681, §p=0.9024.

Chapter 3: Mutation of *gabra1* is associated with seizures and abnormal expression of proteins critical for ion homeostasis and synaptic vesicle transport.

This chapter presents a research manuscript written and submitted to Plos One Journal on April 21st, 2023. It has been deposited to the BioRxiv preprint server. It was resubmitted on two occasions and is pending validation of Gabra1 protein expression, mRNA validation of alpha1 subunits, and protein expression of Gabra4 protein levels. In this manuscript, we identified light-induced seizure light behavior upon genetic disruption of *gabra1.* Previous research has shown that *gabra1* plays an essential role in neurodevelopment and locomotion, from larval to juvenile stages in zebrafish. We previously reported hypolocomotion upon transient knockdown of *gabra1,* whereas seizure-like behavior was reported in a germline mutant of *gabra1* (58,80). Interestingly, knockdown and germline mutation of *gabra1* resulted in contrasting behavioral phenotypes. Hence, the need for complemental model systems to further elucidate the contribution of *gabra1* in neural development and disease is highlighted. In this manuscript, the behavioral and molecular patterns associated with non-sense mutation of *gabra1* (*sa43718* allele) in zebrafish were investigated. We hypothesized that homozygous carriers of the *sa43718* allele will exhibit seizure-like behavior phenotype and differential expression of $GABA_AR$ subunits. Homozygous carriers showed a 90% decrease in total *gabra1* mRNA, confirmed by quantitative PCR analysis, but could not be confirmed by western blot analysis with GABRA1 specific antibodies. Behavioral analysis demonstrated that homozygous carriers of the *sa43718* allele exhibit seizure-like behavior upon light stimuli at 5 days post fertilization. We further evaluated larval response to $GABA_AR$ antagonists to determine the presence of a functional $GABA_AR$.

Importantly, response to PTZ was abrogated in mutant larvae, suggesting the presence of a receptor with deficient function. We then analyzed the expression levels of *gamma2* and *beta2* subunits, which, together with *gabra1* encode for the major $GABA_AR$ isoform. We did not observe major changes in transcripts that encode for these subunits. However, we did report upregulation of *gabra4,* which encodes for the alpha-4 subunit of the $GABA_AR$. Analysis not included here discerned that *rpl13a*, our endogenous control for qPCR was abnormally expressed according to proteomics. Additional qPCR of all subunits is required prior to publication. Although seizure-light behavior was associated with up-regulation of *gabra4* transcript*,* the protein levels of Gabra4 were not increased as reported by our proteomic analysis. Subsequent western blot with anti-Gabra4 antibodies by the Quintana Laboratory revealed reduced Gabra4 protein levels, raising questions as to the veracity of the mRNA expression analysis. This discrepancy in addition to the differential expression of *rpl13a* in mutant animals warrants additional validation of mRNA expression be performed. Importantly, proteomic analysis identified differential expression of proteins involved in neurotransmitter release, vesicle transport, proton homeostasis, and mitochondrial function. However, only the most abundant proteins were reliably detected across technical and biological replicates. In closure, our findings provide further understanding on the development of the GABAergic system, its contribution to neurodevelopmental disorders, and epilepsy.

AUTHOR CONTRIBUTIONS

The following manuscript discusses the findings and observations in a *GABRA1* germline mutant zebrafish, the *gabra1*^{sa43718} allele. The manuscript includes data from six authors, Nayeli G. Reyes-Nava (NGR), Isaiah Perez (IP), Brian Grajeda (BG), Igor L. Estevao (ILE), Cameron C. Ellis (CCE), and Anita M. Quintana (AMQ). NGR performed experiments, provided experimental conceptualization, wrote aspects of the manuscript, performed zebrafish care and maintenance, supervised trainees that provided input/data analysis or acquisition. AMQ performed data analysis, wrote portions of the manuscript, obtained funding, provided mentorship to NGR and all other Quintana Lab members contributing to the goals of the project, and performed data analysis. IP performed survival analysis and produced graphs related to survival. BG, ILE, and CCE performed mass spectrometry, protein preparation, and data analysis for proteomics.

Title: Mutation of *gabra1* is associated with seizures and abnormal expression of proteins critical for ion homeostasis and synaptic vesicle transport.

Authors: Nayeli G. Reyes-Nava[1], Isaiah Perez[1], Brian Grajeda[1¶], Igor L. Estevao[1¶], Cameron C. Ellis[1¶], and Anita M. Quintana[1*].

Affiliations:

[1] Department of Biological Sciences, Border Biomedical Research Center, The University of Texas at El Paso, El Paso, Texas, United States of America

[¶]These authors contributed equally

***Corresponding author**

Email: amquintana8@utep.edu (AQ)

ABSTRACT

Mutation of the *GABRA1* gene is associated with neurodevelopmental defects and epilepsy phenotypes. *GABRA1* encodes for the α1 subunit of the gamma-aminobutyric acid type A receptor ($GABA_AR$), which regulates the fast inhibitory impulses of the nervous system. Multiple model systems have previously been developed to understand the mechanism by which mutations in *GABRA1* cause disease, but these models have produced complex and incongruent data. Thus, additional model systems are required to validate and substantiate previously published results. We investigated the behavioral patterns associated with a non-sense mutation of the zebrafish *gabra1* (*sa43718* allele) gene. The *sa43718* allele has a 90% decrease in total *gabra1* mRNA expression, which is associated with a light induced seizure-like behavior. Mutation of *gabra1* was accompanied by increased mRNA expression of *gabra4,* which encodes for alpha-4 subunit of the $GABA_AR$. Despite increased expression at the RNA level, Gabra4 protein was not increased according to proteomics analysis. Thus, implying that RNA expression patterns of alpha sub-units may not accurately reflect the mechanism underlying seizure. Interestingly, proteomics analysis identified significant enrichment of genes that regulate proton transport, ion homeostasis, vesicle transport, and mitochondrial protein complexes. Collectively, our analysis validates that mutation of *gabra1* results in seizure like phenotypes and provides a blueprint of putative proteins which may mediate these phenotypes *in vivo*.

INTRODUCTION

The gamma-aminobutyric acid type A receptor ($GABA_AR$) is a multi-subunit ion channel that mediates inhibitory synapses of the nervous system. The $GABA_AR$ can be composed of unique combinations of any of the following: 6 α subunits, 3 β subunits, 3 γ subunits, and one ε, δ, θ, or π subunits. The most common $GABA_AR$ in mammals consists of 2 α subunits, 2 β subunits, and γ subunit. Each of the subunits is encoded by an independent gene, which are located on different chromosomes. Mutations in many of these subunits have been associated with seizure phenotypes in humans (98) and most recently we used whole exome sequencing to identify a putative heterozygous mutation in the *GABRA1* gene (c.875C>T) associated with seizure phenotypes (99). *GABRA1* encodes for the α1 subunit of the $GABA_AR$ and to date, over 30 different variants in the *GABRA1* gene have been reported and associated with neurological disorders and neurodevelopmental defects (13,15,16,19,66,99–103).

Because of its indicated role in neural development, several murine models have been developed to investigate the physiological and behavioral functions of *GABRA1* in mammals, however, the phenotypic outcomes are heterogeneous. For instance, deletion of *Gabra1* or the knock-in of the p.Ala332Asp allele cause behavioral phenotypes that range from tremors/absence-like seizures to development of myoclonic seizures at postnatal stages (5,35,36,104). Noteworthy, these phenotypes are generally strain, age, and sex specific, which makes interpretation of results difficult. Additional zebrafish models have been characterized including a germline mutant via CRISPR/Cas9 and a morpholino mediated transient knockdown. These two studies yielded contrasting results

whereas hypermotility was observed in a nonsense mutant of *gabra1* and hypomotility was observed after transient knockdown (99,105). Thus, additional complementary models are warranted.

In 2016, the zebrafish mutation project was completed by the Wellcome Sanger Institute, where over 40,000 mutant alleles, covering 60% of zebrafish protein-coding genes, were generated (106). However, only a small number of alleles have been characterized or associated with a specific phenotype. An allele carrying a nonsense mutation in the *gabra1* gene (sa43718) was generated and remains uncharacterized. We hypothesized that a more comprehensive analysis of this allele is necessary to discern the disparate phenotypes observed across other zebrafish approaches. We therefore performed behavioral and molecular analysis of the sa43718 allele.

Our results indicate that homozygous *gabra1*$^{sa43718/sa43718}$ larvae show hyperactive locomotion (seizure-like behavior) upon a light stimulus. These behavioral changes are associated with a moderate increase in the expression of *gabra4* transcript, but no change at the level of Gabra4 protein expression. However, differential expression of proteins identified via proteomics approaches revealed abnormal expression of proteins that regulate proton transport, sodium ion homeostasis across the plasma membrane, and the mitochondrial inner membrane protein complex and respiratory chain.

METHODS

Experimental model and animal husbandry

The *gabra1*$^{sa43718/+}$ allele (N=10 female fish) was obtained from Sanger Institute through the Zebrafish International Resource Center (ZIRC). Female carriers were outcrossed with wildtype (AB) males to generate independent families of heterozygous male and female carriers. For all experiments, zebrafish larvae were obtained by mating adult heterozygous *gabra1*$^{sa43718/+}$ fish. Collected zebrafish embryos were maintained in E3 media (5mM NaCl, 0.17mM KCl, 0.33mM CaCl, 0.33mM MgSO4, 0.05% methylene blue, pH 7.4) at 28°C under 14:10 light: dark cycle. All experimental procedures were performed at 5 days post fertilization (DPF). All animals were maintained and used in accordance with the guidelines from the University of Texas at El Paso Institutional Animal Care and Use Committee (Animal Protocol Number 811869-5). Euthanasia and anesthesia were performed according with the American Veterinary Medical Association (AVMA) guidelines for the euthanasia, 2020 edition.

Genotyping

Genotyping of the *gabra1*^{sa43718} allele was performed by PCR amplification and restriction enzyme digest. Adult fin clips and larval tails were lysed in lysis buffer (30ul) (50mM NaOH) for 5 minutes at 95°C followed by 10 minutes at 4°C. DNA was then neutralized by addition of 500mM Tris-HCL solution (6ul) and used directly for PCR. The fragment of interest (237bp) was amplified by standard PCR at an annealing temperature of 60°C (forward: TTGTGACTCAAAGCCACGAG and reverse: TGAGACGAGAACCATCGTCA). PCR amplicon containing the *sa43718* allele region, was digested with XhoI (NebBiolabs)

at 37°C according to manufacturer's guidelines. The mutation present in the *sa43718* inhibits cleavage by XhoI allowing differentiation of wildtype, heterozygous, and homozygous offspring.

Behavioral analysis and pentylenetetrazole (PTZ) treatment

Behavioral analysis was performed using the ZebraBox (ViewPoint Behavioral Technology, Montreal, Canada). Briefly, embryos were obtained from natural spawning and raised to 5 DPF. Larvae (5 DPF) were individually tracked for swim speed and total distance swam in a 96-well plate. The behavioral analysis consisted of 15 minutes divided into 5-minute intervals of dark/light/dark conditions. All larvae were acclimated to the chamber for 1 hour prior to data acquisition (99). Data was collected each minute, for a total of 15 minutes and total distance traveled (mm) and speed (mm/s) was calculated as previously described (99). Experiments were performed in biological duplicates using a minimum of N=30 larvae per trial. Treatment with 10mM pentylenetetrazole (PTZ) (Millipore-Sigma) was performed as previously described (99). Genotyping of each larva was performed after behavioral analysis.

Quantitative real time PCR (QPCR)

Total RNA was isolated from brain homogenates at 5 DPF from wildtype, heterozygous, and homozygous larvae with TRIzol reagent (Invitrogen) according to manufacturer's instructions. RNA was reverse transcribed using the Verso cDNA Synthesis Kit (ThermoFisher Scientific) and total RNA (500ng) was normalized across samples. Gene expression was measured in biological quadruplicates using a pool of at least N=5 larvae

per biological replicate. For each individual biological replicate, technical replicates were performed as internal controls. The Applied Biosystems StepOne Plus machine with Applied Biosystems associated software was used for quantitative PCR (qPCR) analysis. Sybr green (ThermoFisher Scientific) based primer pairs were designed for each gene analyzed: *gabra1* (FWD: AGAGCGTGTAACCGAAGTCA, REV: TCGGGAGTCCAGATTTTGCT), g*abra2a* (FWD: GATGGCTACGACAACAGGCT, REV: TGTCCATCGCTGTCGGAAAA), *gabra3* (FWD: GCTGAAGTTCGGGAGCTATG, REV: GGAGCTGATGGTCTCTTTGC), *gabra4* (FWD: GACTGCGATGTACCCCACTT, REV: ATCCAGGTCGGAGTCTGTTG), *gabra5* FWD: CATGACAACACCCAACAAGC, REV: CAGGGCCTTTTGTCCATTTA), *gabra6a* (FWD: TCGCGTACCCATCTTTCTTC, REV: CCCTGAGCTTTTCCAGAGTG), *gabra6b* (FWD: CGGAGGAGTGCTGAAGAAAC, REV: GGGAAAAGGATGCGTGAGTA), *gabrb2* (FWD: CCCGACACCTATTTCCTCAA, REV: TCTCGATCTCCAGTGTGCAG), *gabrg2* (FWD: ACACCCAATAGGATGCTTCG, REV: AGCTGCGCTTCCACTTGTAT). The *rpl13a* gene was used as a reference gene for $2^{\Delta\Delta ct}$ quantification. Statistical analysis performed using a *t-test* assuming equal variance. t-test was performed taking into consideration variances by means of the f-test.

Proteomic analysis

Protein isolation

For protein analysis, total protein was obtained from a pool of whole brain homogenates (n=9) per genotype. Two biological replicates per genotype were collected. Brains were excised and stored for protein isolation in 1X Cell Lysis Buffer (ThermoFisher Scientific) with protease inhibitors cocktail (ThermoFisher Scientific). DNA was isolated from the tail

tissue for genotyping and protein was isolated from brain homogenates using manual homogenization. Protein quantification was performed using Precision Red Protein Assay Reagent (Cytoskeleton) according to manufacturer's instructions. Samples were then sent to the Biomolecule Analysis and Omics Unit (BAOU) at The University of Texas El Paso for sample processing and proteomic analysis.

Sample preparation for proteomics

Proteins were removed from 1X Cell Lysis Buffer by trichloroacetic acid (TCA) protein precipitation. Fifty microliters of 100% TCA (Sigma/Millipore - cat# T6399-5G) was added to 200 µL of sample in 1x Cell Lysis Buffer (Safe Seal microcentrifuge tubes, Sorenson BioScience, cat. No. 12030) and incubated at 4°C for 10 minutes. Total protein ranged from 2 – 5 µg per sample. The precipitated proteins were pelleted by centrifugation for five minutes at 14,000 rcf and the supernatant was discarded. The protein pellet was subsequently washed a total of three times with 200 µL LCMS grade acetone by resuspension and pelleting, the acetone supernatant was discarded each time. Residual acetone was evaporated with a heating block at 95°C for 2 minutes. Samples were stored as a pellet at -80°C until processing for proteomic analysis. Stored pellets were resuspended in 8M Urea prior and subjected to enzymatic tryptic digestion using the PreOmics iST sample preparation kit (catalog no. iST 96x P.O.00027). Briefly, denaturation, alkylation, and reduction were performed with 10 µL LYSE buffer per 1 µg of protein and heated at 80 °C for 20 min while being mixed every 5-minutes. Remaining droplets on the cap were given a brief centrifugation (RT; 300 rcf; 10 sec) and samples were sonicated ten times at 30-second on/off intervals for a total of 5 minutes. Fifty

microliters of resuspended DIGEST solution were added to the samples for protein digestion. Sample-filled microtubes were gently vortexed, centrifuged and kept for 90 minutes at 37°C in a heating block. Throughout the 90-minute incubation period, samples were gently mixed every 10 minutes. One hundred microliters of STOP solution were added and mixed by pipetting ten times. Samples were then transferred to the cartridge and centrifuged for 1 minute at 3,800 rcf, followed by subsequent 200 µL washes with WASH 1 and WASH 2 solutions according to the manufacturer's instructions. Peptides were eluted in two cycles of 100 µL of ELUTE solution and dried completely in a vacuum evaporator (Savant; Thermo Fisher Scientific) for 90 minutes at 45 °C and 100-mTorr and stored at -80°C until LC-MS/MS acquisition.

Liquid chromatography–tandem mass spectrometry (LC-MS/MS)

Peptides were resuspended in LCMS grade 4% acetonitrile (ACN) with 0.1% formic acid (FA) at a concentration of 1µg/µL. Peptides were separated by a Dionex Ultimate 3000 UHPLC system (Thermo Scientific) tandem with a Q-Exactive Plus Hybrid Quadrupole-Orbitrap Mass Spectrometer (Thermo Scientific) with Xcalibur software (v. 3.0.63) for data acquisition in positive mode. Peptides were separated on a C18 Acclaim PepMap nanoLC column (75 µm x 50 cm nanoViper, PN 164942, Thermo Fisher Scientific) equilibrated with 4% solvent B (99.9% acetonitrile, 0.1% formic acid) and 96% solvent A (99.9% H2O, 0.1% formic acid) kept at 55°C throughout the entire acquisition. One microliter of peptides was loaded onto the column for 15-minutes at a flow rate of 0.5 µL/min and eluted with a multi-step gradient. The flow rate was reduced to 0.3µL/min over the course of 15 min, and solvent B was set to 20% over 100-minutes, then increased to 32% and

maintained for 20-minutes before increasing to 95% over 1-minute. The column was washed with 95% solvent B at a flow rate of 0.4 µL/min for 4-minutes to remove/clean any remaining peptides. The column was then re-equilibrated with 4% solvent B at 0.5µL/min until a 180-minutes total runtime. Blank injections were added after each biological duplicate, using a 60-minute two sawtooth gradient from 4-95% solvent B, and column re-equilibration at 4% solvent B. The mass spectrometer was set to top10 data-dependent acquisition (DDA), with a scan range of 375 to 1500 m/z and a full MS resolution of 70,000; AGC target 3e6. Ions were fragmented with NCE at 27 and collected with an AGC target of 1e5 at 17,500 resolution, 2 m/z isolation window, maximum IT of 60 ms. Charged exclusion ions were unassigned, 1, 6–8, and >8 charges.

Bioinformatics data analysis

After LC-MS/MS analysis, Proteome Discover (PD) 2.5.0.400 (Fisher Scientific) was utilized to identify the proteins from each peptide mixture. The database for Danio rerio was downloaded from UniProtKB; http://www.uniprot.org/ on 21 October 2021 with a database 61,623 sequences. A contaminant dataset was run in parallel composed of trypsin autolysis fragments, keratins, standards found in CRAPome repository and in-house contaminants. PD analysis parameters are as follows: false-discovery rate (FDR) of 1%, HCD MS/MS, fully tryptic peptides only, up to 2 missed cleavages, parent-ion mass of 10 ppm (monoisotopic); fragment mass tolerance of 0.6 Da (in Sequest) and 0.02 Da (in PD 2.1.1.21) (monoisotopic). Two-high confidence peptides per protein were applied for identifications. PD dataset was processed through Scaffold Q+S 5.0.1. Scaffold (Proteome Software, Inc., Portland, OR 97219, USA) was used to probabilistically

validate protein identifications derived from MS/MS sequencing results using the X!Tandem and Protein Prophet. Data was transferred to Scaffold LFQ (Proteome Software, Portland, Oregon, USA) which was used to validate and statistically compare protein identifications derived from MS/MS search results. A protein threshold of 95%, peptide threshold of 95%, and a minimum number of 2 peptides were used for protein validation. Normalized weighted spectral counts were used when comparing the samples. To ascertain p-values, Fisher's Exact was run with a control FDR level q * .05 with standard Benjamini-Hochberg correction.

RESULTS

Characterization of the sa43718 allele

The sa43718 allele results in a single base pair substitution in exon 6, which is predicted to result in a premature stop codon (Figure 3.1A). Exon 6 encodes part of the extracellular domain. We used Sanger sequencing to validate the single base pair substitution shown in figure 3.1B&B'. Based on the sequence change present in the sa43718 allele, we developed a restriction enzyme based genotyping strategy. The sa43718 allele abolishes an XhoI cleavage site and therefore cannot be cleaved by XhoI in a restriction digest. We performed PCR amplification using primers that flank the substituted nucleotide and used restriction digest to identify wildtype, heterozygous, and homozygous larvae. DNA from wildtype siblings was completely digested as predicted (Figure 3.1C, lane 2), while DNA from homozygous larvae was completely undigested and DNA from heterozygous carriers was partially digested (Figure 3.1C, lane 4 and 3, respectively).

Homozygous mutation in zebrafish *gabra1* has been associated with early lethality. Consequently, we performed a survival assay and monitored the survival for 22 DPF. We observed a 50% survival rate in wildtype and heterozygous siblings, but all homozygous carriers of the sa43718 allele died by 22 DPF (Figure 3.1D). The remaining heterozygous individuals survived into adulthood.

Expression of $GABA_A$ receptor subunits in the sa43718 allele.

Based on our previous studies, we hypothesized that the expression of other $GABA_AR$ receptor subunits were disrupted in the sa43718 allele. We first measured the expression of β2 and γ2 subunits, as these are present in the most common form of the $GABA_AR$ receptor, alongside α1. We validated that the sa43718 allele reduced the expression of *gabra1* (Figure 3.2A), but that decrease was not associated with decreased expression of β2 and γ2 transcripts (Figure 3.2A). We therefore hypothesized that these subunits were in complex with other α subunits to compensate for the loss of α1. We measured the expression of α2-6 (including 6a and 6b due to gene duplication). We observed a mild increase in *gabra4* (α4) gene expression, which was statistically significant (Figure 3.2B). However, we did not detect a significant difference in any other α subunit (Figure 3.2B).

Mutation of *gabra1* results in seizure-like behavior

We have previously reported hypoactivity at 5 DPF upon knockdown of *gabra1* (99). In contrast, seizure-like behavior at juvenile stages has been reported in a zebrafish model of *gabra1* loss of function (105). To begin to rectify these differences, we monitored

swimming behavior after a light stimulus, which has been shown to induce seizure like behavior in a previous allele of *gabra1* mutation. We measured baseline activity for a period of 5 minutes in the dark after a 1-hour acclimation period. During this time, we did not observe any differences in baseline swimming patterns according to total distance swam (mm) or swim speed (mm/s) in the sa43718 allele (Figure 3.3A&A'). However, after light stimulus, we detected a marked increase in swim speed in the sa43718 allele (Figure 3.3A&A'). Swim patterns were increased in mutant larvae during the entire light stimulus (Figure 3.3C&C'). Importantly, increased speed (velocity) was associated with rapid circling behavior, hyperactivity burst, and whirlpool behavior (Figure 3.3B) indicative of a seizure-like behavior as defined by the zebrafish behavioral glossary (107). Because we did not observe behavioral changes in heterozygous carriers in comparison to wildtype siblings, all data shown here is focused on homozygous carriers of the sa43718 allele.

Gabra1 sa43718 response to PTZ

We have previously demonstrated that reduced *gabra1* expression does not prohibit receptor responses to pentylenetetrazole (PTZ), a $GABA_AR$ antagonist (99). We also observed increased expression of *gabra4* and therefore, we sought to understand if the sa43718 allele would respond to PTZ, indicating the presence of a functional receptor. As shown in Fig 4A, treatment with PTZ induces increased swimming distance and speed in wildtype larvae. Within the first five minutes post treatment, in dark conditions, wildtype larvae exhibit an average 2-fold change in total distance swam and a 1.54-fold change in swim speed. However, the sa43718 allele had a slightly reduced response to PTZ in the dark accounting for a 1.7-fold change in total distance swam and a 1.2-fold change in

swim speed in dark conditions (minutes 1-5) (Figure 3.4C-D). We continued to monitor the speed and distance swam after light stimulus in PTZ treated larvae. After light stimulus, wildtype sibling larvae showed a 1.5-fold change in average swim speed and a 2.5-fold change in average total distance swam (Figure 3.4C-D). In contrast, the sa43718 allele exhibited a 1.4-fold change in average swim speed and 1.7-fold change in average distance swam in response to PTZ treatment (Figure 3.4C-D). The reduced response to PTZ treatment by the sa43718 allele was statistically significant in dark conditions for speed ($p=0.03$) and distance ($p=0.002$).

Proteomic analysis identifies differentially expressed proteins (DEPs) in the sa43718 allele.

A total of 3500 proteins were identified in the wildtype sibling brain homogenate, 3511 were identified in the heterozygous and 3552 were identified in the homozygous carriers of the sa43718 allele. There does not seem to be a drastic change in the number of proteins identified between the groups.

To begin to understand the underlying molecular mechanisms by which seizure phenotypes occurred, we performed proteomics analysis. We isolated protein from whole brain homogenates isolated from wildtype and homozygous larvae. We identified a total of 173 differentially expressed proteins, from which 81 were up-regulated and 93 down-regulated proteins in the sa43718 allele when compared to wildtype siblings. These DEPs are summarized in the volcano plot shown inf Figure 3.5A. A complete list of DEP can be found in S1 file (table S1). DEPs of interest include Synaptotagmin, Complexin 4a, Dynactin subunit 1, Dynamin GTPase, Secretogranin II, and a Vat1 homolog. Each of

these proteins has a function in synaptic fusion, transport, exocytosis, endocytosis, or direct interactions with small synaptic vesicles. Interestingly, we also noted a significant number of DEPs involved in microtubule growth, microtubule binding, vesicle recycling, retrograde transport along microtubules, or microtubule folding. These include microtubule associated protein, RP/EB family member 3b, Dynactin subunit 1, Dynamin GTPase, and Tubulin-specific chaperone A.

We further annotated DEPs by Biological Process (Figure 3.5B), Molecular Function (Figure 3.5C), and Cellular Process (Fig 5D). According to biological process, DEPs were clustered in Gene Ontology (GO) groups associated with proton transport including sodium and potassium export across the plasma membrane. Some examples of DEPs in this category include Slc82b, Atp1a1b, Atp1b3a, and Atp1a1a.3. All these DEPs are important for sodium and potassium homeostasis consistent with GO analysis. GO analysis by Molecular Function also indicated molecular carrier activity and active transport mechanisms, consistent with the GO analysis according to Biological Process. GO analysis by Cellular Process indicated DEPs in the respiratory chain, mitochondrial protein containing complexes, the cytoskeleton, proton transport, and exocytosis. These data collectively indicate mitochondrial transport, synaptic vesicle regulation, and proton homeostasis as dysregulated after mutation of *Gabra1*.

DISCUSSION

The $GABA_AR$ has previously been associated with seizure and epileptic phenotypes (98,102,104). In support of this notion, we reported a heterozygous missense mutation in humans that is associated with a seizure disease (99). Multiple model systems

have been developed to study early *GABRA1* function. These include mouse and zebrafish models. Survival of homozygous knockouts in mice and zebrafish is compromised (5,105). Due to external fertilization and early juvenile survival of homozygous mutants, zebrafish provide a window of opportunity to analyze developmental and juvenile onset of seizures (23,43,108–111). However, in previous studies germline nonsense mutation of zebrafish *gabra1* and morpholino mediated knockdown of *gabra1* demonstrated different behavioral phenotypes after a light stimulus (99,105). Here we characterized the phenotypes of a novel allele, known as the sa43718 allele. The sa43718 allele is a single base pair change in exon 6, which results in a premature stop codon and leads to a greater than 90% decrease in *gabra1* expression, indicating the possibility of nonsense mediated decay of the mutated transcript. The sa43718 allele reduces viability and homozygous mutants die by 22 DPF. This is consistent with the viability of other zebrafish (105) and mouse models (35).

We observed seizure like behavior upon light stimuli in the sa43718 allele. These data are supported by previously published works, which established seizure like behavior at the juvenile stage of another germline zebrafish mutant (105). Similar results have also been documented in mouse models of *Gabra1* mutation, although these are sex and strain specific (5,35,36). In our experiments, the zebrafish larvae have not yet determined sex and therefore, sex is not a variable considered in our experiments. Hyperactivity and seizure like behavior in the sa43718 allele contrasts with our previous study using morpholino mediated knockdown (99). There are several reasons for these differences. For example, we validated an approximate 50% knockdown of *gabra1* in morphants, which would most likely reflect a haploinsufficency or dosage effect. In

addition, *gabra1* morphants showed decreased expression of other $GABA_A$ receptor subunits. We did not observe statistically significant differences in other subunits, except for the *gabra4* subunit. However, this was only at the mRNA level, as proteomics did not reveal differences in the Gabra4 protein level in the sa43718 allele.

Given the normal expression of other $GABA_AR$ subunits, it is not surprising that sa43718 larvae responded to PTZ treatment. Mutant larvae were capable of a response to 10uM PTZ, which has been shown to induce seizures in zebrafish (55,112). These data are consistent with our previous work, which demonstrated that *gabra1* knockdown did not affect response to PTZ (99). Additionally, Samarut and colleagues demonstrated that the overall brain morphology of *gabra1* mutant brains was normal. Despite an overwhelming normal morphology, Samarut and colleagues did show 460 differentially expressed genes in *gabra1* mutant brains. Of these genes, 3 $GABA_AR$ subunits, in addition to *gabra1*, were down regulated (105). We observed increased expression of *gabra4* here and in a previous study we found *gabra6* to be up regulated after morpholino mediated knockdown (99). However, murine studies have suggested that changes in subunit expression across unique *Gabra1* mutants, backgrounds, and gender are not consistent (38,113). Our results are consistent with the former, that knockdown and mutation has independent effects on mRNA expression. We performed proteomics analysis to determine if these changes translate to actual changes in protein expression. We did not identify a single $GABA_AR$ subunit differentially expressed in the sa43718 allele at the protein level. These data are consistent with the ability of *gabra1* mutants to respond to PTZ, indicating the presence of a receptor, albeit with unknown subunit combinations.

Our proteomics analysis identified proteins with functions in synaptic vesicle transport, microtubule organization/growth, mitochondrial function, and regulation of potassium and sodium homeostasis as differentially expressed. A subset of these data are consistent with data from Samarut and colleagues, who noted decreased expression of kinesin motor proteins (105). However, our analysis is novel in that we identify changes in the expression of proteins rather than mRNA. As noted with $GABA_AR$ subunits, mRNA does not provide an accurate depiction of protein concentration. Thus, there are some differences from our protein data relative to previous results. For example, we did not identify statistically significant changes in neuroligins 2 and 4, nor other $GABA_A$ subunits. We cannot rule out differences in these proteins, however, at the present any differences were not statistically significant. Of note, we identified abnormal expression of synaptotagmin, secretogranin II, and synapsin IIb; all of which are important for synaptic vesicle release at the presynaptic membrane. Synapsin I was also downregulated and has been associated with epileptic phenotypes (114–117). Furthermore, we identified downregulation of proteins implicated in mitochondrial complex I deficiency, including NADH:ubiquinone oxidoreductase core subunit S2 and NADH:ubiquinone oxidoreductase core subunit A10. Remarkably, mutations in the genes encoding these proteins, *NDUFS2* and *NDUFA10* respectively, are associated with Leigh syndrome, one of the most common mitochondrial diseases, in which epilepsy is a primary phenotype (118,119). Interestingly, mutation of *GABRA1* in humans have been prematurely diagnosed as a primary mitochondrial disorder prior to exome sequencing (43). Moreover, none of the DEPs discovered led to an inability to respond to PTZ, a $GABA_AR$ agonist, suggesting that a residual receptor is present. Nonetheless, our proteomics data

implicates neurotransmitter release, vesicle transport, microtubule structure, proton homeostasis, and regulation of mitochondrial proteins as putative underlying mechanisms resulting in seizure-like phenotypes after mutation of *gabra1*.

Here we have characterized an additional germline mutant of the zebrafish *gabra1* gene. We observed early lethality, seizure-like hypermotility after light stimuli, and abnormal expression of proteins involved in vesicle transport, synaptic vesicle release, exocytosis, and endocytosis. Our data support the hypermotility and expression patterns previously described in a secondary zebrafish germline mutant (105). Collectively, these data suggest that models derived from germline mutation of *gabra1* rather than transient knockdown are more physiologically relevant to human disease.

ACKNOWLEDGEMENTS

The authors would like to thank the members of the Quintana Lab, past and present, for discussions, animal care, genotyping, and general laboratory maintenance. A special thank you to Pamela Rodriguez and Carla Canales for their efforts in the laboratory and their explicit help with genotyping embryos related to this manuscript. The work provided herein could not be completed without the support of The University of Texas El Paso core facilities and Border Biomedical Research Center (BBRC). We graciously thank Dr. Robert Kirken, Dr. Igor C. Almeida, and Dr. Renato Aguilera for their directorships of the BBRC and core facilities.

DATA AVAILABILITY

All data and reagents are available upon request from the corresponding author.

COMPETING INTERESTS

Authors declare no competing or financial interests.

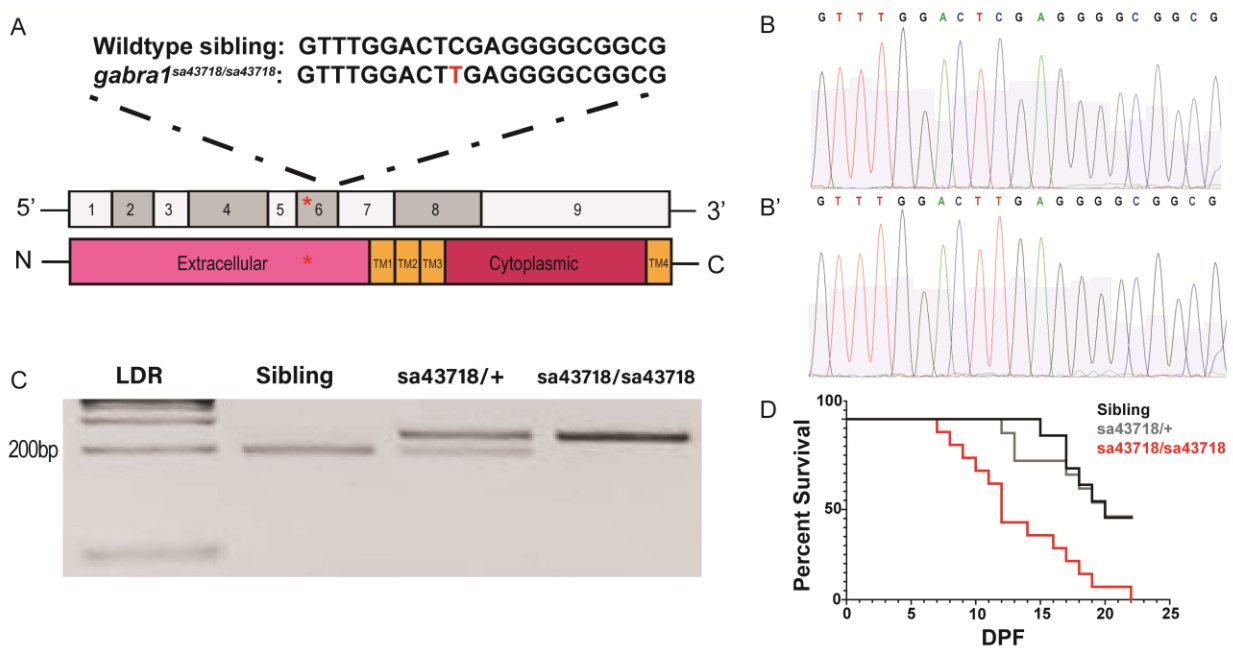

Figure 3.1. The sa43718 allele carries a single non-sense mutation in the *gabra1* gene.

(A) Schematic representation of the gabra1 sa43718 allele. Homozygous individuals of the sa43718 allele (gabra1sa43718/sa43718) carry a non-sense mutation (C>T) in the gabra1 gene (ENSDART0000010000), predicted to result in a premature stop. Schematic of exon structure of the gabra1 gene, not to scale. The sa43718 site is indicated with a red asterisk within exon 6, which encodes the extracellular domain of Gabra1. (B-B') Chromatograph showing confirmation of the sa43718 allele through Sanger sequencing of gabra1sa43718/+ offspring. (B) Wildtype sibling sequence. (B'): gabra1sa43718/sa43718 sequence. (C) Restriction enzyme digest gel showing digestion of PCR fragments of genomic gabra1. The sa43718 allele abolishes the XhoI recognition site. Therefore, digestion of homozygous (sa43718/sa43718) sample results in an uncut fragment, whereas digestion of wildtype (sibling) sample results in a fully digested fragment. LDR: 1kb plus ladder. (D) The offspring of gabra1sa43718/+ fish was genotyped by tail-clipping at 3 days post fertilization (DPF). Larvae were raised separately

according to their genotypes (sibling n=11, sa43718/+ n=13, sa43718/sa43718 n=14), and their survival was monitored until day 22. Premature death of homozygous carriers of the sa43718 allele (sa43718/sa43718) was observed starting at day 7 post fertilization, when compared to the wildtype (sibling) and heterozygous (sa43718/+) siblings.

A

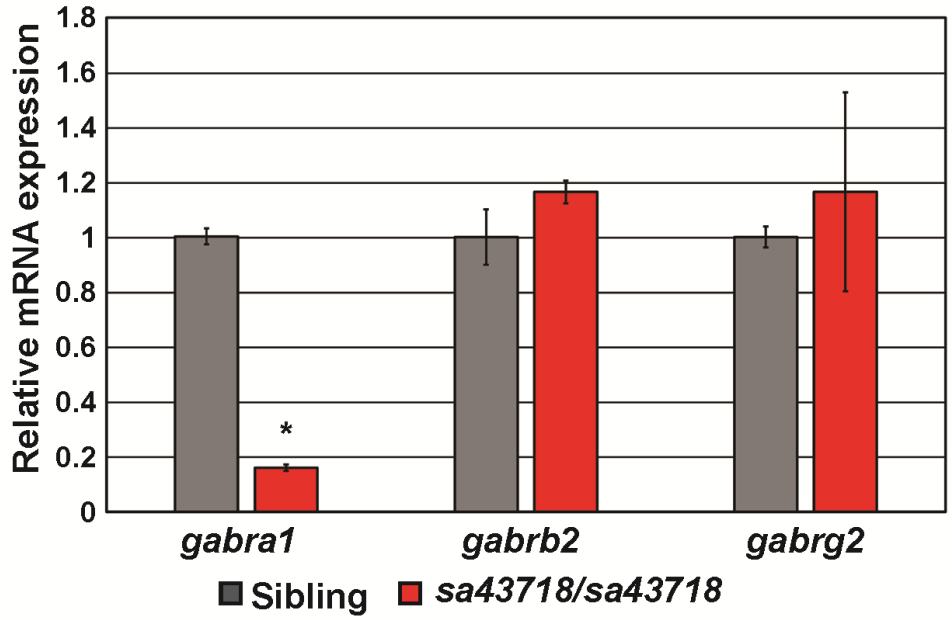
Relative mRNA expression
1.8
1.6
1.4
1.2
1
0.8
0.6
0.4
0.2
0
*
gabra1
gabrb2
gabrg2
Sibling
sa43718/sa43718

B

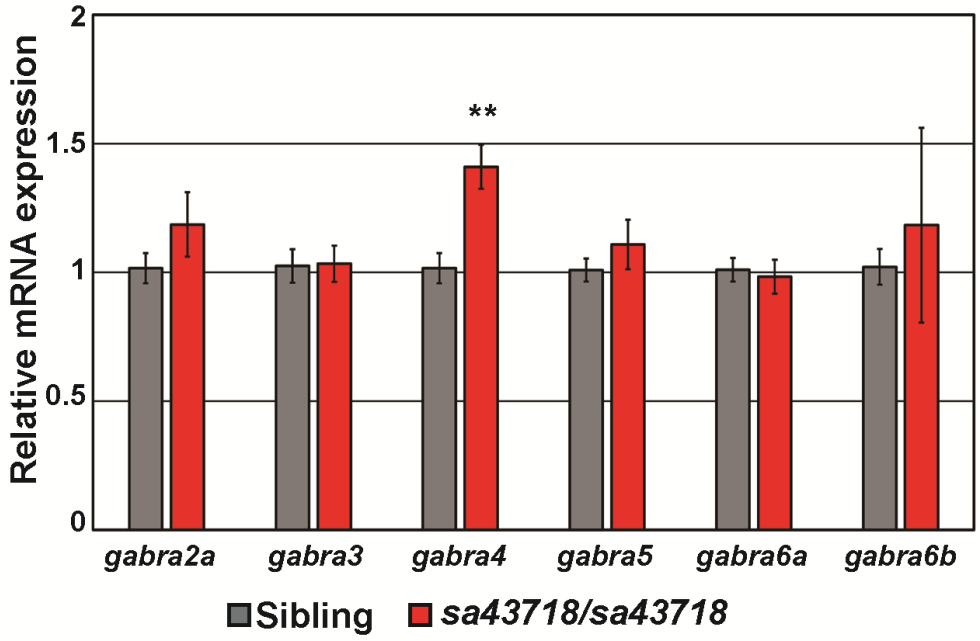
Relative mRNA expression
2
1.5
1
0.5
0
**
gabra2a
gabra3
gabra4
gabra5
gabra6a
gabra6b
Sibling
sa43718/sa43718

Figure 3.2. Non-sense mutation of *gabra1* results in decreased expression of *gabra1*. (A) Quantitative real time PCR (qPCR) analyzing the relative mRNA expression of major GABAAR subunits, α1 (gabra1), β2 (gabrb2) and, γ2 (gabrg2) at 5 days post fertilization (DPF). n≥5 larvae per group with five biological replicates. Error bars represent the standard error of the mean of biological replicates. *p=1.00511E-07. (B) Relative expression of genes encoding for alpha type subunits, gabra2a (α2), gabra3 (α3), gabra4 (α4), gabra5 (α5), gabra6a (α6a), and gabra6b (α6b), was analyzed in wildtype siblings (sibling) and homozygous (sa43718/sa43718) mutants. n≥5 larvae per group in four independent biological replicates. Error bars represent the standard error of the mean. **p=0.002884.

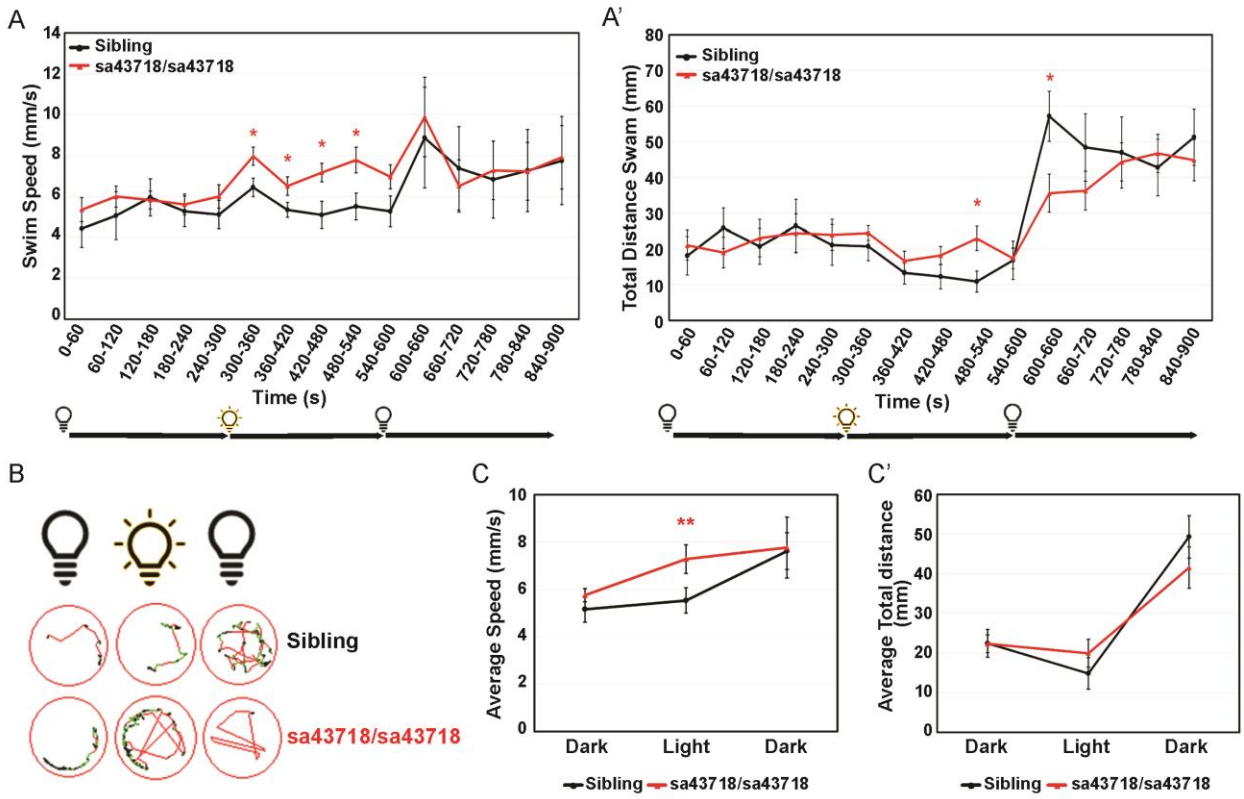

Figure 3.3. *gabra1*$^{sa43718/sa43718}$ larvae undergo seizure-like behavior upon light stimuli.

(A & A') Behavioral analysis of *sa43718* allele and wildtype siblings at 5 days post fertilization. (A) Swim speed (mm/s) over 15 minutes (900 seconds) in dark-light-dark transitions [5 minutes (0-300 seconds) in the dark, 5 minutes (300-600 seconds) in the light, and 5 minutes (600-900 seconds) in the dark) was analyzed using the Zebrabox technology. Data was collected every minute (60 seconds). *gabra1*$^{sa43718/sa43718}$ larvae undergo hyperlocomotion upon light stimuli when compared to their wildtype siblings (Sibling). *p<0.05. (A') Total distance swam over 15 minutes in dark-light-dark transitions. Homozygous carriers (*sa43718/sa43718*) larvae showed increased distance swam across the light phase, showing a statistically significant increase at seconds 480-540

(minute 9), when compared to their wildtype counterparts (sibling). *gabra1*$^{sa43718/sa43718}$ larvae then show decreased distance swam under dark conditions (600-660s) when compared to their wildtype siblings (sibling) *p<0.05. (B) Representative images of swimming track of a single larvae, representing each genotype, generated from the Viewpoint Zebralab Tracking software in dark (180-240s), light (480-540s), and dark (600-660s) conditions. Green lines indicate movements between 4-8mm/s and red lines indicate burst movements (>8mm/s). (C) Average total speed representing overall behavioral responses in dark-light-dark conditions of *gabra1* wildtype (sibling) and homozygous (sa43718/sa43718) larvae. Homozygous carriers (sa43718/sa43718) showed increased average swim speed in light conditions when compared to their wildtype (sibling) counterparts. (C') Average total distance swam representing overall behavioral responses in dark-light-dark conditions of *gabra1* wildtype (sibling) and homozygous (sa43718/sa43718) larvae. No statistically significant changes were observed in homozygous larvae (sa43718/sa43718) when compared to their wildtype siblings for average distance measurements. All behavioral analysis was performed using a minimum of 30 larvae per biological replicate, over three independent biological replicates. Representative analysis of a single biological replicate is shown here. Sibling (n=13) and *gabra1*$^{sa43718/sa43718}$ (n=26).

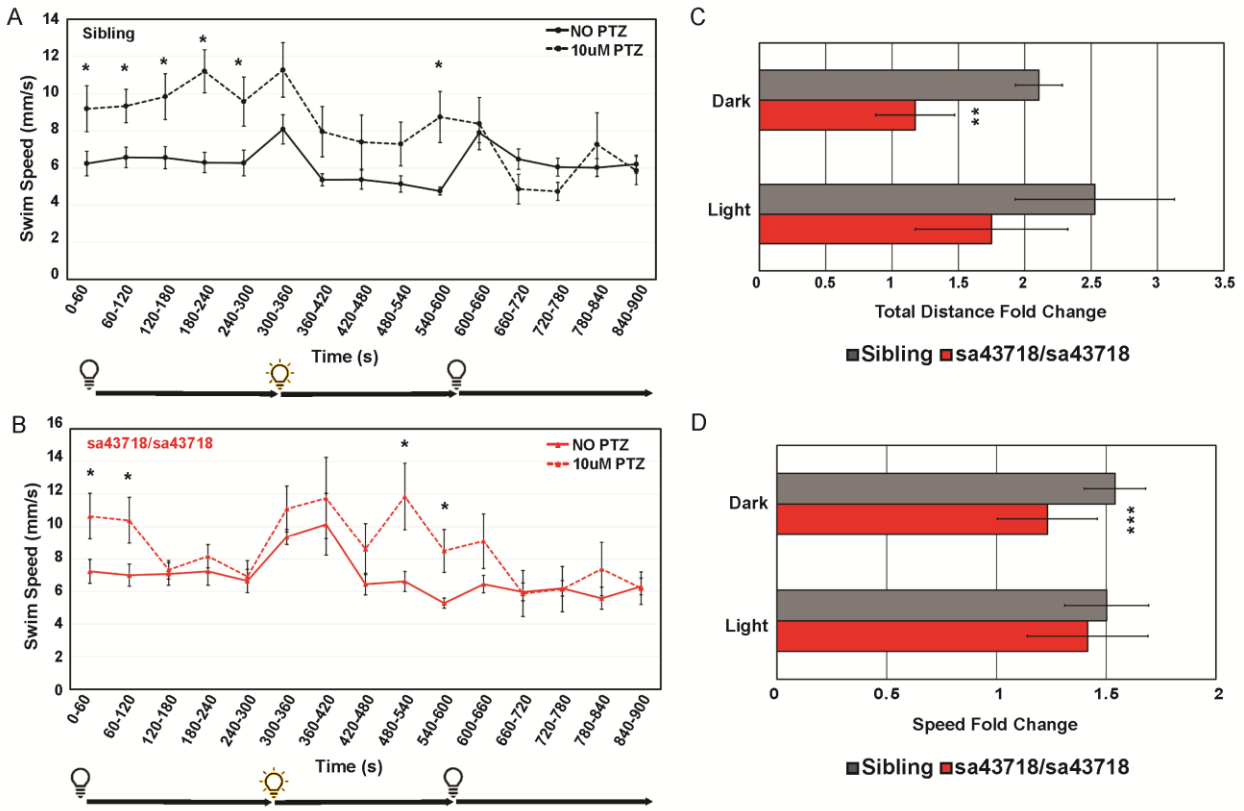

Figure 3.4. Locomotion response to pentylenetetrazole (PTZ) in the sa43718 allele.

(A-B). Behavioral responses of the sa43718 allele at 5 days post fertilization (DPF) were analyzed using the Zebrabox. (A) Comparison of wildtype sibling (Sibling) larvae response to treatment with 10uM PTZ (10uM PTZ) or no treatment (NO PTZ) at 5 days post fertilization. NO PTZ n=18, 10uM PTZ n=16. *p<0.05 (B) Comparison of homozygous carriers (sa43718/sa43718) response to treatment with 10uM PTZ (10uM PTZ) or no treatment (NO PTZ) at 5 days post fertilization. NO PTZ n=13, 10uM PTZ n=14. *p<0.05. Swim speed (mm/s) was analyzed using the distance swam and swimming duration data generated by ViewPoint software. The larvae were monitored for 5 minutes in the dark (0-300 s), 5 minutes in the light (300-600 s), and 5 minutes in the dark (600-900 s). Data was collected every minute (60 s). Error bars represent the standard error of the mean.

(C) Average fold change (total distance) response to treatment with PTZ in dark (0-300s) and light (300-600s) conditions by wildtype (sibling) and sa43718/sa43718 mutants. **p=0.002. (D) Average fold change (swim speed) response to treatment with PTZ in dark (0-300s) and light (300-600s) conditions by wildtype (sibling) and sa43718/sa43718 mutants. ***p=0.03. Error bars represent standard deviation in C-D.

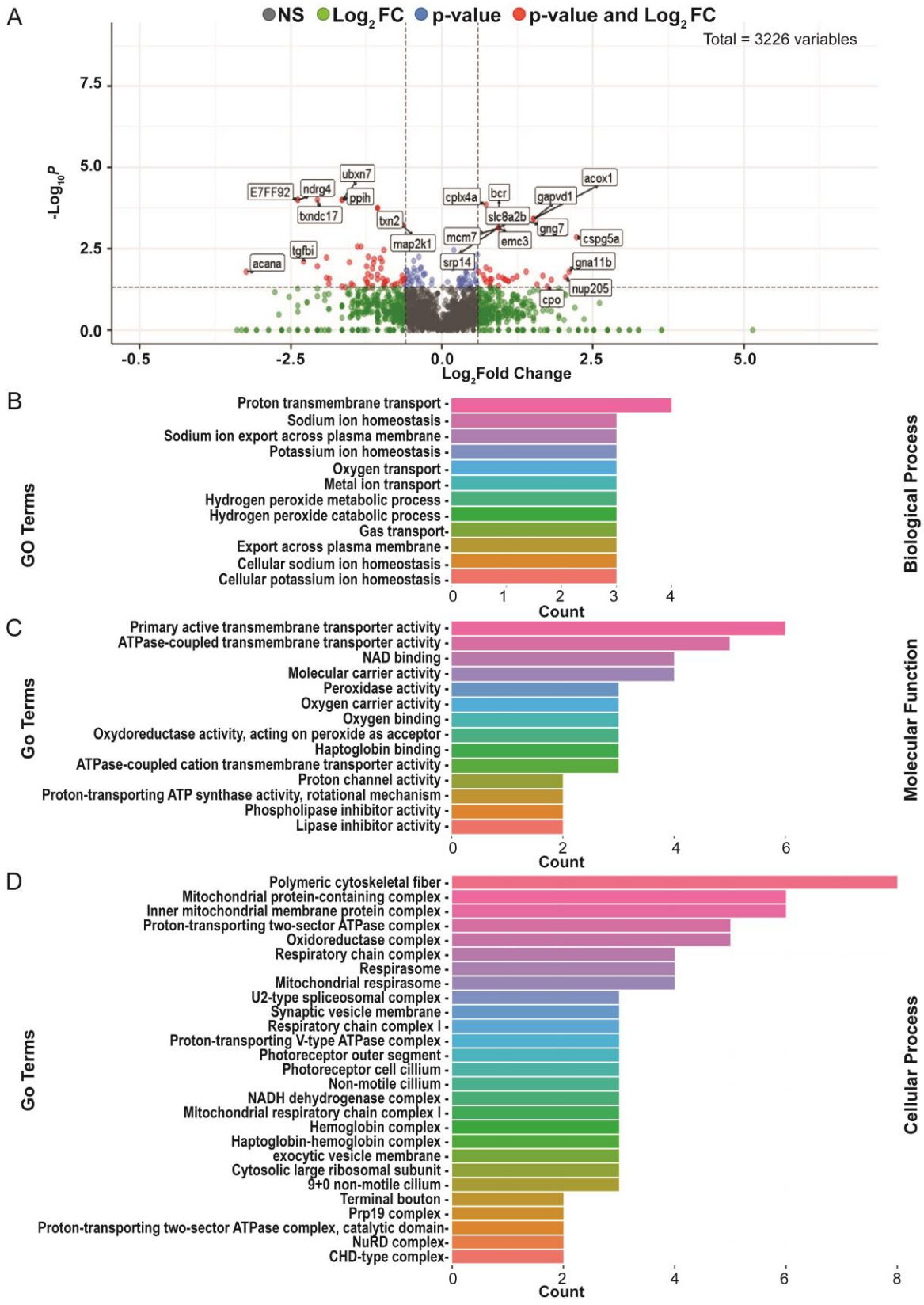
A
NS
Log2 FC
p-value
p-value and Log2 FC
Total = 3226 variables
-Log10P
Log2Fold Change
ubxn7
E7FF92
ndrg4
ppih
txndc17
txn2
map2k1
tgfbi
acana
cplx4a
bcr
acox1
gapvd1
slc8a2b
gng7
cspg5a
mcm7
emc3
srp14
gna11b
nup205
cpo
B
GO Terms
Proton transmembrane transport
Sodium ion homeostasis
Sodium ion export across plasma membrane
Potassium ion homeostasis
Oxygen transport
Metal ion transport
Hydrogen peroxide metabolic process
Hydrogen peroxide catabolic process
Gas transport
Export across plasma membrane
Cellular sodium ion homeostasis
Cellular potassium ion homeostasis
Count
Biological Process
C
Go Terms
Primary active transmembrane transporter activity
ATPase-coupled transmembrane transporter activity
NAD binding
Molecular carrier activity
Peroxidase activity
Oxygen carrier activity
Oxygen binding
Oxydoreductase activity, acting on peroxide as acceptor
Haptoglobin binding
ATPase-coupled cation transmembrane transporter activity
Proton channel activity
Proton-transporting ATP synthase activity, rotational mechanism
Phospholipase inhibitor activity
Lipase inhibitor activity
Count
Molecular Function
D
Go Terms
Polymeric cytoskeletal fiber
Mitochondrial protein-containing complex
Inner mitochondrial membrane protein complex
Proton-transporting two-sector ATPase complex
Oxidoreductase complex
Respiratory chain complex
Respirasome
Mitochondrial respirasome
U2-type spliceosomal complex
Synaptic vesicle membrane
Respiratory chain complex I
Proton-transporting V-type ATPase complex
Photoreceptor outer segment
Photoreceptor cell cillium
Non-motile cillium
NADH dehydrogenase complex
Mitochondrial respiratory chain complex I
Hemoglobin complex
Haptoglobin-hemoglobin complex
exocytic vesicle membrane
Cytosolic large ribosomal subunit
9+0 non-motile cilium
Terminal bouton
Prp19 complex
Proton-transporting two-sector ATPase complex, catalytic domain
NuRD complex
CHD-type complex
Count
Cellular Process

Figure 3.5. Proteomic analysis of sa43718 allele carriers.

(A) Volcano plot of differentially expressed proteins between wildtype siblings and homozygous (sa43718/sa43718) larvae. Volcano plot of –log10 P-values from the normalized proteomics data exported from Scaffold LFQ versus log2foldchange (FC) across each contrast. Thresholds were set at p-value ≤ 0.05 and Log2FC ≤ -1.5 or ≥ 1.5. (B-D) Gene Ontology terms enriched by proteins with significant expression (p-value <0.05) between wildtype sibling and sa43718 homozygous mutant larvae at 5 days post fertilization. Terms are separated by (B) Biological Process, (C) Molecular Function, (D) Cellular Process.

SUPPLEMENTAL MATERIAL

Table S3.1. Table of differentially expressed proteins in the *gabra1*^{sa43718} allele.

Protein Name	Accession Number	Gene Name	MW	Exclusivity	t-test CL: Group BRL: Scaffold BioSample	MT	WT
Group of Aggrecan	F1QDA1	acana	-	100%	0.016	1.94	18.29
Group of Acyl-coenzyme A oxidase	F1R3V9	acox1	-	100%	0.00039	5.83	2.03
Actinodin2	A9JRX1	and2	57 kDa	100%	0.0066	23.33	50.79
Group of Annexin	Q804H2	anxa1a	-	100%	0.023	34.99	18.29
Annexin	Q804G9	anxa2a	38 kDa	100%	0.039	57.35	45.71
Apolipoprotein D	Q0D290	apoda.1	21 kDa	100%	0.032	8.75	4.06
Apolipoprotein Eb (Fragment)	A4VAJ8	apoeb	18 kDa	56%	0.023	61.24	25.90
ADP-ribosylation factor 2	Q7ZUA0	arf2a	21 kDa	62%	0.027	27.70	42.07
Group of Arhgdia protein	Q802W6	arhgdia	-	100%	0.00018	1.94	4.06
Group of Arhgef7b protein	Q5PRA8	arhgef7b	-	100%	0.00018	1.94	4.06
Group of Aryl hydrocarbon receptor nuclear translocator 2	A0A0R4ILG9	arnt2	-	100%	0.00018	1.94	4.06
cAMP-regulated phosphoprotein 19b	Q7ZUT5	arpp19b	12 kDa	83%	0.032	4.37	2.03
Sodium/potassium-transporting ATPase subunit alpha	Q9DEY3	atp1a1a.3	113 kDa	22%	0.045	25.12	20.57
Group of Sodium/potassium-transporting ATPase subunit alpha	B0R068	atp1a1b	-	55%	0.0034	186.04	162.02
Sodium/potassium-transporting ATPase subunit alpha	Q6P271	atp1a3a	113 kDa	50%	0.029	195.48	218.02

Sodium/potassium-transporting ATPase subunit beta	Q8QHI1	atp1b3a	32 kDa	100%	0.025	4.86	18.29
ATP synthase F1 subunit delta	Q6P1J5	atp5f1d	17 kDa	75%	0.035	11.66	17.27
ATP synthase membrane subunit DAPIT	H0WES8	atp5md	6 kDa	100%	0.012	38.88	29.46
H(+)-transporting two-sector ATPase	E7FCD8	atp6v1ab	68 kDa	61%	0.019	36.45	52.82
V-type proton ATPase subunit D	Q7ZVX8	atp6v1d	28 kDa	100%	0.015	20.41	30.47
V-type proton ATPase subunit G	Q6PBR5	atp6v1g1	13 kDa	64%	0.029	49.09	38.60
Group of BCR activator of RhoGEF and GTPase	A0A2R8Q802	bcr		100%	0.00073	3.89	2.03
Group of Ca2+-dependent activator protein for secretion b	F1RCD5	cadpsb		100%	0.03	39.85	56.89
Calretinin	Q6PC56	calb2b	31 kDa	86%	0.0027	23.81	62.64
Calcium/calmodulin-dependent protein kinase	Q4V9P8	camk2g1	63 kDa	70%	0.016	24.95	34.17
F-actin-capping protein subunit alpha	Q6NWK1	capza1a	33 kDa	87%	0.032	14.90	23.70
T-complex protein 1 subunit delta	Q6P123	cct4	57 kDa	100%	0.025	146.77	113.77
CCT-epsilon	Q6NVI6	cct5	59 kDa	100%	0.0058	125.39	115.80
Creatine kinase	Q90X19	ckma	43 kDa	82%	0.0049	242.60	161.13
Calmegin	Q08BY9	clgn	72 kDa	100%	0.047	6.80	13.21
Clathrin light chain	Q6P937	clta	26 kDa	61%	0.029	34.99	54.85
Calponin	Q7T303	cnn3a	37 kDa	88%	0.00018	1.94	4.06
Collagen, type I, alpha 3	Q6PEI9	col1a1b	137 kDa	57%	0.049	4.37	13.21
Group of Col2a1a protein	B3DLK0	col2a1a		93%	0.026	13.61	26.75
Collagen, type VI, alpha 4a (Fragment)	F1Q924	col6a4a	278 kDa	100%	0.038	1.94	7.11

Group of Cytochrome c oxidase subunit	A9C462	cox6a1		100%	0.028	95.26	53.84
Complexin 4a	**Q08BK6**	**cplx4a**	**18 kDa**	**100%**	**0.00014**	**57.35**	**34.54**
Carboxypeptidase O	B8JLQ9	cpo	41 kDa	100%	0.046	6.80	2.03
Crystallin, beta B1,-like 2	A7E2K5	crybb1l2	26 kDa	85%	0.039	66.10	86.34
Chondroitin sulfate proteoglycan 5a	A0A2R8RMD7	cspg5a	54 kDa	100%	0.0014	57.35	12.19
Ribeye b protein	Q5BU17	ctbp2l	93 kDa	34%	0.026	1.10	4.01
Aspartate--tRNA ligase, cytoplasmic	F1R246	dars1	61 kDa	100%	0.03	49.57	38.60
Dynactin subunit 1	F6PC33	dctn1b	141 kDa	83%	0.0027	5.83	14.73
Group of D-dopachrome tautomerase	F1QJV7	ddt	-	100%	0.047	2.92	9.14
Group of Dihydrolipoyllysine-residue succinyltransferase component of 2-oxoglutarate dehydrogenase complex, mitochondrial	F1QFQ6	dlst	-	100%	0.025	34.02	27.43
Dynamin GTPase OS=Danio rerio	**E9QF63**	**dnm1b**	**95 kDa**	**59%**	**0.012**	**49.65**	**62.73**
Dynamin GTPase	Q5RHR9	dnm3a	93 kDa	75%	0.02	3.65	7.62
Group of Dynein light chain (Fragment)	Q1RM30	dynll2a		85%	0.044	31.69	18.29
Novel alpha-globin	Q7SZV8	dZ118J2.6-001	16 kDa	34%	0.014	61.72	35.55
Synaptotagmin	**E7FF92**	**Syt1**	**29 kDa**	**88%**	**0.0001**	**1.94**	**10.16**
ER membrane protein complex subunit 3	Q7SXW4	emc3	30 kDa	100%	0.00073	3.89	2.03
Zgc:194578	B3DIW6	epn1b	54 kDa	100%	0.013	27.22	37.59
Enhancer of rudimentary homolog	Q98874	erh	12 kDa	100%	0.0055	28.19	36.57

Group of EWS RNA-binding protein 1a	A0A0B4J1A5	ewsr1a		100%	0.023	20.41	28.44
Phenylalanyl-tRNA synthetase beta subunit OS=Danio rerio	F1Q820	farsb	66 kDa	100%	0.023	6.80	15.24
Fascin	F1QET7	fscn1a	55 kDa	100%	0.0081	16.52	47.74
Group of GTPase-activating protein and VPS9 domains 1	A0A2R8Q516	gapvd1		100%	0.00039	5.83	2.03
Group of H/ACA ribonucleoprotein complex subunit 1	Q7ZVE0	gar1		100%	0.045	7.78	17.27
GATA zinc finger domain-containing 2Ab	A0A0R4IN87	gatad2ab	82 kDa	75%	0.0063	4.86	4.06
Group of Glyoxylate reductase 1 homolog	A0A0R4IMF9	glyr1		100%	0.0019	7.78	10.16
Glia maturation factor	Q7ZUD3	gmfb	17 kDa	100%	0.045	17.50	26.41
Guanine nucleotide-binding protein (G protein), alpha 11b (Gq class)	Q5RKP9	gna11b	42 kDa	100%	0.016	8.75	2.03
Guanine nucleotide-binding protein subunit gamma	Q6DGZ5	gng7	8 kDa	100%	0.00043	21.38	8.13
Glycerol-3-phosphate dehydrogenase 1-like protein	Q5XIZ6	gpd1l	38 kDa	100%	0.049	31.10	24.38
Glycoprotein M6Ab OS=Danio rerio	Q6DI17	gpm6ab	32 kDa	75%	0.041	43.74	62.98
Group of Glutathione transferase	B8JIS8	gstm.1		93%	0.027	31.10	18.96
Group of Embryonic alpha globin e1	Q7ZT21	hbae1.1		78%	0.021	179.34	111.74
Embryonic globin beta e2	Q7T1B0	hbbe2	17 kDa	94%	0.044	58.32	30.47
Hemoglobin beta embryonic-3	Q5BLF6	hbbe3	17 kDa	56%	0.047	24.79	14.22

Heterogeneous nuclear ribonucleoprotein A0,-like	Q7ZU48	hnrnpa0l	32 kDa	100%	0.016	53.46	40.63
78 kDa glucose-regulated protein	Q6P3L3	hspa5	72 kDa	95%	0.046	336.61	240.80
Keratin 17	Q1LXJ1	krt17	46 kDa	47%	0.034	102.81	62.11
Group of Keratin 4	F1QK60	krt4		76%	0.021	792.68	550.23
Group of Lamp2 protein	A4QP49	lamp2		100%	0.00018	1.94	4.06
Galectin	Q7SXJ0	lgals2b	13 kDa	62%	0.028	4.86	11.68
LOC795505 protein (Fragment)	A3KPA2	LOC795505	23 kDa	100%	0.00073	3.89	2.03
Low density lipoprotein receptor-related protein-associated protein 1	A0A2R8QMD9	lrpap1	41 kDa	54%	0.036	35.48	28.44
Lysophospholipase 2	Q6PBW8	lypla2	25 kDa	100%	0.044	12.64	22.35
Map2k1 protein	Q7ZTX6	map2k1	36 kDa	100%	0.00059	3.89	6.10
Microtubule-associated protein, RP/EB family,	Q6GMJ3	mapre3b	30 kDa	53%	0.0012	8.31	12.52
DNA replication licensing factor MCM7	Q7ZVL6	mcm7	81 kDa	100%	0.00073	3.89	2.03
Group of Metastasis-associated 1 family, member 2	F1QLG2	mta2		100%	0.028	29.16	14.22
Mitochondrial carrier homolog 2	Q9PUL9	mtch2	33 kDa	100%	0.0018	5.83	4.06
Myosin, light chain 6, alkali, smooth muscle and non-muscle	E9QB41	myl6	17 kDa	80%	0.028	46.41	67.81
Ndel1b protein OS=Danio rerio	B2GRS6	ndel1b	38 kDa	100%	0.00018	1.94	4.06
Group of N-myc downstream regulated gene 4	Q1JPS5	ndrg4		100%	0.0001	1.94	10.16

NADH dehydrogenase [ubiquinone] 1 alpha subcomplex subunit 10, mitochondrial	**Q6IQS0**	**ndufa10**	**40 kDa**	**100%**	**0.021**	**53.46**	**66.03**
Group of Acyl carrier protein	F1R611	ndufab1a		100%	0.0021	31.10	22.35
Group of Complex I-SGDH	A8E5B7	ndufb5		100%	0.012	25.27	15.24
Complex I-B22	Q567Y4	ndufb9	21 kDa	62%	0.024	13.12	17.27
Complex I-49kD	**F1Q4N4**	**ndufs2**	**53 kDa**	**100%**	**0.0078**	**19.44**	**38.60**
Neurofilament, light polypeptide a (Fragment)	E9QFD5	nefla	69 kDa	38%	0.043	5.49	15.20
NOP56	Q6DRE5	nop56	61 kDa	62%	0.015	9.23	12.19
NOVA alternative-splicing regulator 1	Q1LYC7	nova1	51 kDa	57%	0.019	43.42	53.50
sp|Q7T3C6|CPSF5_DANRE Cleavage and polyadenylation specificity factor subunit 5	Q7T3C6	nudt21		100%	0.032	5.83	11.17
Group of C7orf14-like	Q6DRN9	nup205		100%	0.024	12.64	3.05
sp|Q9W6A5|OPSG1_DANRE Green-sensitive opsin-1	Q9W6A5	opn1mw1		100%	0.039	22.36	34.54
Group of Opsin 1 (Cone pigments), short-wave-sensitive 2	A8E5J4	opn1sw2		100%	0.00018	1.94	4.06
Ubiquitinyl hydrolase 1	Q6DGP0	otub1b	29 kDa	100%	0.037	3.89	9.14
Protein disulfide-isomerase	A0A0R4IPV5	p4hb	57 kDa	100%	0.039	117.61	132.06
Piccolo presynaptic cytomatrix protein a	A0A2R8QC86	pcloa	521 kDa	98%	0.026	34.51	15.24
Group of Programmed cell death protein 4	F1QBM2	pdcd4a		100%	0.016	10.69	4.06
Phosphodiesterase	Q6P4P8	pde6c	98 kDa	100%	0.038	97.20	162.53

D-3-phosphoglycerate dehydrogenase	F1QEY8	phgdh	56 kDa	61%	0.0034	10.69	20.82
Phosphatidylinositol-5-phosphate 4-kinase, type II, alpha b OS=Danio rerio OX=7955 GN=pip4k2ab PE=1 SV=1	B0UXW0	pip4k2ab	47 kDa	60%	0.0087	4.86	10.67
Group of Peptidyl-prolyl cis-trans isomerase	F6NLI6	ppib		100%	0.02	170.10	126.98
Peptidyl-prolyl cis-trans isomerase	Q6IQF8	ppih	24 kDa	100%	0.0001	1.94	6.10
Serine/threonine protein phosphatase 2A regulatory subunit	Q8AXX6	ppp2r5ea	55 kDa	83%	0.041	9.07	3.05
Pre-mRNA-processing factor 19	Q7ZV92	prpf19	55 kDa	100%	0.048	65.13	48.76
Peripherin 2a (retinal degeneration, slow)	Q66HW7	prph2a	39 kDa	100%	0.034	3.89	9.14
Prothymosin alpha-B	A5PLC8	ptmab	12 kDa	100%	0.016	26.24	17.27
Parvalbumin 1	Q804W0	pvalb1	11 kDa	94%	0.028	170.59	98.03
Parvalbumin 4	Q6IMW7	pvalb4	12 kDa	100%	0.038	52.49	37.59
Parvalbumin 6	Q804W1	pvalb6	12 kDa	100%	0.013	23.33	46.73
RAB5C, member RAS oncogene family	Q7ZVP2	rab5c	24 kDa	54%	0.0074	6.48	8.97
60S ribosomal protein L10 (Fragment)	E9QIR9	rpl10	18 kDa	57%	0.039	4.86	13.71
60S ribosomal protein L13a	Q1LYB7	rpl13a	24 kDa	100%	0.025	96.23	47.74
Ribosomal protein L15	Q6DHS3	rpl15	24 kDa	100%	0.013	22.36	28.44
60S ribosomal protein L31	Q24JV3	rpl31	14 kDa	100%	0.015	43.74	29.46
Ribosomal protein L4	Q7ZW95	rpl4	43 kDa	100%	0.049	112.75	81.27
Ribosomal protein L5b	A0A286YAR2	rpl5b	33 kDa	78%	0.03	47.63	39.11

40S ribosomal protein S18	A3KQW5	rps18	18 kDa	100%	0.019	92.34	111.74
Group of 40S ribosomal protein S27a (Fragment)	Q7ZU62	rps27a		100%	0.026	143.86	219.42
40S ribosomal protein S28	X1WC82	rps28	6 kDa	100%	0.036	89.43	59.93
Metastasin	Q6DGT8	s100b	11 kDa	100%	0.028	4.86	10.16
Secretogranin II	**A0JMK6**	**scg2b**	**66 kDa**	**100%**	**0.013**	**23.33**	**51.81**
Group of Selenoprotein W	F6NSR1	selenow1	-	83%	0.04	4.54	7.79
Group of Selenide, water dikinase 1	Q7ZW38	sephs1	-	100%	0.032	10.69	6.10
Septin	A0A0G2KQA6	sept4b	49 kDa	83%	0.00018	0.97	2.03
Group of Serine (Or cysteine) proteinase inhibitor, clade A (Alpha-1 antiproteinase, antitrypsin), member 1, like	Q24JW6	serpina1l	-	59%	0.019	14.58	34.03
Splicing factor 3b, subunit 2	A7YT51	sf3b2	94 kDa	100%	0.0098	61.24	41.65
Si:ch211-105c13.3	E7FAE7	si:ch211-105c13.3	10 kDa	100%	0.029	12.64	6.10
Si:ch211-278a6.1	F1QL76	si:ch211-278a6.1	127 kDa	100%	0.026	17.50	23.36
Si:ch73-1a9.3	A0A0R4IBX9	si:ch73-1a9.3	10 kDa	100%	0.0049	176.91	144.25
Group of Si:ch73-368j24.11	A0A140LFZ1	si:ch73-368j24.11	-	61%	0.0091	46.38	37.22
Group of Solute carrier family 38 member 3a	A5PLD2	slc38a3a	-	100%	0.048	4.86	11.17
Group of Sodium/calcium exchanger 2 isoform b	B2CZC4	slc8a2b	-	100%	0.00073	3.89	2.03
Synuclein, gamma b (breast cancer-specific protein 1)	A0A2R8RP85	sncgb	11 kDa	100%	0.013	25.27	22.35
Small nuclear ribonucleoprotein E	A0A140LFZ7	snrpe	6 kDa	100%	0.0018	5.83	4.06
SLIT-ROBO Rho GTPase-activating protein 3	A0A0R4IAE2	srgap3	124 kDa	100%	0.022	9.72	3.05

Group of Sorcin OS=Danio rerio	F1R4I7	sri		100%	0.011	25.27	59.93
Signal recognition particle 14 kDa protein	Q4V9I5	srp14	12 kDa	100%	0.00073	3.89	2.03
Sjogren syndrome antigen B (Autoantigen La)	Q7ZTI0	ssb	46 kDa	100%	0.027	81.65	67.04
Zgc:110200	Q568N1	stoml3b	31 kDa	67%	0.0015	10.69	7.11
Small ubiquitin-related modifier 1	Q7SZR5	sumo1	11 kDa	100%	0.027	25.27	19.30
Synapsin I	**B0UXI4**	**syn1**	**72 kDa**	**100%**	**0.0055**	**8.75**	**20.32**
Synapsin IIb	**A0A0R4IJU5**	**syn2b**	**75 kDa**	**57%**	**0.041**	**12.15**	**15.24**
Tubulin-specific chaperone A	Q7ZV25	tbca	13 kDa	100%	0.032	28.19	19.30
Group of Serotransferrin	B8JL43	tfa	-	100%	0.05	132.19	130.02
Group of Transforming growth factor-beta-induced protein ig-h3	Q503K1	tgfbi	-	100%	0.0079	2.92	14.22
Group of Fast muscle troponin I	Q0D2W2	tnni2a.4	-	78%	0.0072	94.24	67.60
Troponin I type 2b (skeletal, fast), tandem duplicate 2	Q6DHP2	tnni2b.2	20 kDa	83%	0.031	112.27	81.60
Group of Target of myb1-like 2 membrane-trafficking protein	R4GEE3	tom1l2	-	93%	0.011	2.59	10.84
Uncharacterized protein	E7FC90	tom1l2	56 kDa	83%	0.04	2.27	4.40
Tropomyosin 4-2alpha	A0A1L6UW65	tpm4b	33 kDa	48%	0.033	72.88	102.71
Tropomyosin alpha-1 chain (Fragment)	A0A1D5NSG1	tpma	15 kDa	27%	0.022	47.61	75.12
Thioredoxin 2	Q6P131	txn2	18 kDa	100%	0.00059	3.89	6.10
sp|Q6DBT3|TXD17_DANRE Thioredoxin domain-containing protein 17	Q6DBT3	txndc17	-	100%	0.0001	1.94	8.13
Zgc:123326	Q3B7F0	ube2v1	17 kDa	75%	0.0059	2.43	9.14

UBX domain-containing protein 7	Q6P3G3	ubxn7	56 kDa	100%	0.0001	1.94	6.10
Group of Ubiquitin carboxyl-terminal hydrolase	Q6YI49	uchl1	-	100%	0.03	13.61	25.40
Ubiquitin carboxyl-terminal hydrolase	Q6NWL6	uchl5	38 kDa	100%	0.031	24.30	31.49
UDP-glucose glycoprotein glucosyltransferase 1	A0A2R8RTT5	uggt1	173 kDa	100%	0.029	10.69	3.05
Cytochrome b-c1 complex subunit 7	Q4VBV1	uqcrb	13 kDa	67%	0.045	42.77	34.54
Ubiquinol-cytochrome c reductase core protein 2a	F1QJE0	uqcrc2a	49 kDa	55%	0.021	25.76	38.09
Synaptic vesicle membrane protein VAT-1 homolog	**Q8JFV8**	**vat1**	**54 kDa**	**100%**	**0.034**	**152.61**	**143.23**
Group of Similar to Xab2 protein	Q1LY92	xab2	-	100%	0.037	5.83	11.17
Tyrosine 3-monooxygenase/tryptophan 5-monooxygenase activation protein, epsilon polypeptide 1	Q7ZW20	ywhae1	29 kDa	75%	0.0073	222.11	173.75
Group of Zgc:100918	F6NJU6	zgc:100918	-	83%	0.036	20.09	15.24
Zgc:110425	F1R314	zgc:110425	20 kDa	41%	0.015	15.12	22.74
Group of Zgc:55733	A0A0R4IKH3	zgc:55733	-	86%	0.0062	13.93	28.10
Zgc:92380	E7FAL7	zgc:92380	57 kDa	100%	0.017	64.15	48.76
Si:ch211-212k18.4	A0A0R4IZ89	znf638	241 kDa	100%	0.029	19.44	13.21

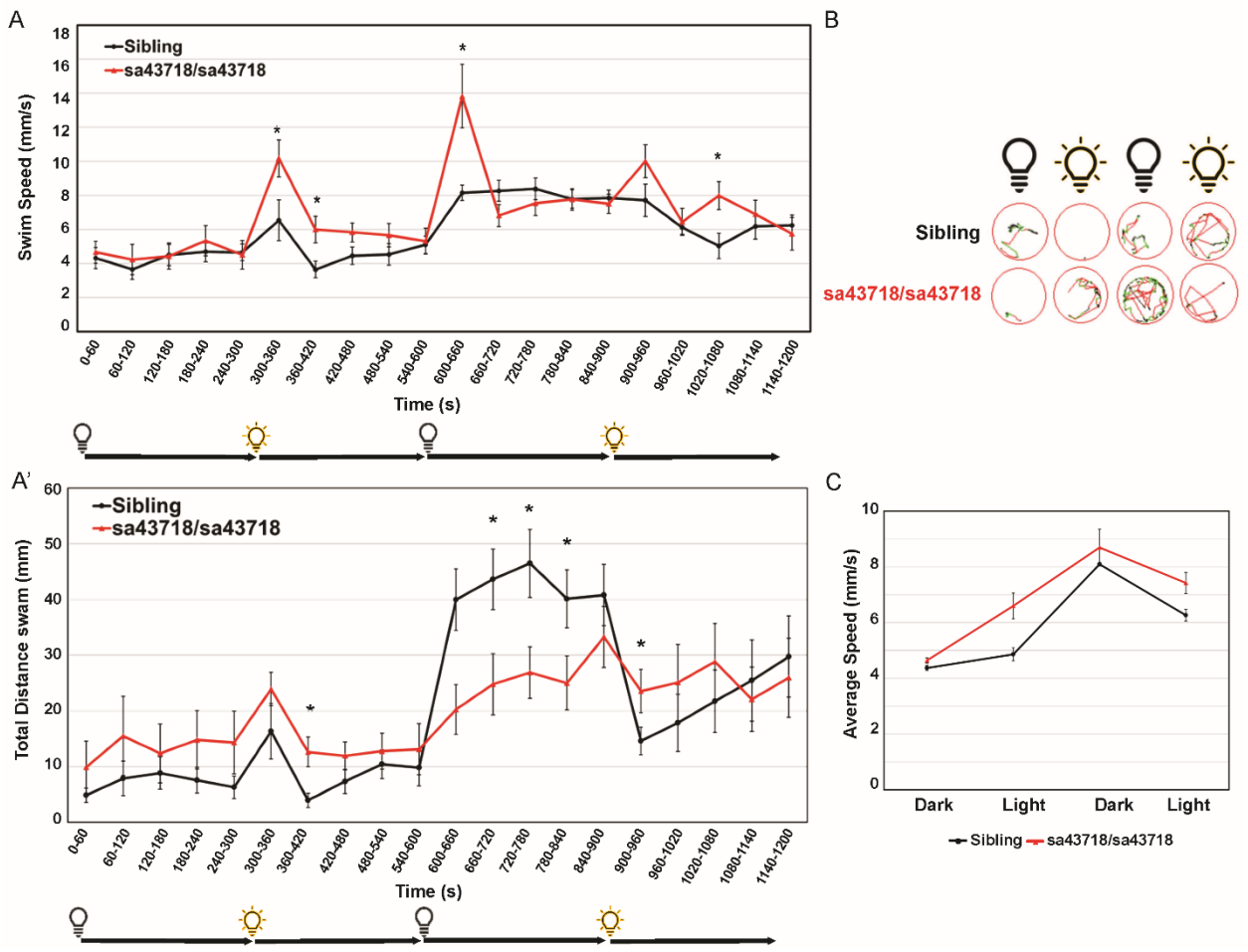

Figure S3.1. Light stimuli induce hyperactive locomotion of *gabra1*$^{sa43718/sa43718}$ larvae.

A & A'. Behavioral analysis of gabra1$^{sa43718/+}$ offspring at 5 days post fertilization. A. Swim speed (mm/s) over 20 minutes (1200 seconds) in dark-light-dark-light transitions [5 minutes (0-300 seconds) in the dark, 5 minutes (300-600 seconds) in the light, 5 minutes (600-900 seconds) in the dark, and 5 minutes (900-1200 seconds) in the light] by 5-day post fertilization (DPF) larvae, analyzed using the Zebrabox technology. Data was collected every minute (60 seconds). *gabra1*$^{sa43718/sa43718}$ larvae exhibit hyperlocomotion upon light stimuli when compared to wildtype siblings (Sibling). *p<0.05. A'. Total distance swam over 20 minutes in dark-light-dark-light transitions. Homozygous carriers

(*sa43718/sa43718*) larvae showed increased distance swam across the light periods (seconds 300-600 and 900-1080), when compared to wildtype siblings (sibling). Homozygous larvae then show decreased distance swam under dark conditions (seconds 600-900) when compared to wildtype siblings (sibling) *p<0.05. B. Representative images of swimming track of a single larvae, representing each genotype, generated from the Viewpoint Zebralab Tracking software in dark (0-60s), light (300-360s), dark(600-660s), and light (1020-1080s) conditions. Green lines indicate movements between 4-8mm/s and red lines indicate burst movements (>8mm/s). C. Average total speed representing overall behavioral responses in dark-light-dark conditions of *gabra1* wildtype (sibling) and homozygous (sa43718/sa43718) larvae. Homozygous carriers (sa43718/sa43718) showed global increased average swim speed when compared to wildtype (sibling) counterparts. Error bars represent the standard error of the mean. *Wildtype sibling (n=21) and gabra1*$^{sa43718/sa43718}$ *(n=19).*

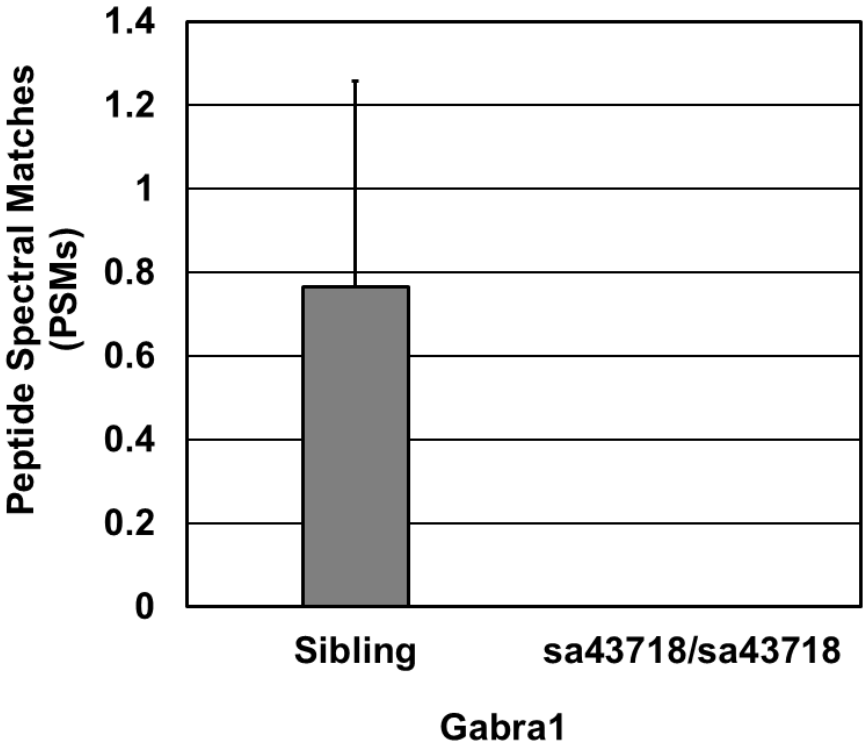

Figure S3.2. Peptide Spectral Matches of Gabra1.

Gabra1 peptides were identified through proteomic analysis of whole brain 5 days post-fertilization zebrafish larvae. Gabra1 peptides were undetectable in homozygote mutants. While identified in wildtype samples, the peptides were not considered for differential expression due to the lack of matches in homozygous samples. This presented a challenge for statistical analysis as it violated the assumption of normal distribution.

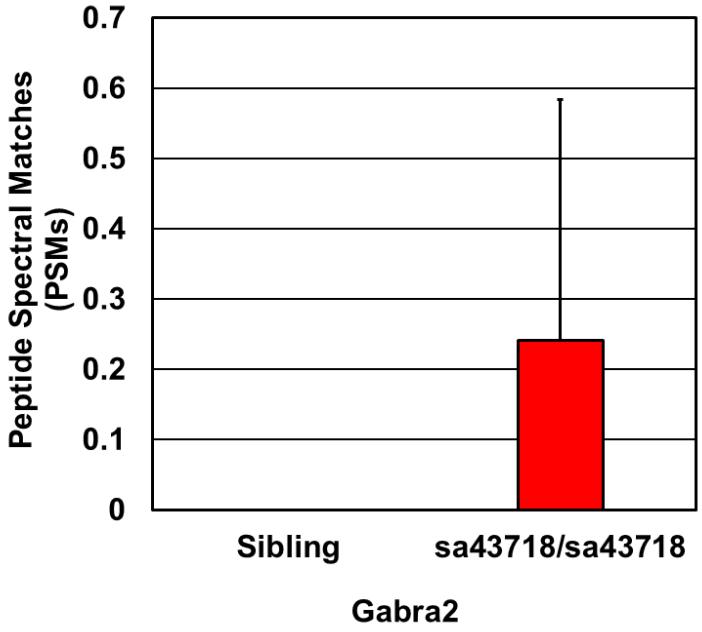

Figure S3.3. Peptide Spectral Matches of Gabra2.

The Gabra2 peptides were not detected in wildtype sibling samples but were detected in homozygous samples (sa43718/sa43718). The fact that no spectral matches were found in wildtype samples contradicts the assumption of normal distribution. Consequently, the software is unable to generate p-values for the protein due to a zero value in one group. Therefore, Gabra2 protein is unsuitable for differential expression analysis.

Chapter 4: Discussion

The data presented in this dissertation demonstrates the critical role of *GABRA1* during brain development, behavior, and disease. This dissertation presents the functional analysis of *GABRA1* using zebrafish as model. The hypothesis that abnormal expression of *GABRA1* results in abnormal behavioral phenotypes, mediated in part by differential expression of $GABA_AR$ subunit, was tested. We used a behavioral paradigm to investigate the effects of *gabra1* loss of function, utilizing two independent genetic models. Transient knockdown of *gabra1* was associated with hypolocomotion phenotype, whereas nonsense mutation of *gabra1* resulted in light-induced seizure-like phenotype. To determine the putative molecular mechanisms underlying these phenotypes, expression of $GABA_AR$ subunits transcripts was analyzed in both morphant and mutant animals. These results will be further discussed in this chapter. Furthermore, we performed proteomic analysis on *gabra1*-mutant developing brains and identified 174 differentially expressed proteins (DEPs) when compared to wildtype siblings. The identified DEPs play essential cellular, molecular, and functional roles. However, our proteomics analysis was limited by abundance of protein and detection rates. Therefore, the 174 proteins differentially expressed represent only those with reliable detection in technical and biological replicates. Collectively, our data suggest that *GABRA1*-dependent epileptic phenotypes are potentially underlying by a combination of molecular cues, including dysregulation of $GABA_AR$ assembly, proton homeostasis, mitochondrial function, and synaptic vesicle regulation.

NOVEL ALLELIC VARIANT IN *GABRA1* (C.875C>T, P.THRE292ILE) IS ASSOCIATED WITH NEURODEVELOPMENTAL DEFECTS AND EPILEPSY.

Mutation of *GABRA1* has been associated with neurodevelopmental and neurological disorders in humans. To date, there are 588 clinical variants in *GABRA1* reported in the ClinVar database (20). Strikingly, the variant (c.875C>T, p.Thre292Ile) identified by our laboratory in 2020 and previously reported by the Epi4K consortium (15) has not yet been added to the ClinVar database. Thus, the variant identified as part of this dissertation research adds to the long list of allelic variants potentially contributing to genetic epileptic syndromes. The c.875C>T (p.Thr292Ile) variant was identified in a pediatric case of multiple congenital anomaly syndrome, characterized by a severe seizure disorder (99). Moreover, the p.Thr292Ile mutation is predicted to be in one of the four transmembrane domains of GABRA1, specifically TM2, which forms part of the inner channel pore and is essential for overall receptor function. Like many previously identified variants, this variant is a *de novo* heterozygous missense variant. The clinical manifestations associated with this variant included early onset infantile spasms that evolved into Lennox-Gastaut syndrome[7]. The seizure disorder consisted of light-sensitive myoclonic epilepsy and generalized clonic seizures resistant

[7] The Lennox-Gastaut syndrome (LGS) is a severe form of epilepsy in which seizures have an early onset (before the age of four). The seizure spectrum in LGS is highly heterogeneous among individuals and is associated with developmental delay and behavioral disturbances.

to multiple treatments[8]. Additionally, the patient was presented with hypotonia, visual impairment, developmental delay, bilateral neuromuscular hip dysplasia, and metabolic defects.

More recently Chen *et al.* (2022) identified a novel variant in the p.Thr292 residue of *GABRA1,* same residue in which the p.Thr292Ile variant occurs. Interestingly, the *de novo* missense variant p.Thr292Ser was identified in a pediatric patient with developmental delay, but no epileptic activity was reported (120). *In vitro* functional analysis of these two variants revealed contrasting effects on $GABA_AR$ function. Biochemical assays and patch-clamp recordings were conducted by Chen and colleagues on HEK293 cells with overexpressed recombinant mutated or wildtype $GABA_AR$. Functional alterations of either variant (p.Thr292Ser or p.Thr292Ile) did not affect the surface/total expression of the alpha-1 subunit. Thus, indicating that $GABA_AR$ is made. Single cell recordings revealed distinct functional effects of each variant. The p.Thr292Ser variant was associated with increased GABA-evoked currents and increased channel opening time and probability, whereas the p.Thr292Ile variant reduced GABA-evoked currents and decreased channel opening time and probability (120). Overall, this suggests that the p.Thr292Ser mutation induced $GABA_AR$ gain of function, whereas the p.Thr292Ile has a loss-of-function effect.

[8] Seizure treatment included adrenocorticotropic hormone, multiple antiepileptic medications, and ketogenic diet.

Moreover, as part of the work presented in this dissertation, the effect of the c.875C>T (p.Thr292Ile) *GABRA1* variant was evaluated (99). Our results, discussed on chapter two and in the following sections, suggest that the c.875C>T is a loss-of-function variant, primarily because overexpression of mRNA encoding this variant failed to restore the hypolocomotion behavioral phenotype exhibited by *gabra1* morphant larvae. Our results, consistent with the findings by Chen *et al.,* (2022), collectively support the premise that the p.Thr292Ile mutation is a pathogenic allelic variant.

Importantly, *in vitro* functional analysis of the p.Thr292Ile and p.Thr292Ser variants indicates that the p.Thr292 residue is critical for $GABA_AR$ gating and overall receptor function. Moreover, identification of the unique effects associated with each mutation on $GABA_AR$ function *in vitro* led to identification of potential therapeutic options that directly or indirectly modulate and restore $GABA_AR$ function to normal levels (120). Hence highlighting the necessity of investigating the functional effects of individual *GABRA1* variants to aid in searching for targeted therapeutic options for *GABRA1*-associated epilepsies.

Albeit Chen *et al.,* (2022) work provides a an insight into the functional effects of the p.Thr292Ile allelic variant, their work only describes the *in vitro* consequences associated with *GABRA1* allelic variants. Moreover, functional studies were performed in a non-neuronal cell line. Thus, raising questions regarding the functional effects of mutation of *GABRA1* in neuronal populations and further *in vivo.* Moreover, treatment with combination of verapamil and diazepam resulted in partial restoration of the $GABA_AR$ function caused by the p.Thr292Ile mutation. Thus, it is possible that additional factors

may be contributing to the impaired function of the $GABA_AR$ upon mutation of *GABRA1*. In that sense, investigation on the *in vivo* functional consequences of *GABRA1* loss-of-function effects is necessary. Importantly, the work presented in this dissertation further delves into the functional role of *GABRA1 in vivo* and contributes to the understanding of the role of *GABRA1* during development and disease*.* Our work explores the *in vivo* consequences of knockdown and nonsense mutation of *gabra1,* by investigating $GABA_AR$ subunit expression, neurobehavioral responses, and for the first-time proteomic analysis of a germline mutant of *gabra1.* The sections below discuss these factors, their implications, and limitations.

WHAT ARE THE MOLECULAR MECHANISMS/CONTRIBUTING FACTORS UNDERLYING SEIZURE PHENOTYPES EARLY IN DEVELOPMENT?

$GABA_AR$ subunit composition and neurobehavioral responses

Although mutation of *GABRA1* is thought to cause epilepsy, the mechanisms underlying these phenotypes have not been completely elucidated. Murine models of *Gabra1* loss of function have provided insight into the physiological, pharmacological, and behavioral role of the gene. However, murine models offer limited scope to the developmental component of *GABRA1*-associated epileptic syndromes. Hence, the initial stages of our research involved the development of a novel knockdown model of *gabra1* using zebrafish*.* Our studies were performed at five days post fertilization, a developmental stage prior to sexual dimorphism and feeding, yet a time point where larvae already exhibit a broad spectrum of complex behaviors, including optic/motor behavior and prey chase (107). Hence being an optimal stage for developmental

behavioral analysis. Interestingly, morpholino-mediated knockdown of *gabra1* resulted in hypomotile phenotypes, characterized by decreased total distance swam and swim speed. Although phenotypes reported in murine models are sex and strain-dependent, behavioral impairment, primarily characterized by decreased locomotion, has been described in *Gabra1*-KO mice (5), consistent with our morpholino findings.

The hypoactive behavior observed in morphant larvae was correlated with altered expression of transcripts encoding $GABA_AR$ subunits (99). Specifically, we reported downregulation for *gabrb2* and *gabrg2*, transcripts that encode for β2 and γ2 subunits, and upregulation of *gabra6a,* which encodes for the α6a subunit. Our discoveries are consistent with previous reports in which downregulation of gamma-2 and beta-2/3 subunits are reported in alpha-1 depleted mice brains (31). Further, upregulation of alpha-type subunits, including alpha-2 and alpha-3 subunits, upon deletion of *Gabra1* has been described (31,36). Moreover, downregulation of *gabrg2* has also been documented in a zebrafish germline mutant of *gabra1* (105). However, this data was not validated by our proteomic analysis nor their functional contribution was tested.

gabra1 mutants generated by Samarut and colleagues were overall hypoactive but become hyperactive when exposed to light, showing convulsions and whirlpool swimming (105). This response was not observed in *gabra1* morphants, which were hypoactive under both light and dark conditions (99). Further, we report hypoactive phenotypes at five days post-fertilization, while Samarut and colleagues report light-induced light-dependent hyperactivity starting at four days post-fertilization to five weeks post-fertilization, a stage where fish are considered juveniles. The distinct behavioral

phenotypes of these two zebrafish models raised questions regarding the effects of *gabra1* on developmental behavior and disease.

Therefore, to address these questions and to further validate the current available zebrafish models of *gabra1* deficiency, we sought to characterize a novel germline mutant of *gabra1* (sa43718 allele). The sa43718 allele, an uncharacterized zebrafish line generated by the Wellcome Sanger Institute as part of the zebrafish mutation project in 2016, harbors a non-sense mutation in *gabra1* (Figure 3.1). Thus, we performed behavioral analysis, targeted gene expression, and proteomic analysis of the *gabra1*^{sa43718} allele. Importantly, *gabra1* knockout resulted in light-induced hyperactive phenotype, consistent with Samarut *et al.* (2018) findings. Yet, in contrast to our previous work using morpholinos technology. The contrasting behavioral phenotypes observed between morphant and mutant larvae could be related to the expression level of *gabra1,* where knockdown of *gabra1* was associated with a 50% decrease in *gabra1* expression. In contrast, homozygous mutants showed a 90% reduction in *gabra1* mRNA expression.

We reported increased swim speed and total distance swam upon light stimulus depicted by *gabra1* homozygous mutants at 5 DPF. According with the glossary of zebrafish behavior, increased velocity and distance traveled correspond to a seizure-like phenotype (107). Moreover, the seizure-like phenotype was accompanied by differential expression of $GABA_AR$ subunits, specifically up-regulation of *gabra4,* which encodes the α4 subunit. However, we did not observe changes in expression of gamma/beta subunits, previously described by Samarut *et al.* and our research group, in both *gabra1* mutant and morphant larvae. Behavioral and gene expression differences observed between

morphant and sa43718 larvae, could be related to the expression level of *gabra1.* Specifically, we observed upregulation of *gabra6b* and *gabra4* associated with a 50% and 90% decrease expression of *gabra1* respectively. Upregulation of different alpha subunits could be a compensatory mechanism for losing the alpha-1 subunit; this has been reported in murine models of *Gabra1* loss of function. For example, the deletion of *Gabra1* in murine models has been associated with the upregulation of *Gabra3* (which codes for alpha-3 subunits) and absence seizure phenotype (113). This could suggest that the deletion of *Gabra1* is compensated by increasing the expression of different receptor isoforms, which may contribute to different behavioral outcomes. Moreover, differential expression of $GABA_AR$ subunits in both morphant and mutant larvae, could imply that *gabra1* is essential for $GABA_AR$ assembly and composition.

Remarks on transient knockdown and germline mutant of GABRA1.

Although it is not considered a true genetic approach, the use of antisense morpholino oligomers (MOs) has been widely used to evaluate gene function in zebrafish (128). MOs can be designed to globally block translation or splicing of a specific gene, providing a relatively easy, rapid, and straightforward approach for gene knockdown in the zebrafish embryo. They can be quickly injected into one-cell stage zebrafish embryos, enabling widespread gene functional analysis. Using MOs to knockdown candidate genes has had an impactful role in using zebrafish as a model system. However, a study by Kok *et al.* (2015) described that only a small portion of mutant phenotypes recapitulate published morpholino-induced phenotypes. In our case, this is partially true. Although we

observed contrasting behavioral phenotypes, our findings highlight that *gabra1* is essential for larval locomotion and development overall.

There are still some questions that still need to be answered regarding the use of morpholinos. Is there a good or poor correlation between morpholino-induced and mutant phenotypes in zebrafish? Which one should one prefer or trust? There are multiple advantages when using MOs to investigate gene function. First, morpholino technologies provide powerful approaches to the study of early development. Because they can be injected into the single-cell stage and are highly effective through the first days post-fertilization, they can be used to analyze gene function during the entire course of embryonic development (121). Another significant advantage is the ease of inducing knockdowns quickly, which allows for subsequent phenotypic characterization relatively quicker than the time required to generate data from a mutant line.

According to Eisen and Smith (2008), appropriate controls are essential to provide high confidence and validity of the results. Our morpholino studies were highly controlled. First, knockdown analysis was performed by means of two independent morpholinos targeting exclusively *gabra1* transcript. Regardless of translation blocking (tbMO) or splicing morpholino (sMO) utilized, morphant larvae exhibited hypoactive phenotypes. Further, the behavioral phenotypes were *gabra1*-dependent and validated through restoration experiments. The co-injection of MO and *GABRA1* encoding mRNA restored the total distance swam back to control levels. Noteworthy, co-injection of *GABRA1* mRNA harboring the c.875C>T variant failed to restore behavioral phenotypes observed in morphant larvae. Thus, implying this variant is pathogenic. Moreover, larvae injected

with either morpholino, tbMo or sMO, showed differential expression of $GABA_AR$ subunits. Lastly, to further validate the role of *gabra1* during development we utilized and analyzed a nonsense germline mutant of *gabra1* (sa43718 allele). Specifically, mutation of *gabra1* resulted behavioral phenotypes (seizure-like behavior) similar to those observed in patients and in line with work by Samarut and colleagues. Thus, our studies suggest that data collected from germline mutation are more physiologically relevant to human disease.

Putative implications of DEP in behavior and epileptogenesis

Using SWISS model software, we generated the predicted protein models of both wild-type (sibling) and mutant (*gabra1*$^{sa43718/sa43718}$) alpha-1 subunit (Figure 4.1). Carriers of the sa43718 allele harbor a nonsense mutation in the extracellular domain of *gabra1*, which is predicted to result in a premature stop codon. The SWISS model depicts a truncated protein, where all four transmembrane domains and intracellular components are lost. Importantly, transmembrane domains are essential for protein anchoring into the cell membrane. Thus, suggesting that, if synthesized, this truncated peptide will likely not be assembled in a receptor thus transcript encoding the alpha-1 subunit will likely be degraded through nonsense-mediated mRNA decay. This predicted model is consistent with our qPCR analysis, which showed close to 90% decreased mRNA expression of *gabra1* compared to wild-type siblings (Figure 3.2A). Moreover, as shown in supplemental figure 3.2, peptide spectral counts of Gabra1 were undetected in homozygote fish. These numbers, however, have several limitations. One of which is that spectral counts were not detectable in technical replicates from wildtype larvae. This is

likely due to low Gabra1 peptide abundance and/or low yield on membrane proteins recovery. However, this does call into question the reliability of proteomics to detect Gabra1 peptides. Our proteomic analysis consisted of two biological replicates with two technical replicates each, thus increasing the number of both technical and biological replicates could improve the detection alpha-1 peptides.

We performed proteomics analysis to understand further the underlying molecular mechanisms by which seizure phenotypes occurred in *gabra1* mutants. Specifically, we were interested in 1) determining the composition of $GABA_AR$ upon deletion of *gabra1,* 2) validating our gene expression results, and 3) exploring whether transcriptomic results reported by Samarut *et al.* would correlate with our proteomics data.

Proteomic analysis identified a total of 173 differentially expressed proteins, of which 81 were up-regulated and 93 down-regulated proteins in mutant larvae when compared to wildtype siblings. Very few of the identified differentially expressed proteins in our dataset overlap with the differentially expressed RNAs previously identified by Samarut *et al*. (2018). This is striking as the two fish mutations induce premature stop codons, result in dramatic decreases in mRNA expression of *gabra1*, and cause overlapping phenotypes. Through targeted mRNA analysis we observed increased expression of *gabra4* in mutant larvae and we found *gabra6* to be up regulated after morpholino mediated knockdown. Strikingly, we did not identify a single $GABA_AR$ subunit differentially expressed in the sa43718 allele at the protein level. Samarut and colleagues observed some $GABA_AR$ subunits differentially expressed but these were undetectable in our mutant allele.

Loss of gabra1 alters the expression of presynaptic proteins important for vesicle formation, release, and recycling.

We looked at DEPs of interest that could potentially underlie the seizure phenotypes. Our proteomics analysis is limited by detection of proteins in low abundance as we could not reliably detect them in technical replicates. Therefore, we only identified statistically significant proteins for those proteins in higher abundance. Some of these proteins included synaptotagmin-1, complexin-4a, secretogranin-2, a Vat1 homolog, and synapsin proteins. Each of these proteins has a function in synaptic fusion, transport, exocytosis, endocytosis, or direct interactions with small synaptic vesicles. Further work that validates our proteomic analysis through immunohistochemical analysis is recommended.

Specifically, synaptotagmin-1 (Syt1), a calcium sensor that, under normal conditions, triggers neurotransmitter release at the synapse. Syt1 plays additional roles, including targeting and fusion of vesicles, internalization of vesicles, transmembrane transport of substances, formation of cellular structure, regulation of neuronal polarity, and differentiation of axons (122). Hence, the downregulation of this protein interferes with all these processes. Importantly, axonal differentiation is essential for the establishment of synaptic connections. Moreover, Secretogranin-2 (Scg2), a vesicle matrix protein mainly distributed in dense-core vesicles of neurons (123), is also essential for neurotransmitter release. In tandem, the downregulation of this protein could be implicated in GABA accumulation in the presynaptic terminal, deficient GABA release, and poor synaptic transmission.

Interestingly, the vesicle amino transport protein 1 (Vat1) homolog was upregulated in *gabra1* mutants. The vat1 homolog is a protein that localizes in the cytoplasm and the outer mitochondrial membrane (124,125). Moreover, this protein has been implicated in the regulation of vesicular transport (126). Noteworthy, overexpression of VAT1 indicates poor survival prognosis in glioma cases (124). Importantly, models of *gabra1* deficiency, including the sa43718 allele, have high mortality rates and premature death, which could be the result of Vat1 upregulation. Complexin 4a (Cplx4a) was also upregulated in *gabra1* mutant larval brains. Complexins are small synaptic proteins that regulate the SNARE[9] protein complex-mediated synaptic vesicle fusion, and are known to have a negative regulatory role in synaptic transmission (128). Further, complexins are highly enriched in the mammalian brain and are essential for synaptogenesis (128,129).

We also report downregulation of synapsin proteins, specifically synapsin-1 (Syn1) and synapsin-2b (Syn2b). These proteins are also crucial for synaptic vesicle release at the presynaptic membrane. Moreover, mutation of *SYN1* has been associated with epileptic phenotypes in humans (114–117). Significantly, Syn1 is associated with axon elongation of the axon and regulation of the kinetics of synaptic vesicle fusion. Syn1 also

[9] SNARE (soluble N-ethylmaleimide sensitive factor attachment protein receptor) proteins are fusion proteins that regulate docking of vesicles to target membranes and are implicated in vesicle exocytosis and synaptic transmission (127).

plays an essential role in synapsis formation by minimizing neurotransmitter depletion at the inhibitory synapse by contributing to the anchoring of synaptic vesicles (114,130).

Gabra1 loss of function alters expression of epilepsy associated proteins.

In addition to synapsins (Syn1 and Syn2b), we reported altered expression of proteins that have been previously associated with epileptic phenotypes. We identified downregulation of NADH:ubiquinone oxidoreductase core subunit S2 and NADH:ubiquinone oxidoreductase core subunit A10, proteins implicated in mitochondrial complex I. Each is encoded by *NDUFS2* and *NDUFA10* respectively, and mutation of these genes are associated with Leigh syndrome, one of the most common human mitochondrial diseases, in which epilepsy is a primary phenotype (118,119).

Our proteomics data also showed downregulation of dynamin-1b (Dnm1b), v-ATPase (Atp6v1ab), and the sodium-coupled neutral amino acid transporter (Slc38a3a). Mutation of their human orthologs underlie epileptic syndromes (131,132). These proteins play essential roles in synaptic vesicle recycling, sodium-potassium homeostasis, and GABA synthesis. Dynamin-1 is highly concentrated in presynaptic terminals and is implicated in synaptic vesicle recycling (132). Recent studies on knockdown of *dnm1a ,* one of the two zebrafish orthologs of human *DNM1*, have demonstrated a key role in both axon and synapse formation (133). Moreover, the A subunit of v-ATPase, encoded by *atp6v1ab,* is a multi-subunit complex that acts as an ATP-dependent proton pump. This protein is essential for neurotransmitter loading into synaptic vesicles and synaptic transmission (131). Lastly, the glutamine transporter 1, encoded by *slc38a3a,* is the principal transporter of glutamine. Crucially, glutamine is an essential precursor for GABA

synthesis. Abnormal expression of these epilepsy-associated proteins suggest that synaptic vesicle recycling, sodium-potassium homeostasis, and GABA synthesis defects are contributor factors of seizure development. Moreover, these data support the idea that down-regulation of *gabra1* itself alters the expression of other proepilepsy-related genes previously discussed by Samarut *et al.,* (2018).

Transcriptomic analysis by Samarut *et al.* (2018) reported abnormal expression of 460 transcripts in their *gabra1* mutant larvae brains, including *syt3, atp6v0ab, dnm1b,* and *cplxn1* transcripts (105). Our proteomic analysis identified 173 differentially expressed proteins in the *gabra1* sa43718 mutant brains, from these we pinpointed some gene/protein correlations with Samarut's data, including overlapping proteins or proteins from the same family. For instance, we identified the downregulation of synaptotagmin-1, encoded by *syt1. Syt3* was previously reported downregulated by Samarut *et al.* (2018). Importantly, one overlapping protein was dynamin-1 (Dnm1b), which transcript was reported downregulated by Samarut *et al.* (2018). Due to these overlapping results, in two independent zebrafish *gabra1* mutants, Dnm1b could be considered a pivotal contributor to *gabra1*-associated epileptic phenotypes. When comparing transcriptomic and proteomic data from both *gabra1* loss of function zebrafish models, it can be implied that *gabra1* is essential for synaptic vesicle formation, release, and recycling. The reason being that both transcripts and proteins implicated in synaptic vesicle formation, release, and recycling are abnormally expressed in both zebrafish mutants of *gabra1*. Importantly, these mechanisms are critical for neurotransmitter release and, consequently, synaptic neurotransmission. Our proteomic analysis supports and complements, to an extent,

transcriptomics findings. Thus, it provides validity to the previously reported zebrafish model of *gabra1* loss of function.

Remarkably, our data suggests that mutation of major components of $GABA_AR$s, specifically the alpha-1 subunit, induces abnormal expression of proteins involved in synaptic vesicle formation, release, and recycling *in vivo.* This could also suggest changes in synaptic transmission, primarily due to the role of gabra1 in the aforementioned. Moreover, lack or reduced inhibitory input could be implied, which could lead to changes in excitatory/inhibitory balance. However, the present study did not explore the electrophysiological effects of non-sense mutation of *gabra1.* Hence, further studies could include electrophysiological analysis of the sa43718 allele.

Collectively, our findings suggest that bidirectional communication between pre- and post-synaptic terminals is essential for synaptogenesis and downstream synaptic transmission during development.

REMARKS AND LIMITATIONS OF GENE EXPRESSION AND PROTEOMIC ANALYSIS

Our proteomic analysis is not fully consistent with the transcriptomic analysis by Samarut *et al.* (2018). Only a reduced number of proteins were overlapped even though both mutants harbor a mutation in the extracellular domains of g*abra1*. The sa43718 allele harbors a nonsense mutation predicted to result in a premature stop codon at site p200, while the mutant generated by Samarut *et al* (2018) carries a frameshift mutation leading to a premature stop codon at position 150 of Gabra1. Albeit these mutations are located in close proximity they are not identical. While we could anticipate significant overlap on

results, any phenotypic differences could be related to differences in mutation type/location.

We identified only a total of 11 proteins differentially expressed through proteomic analysis, from which transcripts were reported as differently expressed in the *gabra1* loss of function zebrafish model by Samarut and colleagues. Our study did not find a strong correlation between mRNA and protein levels despite the many similarities shared by both mutants. Research has shown low correlations between mRNA and protein expression levels, which could lead to concerns regarding conclusions drawn solely from mRNA data (134,135). Further, genes altered by experimental manipulation are more likely to display consistent expression under the same experimental conditions than those whose transcription is not significantly impacted by the experimental condition (136). This, however, raises another question, if gabra1 expression was reduced in both mutants by qPCR, why was this change not detected by proteomic analysis. This will be further discussed in the sections below. Other factors, such as translational regulation and protein degradation, can also contribute to low mRNA-protein correlations (136). Perhaps, these factors could explain the reduced transcript-protein correlation between *gabra1* mutants.

The overlapping proteins that could be potentially involved and underlying the seizure phenotype observed in our mutants has been previously discussed. However, multiple ribosomal proteins were also identified as DEP and our proteomics results line up with previous transcriptomic analysis. These include Rpl13a, Rpl10, Rpl31, Rpl18, Rps27a, and Rps28. Interestingly, in both analyses *rpl13a* (Rpl13a) was upregulated in

mutant fish. This could be indicative of *rpl13a* not being an optimal housekeeping gene for our Q-PCR analysis, mainly because an optimal endogenous control gene should be consistently expressed in all conditions/samples tested (137–141).

Although *rpl13a* is a widely and commonly used housekeeping gene due to its stability in zebrafish (99,142–144), upregulation of this gene by proteomic analysis raises some questions and indicates the need for validation with additional endogenous genes. *rpl13a* quantification of copy number by standard curve is required to discern differential mRNA expression in the *gabra1* sa43718 allele. Moreover, analysis using complementary housekeeping genes is required. Additional endogenous controls such as *bactin, gapdh, polr2d,* and *tuba1b* are suggested. Specifically, *bactin* since it has been shown to be a gene with low variability in zebrafish embryo/larvae samples (145), and its expression is unchanged according to proteomic analysis. Moreover, *polr2d* could be also utilized since it has been previously used as endogenous control by Samarut *et al.* (2018). Lastly, *tuba1b* was utilized as endogenous control when characterized the GABA-signaling system in zebrafish by RT-QPCR analysis (56).

A further note should be given to the limitations of proteomic analysis. One of our primary goals of the proteomic analysis was to identify the $GABA_AR$ subunit composition upon loss of *gabra1.* To our surprise, proteomic analysis failed to identify changes in the expression of $GABA_AR$ subunits. Only two $GABA_AR$ subunits were identified, Gabra1 and Gabra2. However, the spectral counts for each protein mentioned above were very low and only detected in one of the genotypes or in one of two technical replicates. For instance, Gabra1 was only detected in wildtype samples but not in heterozygous and

homozygous samples. This was similar for Gabra2, which was only detected in homozygous samples but not in wildtype nor heterozygous samples. This could be due to the abundance level of these proteins. Perhaps $GABA_AR$ proteins are low in abundance in zebrafish larvae. Moreover, $GABA_AR$ proteins are membrane proteins, hence low yield on membrane protein recovery may have also contributed. Importantly, the highly abundant proteins represent a major challenge for proteomic analysis since the MS data collection is biased towards high-abundance peptides (146,147). Thus, certain naturally enriched proteins may suppress the signals of low-abundance proteins, which could be the case of Gabra1 and other $GABA_AR$ proteins. To detect low-abundance proteins, enriching them from brain homogenates is crucial. This could be achieved by using beta-2 and/or gamma-2 antibodies to immunoprecipitate $GABA_AR$, since γ2 and β2 subunits are assembled with α1 in wildtype conditions.

Moreover, we detected variation across technical replicates in our dataset. Multiple factors contribute to technical variability in LC-MS proteomics (148–152). Extraction and instrumental variance are significant variability factors (148). Instrumental variation refers to the short-term run-to-tun instrumental fluctuation when making replicate injections for LC-MS/MS analysis (148). Technical variation across technical replicates is common in proteomics (148,149,152). This variation can be attributed to instrumental variation due to the nature of the process that relies on the random sampling of peptides from the sample for peptide identification (151). Hence, different peptides are or can be detected in each technical replicate. This can be the case for low-abundance peptides, such as Gabra1, and its suggested low abundance could account for increased variation across technical replicates. Yet, inefficient recovery of membrane proteins could also account for

low Gabra1 detection. Due to the nature of nonsense mutations, one could anticipate that the sa43718 results in a transcript with a premature stop codon, which will likely be degraded by nonsense mRNA-mediated decay; thus, the abundance of Gabra1 peptides in both heterozygous and homozygous mutants would likely be present in lower abundance than wildtype counterparts. However, Gabra1 was also not reliably detected in wildtype larvae. Significant efforts focused on improving instrument variability, however even in the best/ideal scenarios it has been suggested that significant variability will always exist for most sample types (148). However, increasing the number of both technical and biological replicates could improve the detection of low abundance peptides.

In general, data obtained from these high throughput analyses should be taken with caution and ideally validated by quantitative means, for example immunohistochemical analysis or by western blot. Unfortunately, detection of certain proteins in fish is sometimes difficult due to the limited number of zebrafish specific antibodies.

We utilized expression levels of *gabra1* by QPCR to validate the *gabra1* sa43718 allele. However, upregulation of our selected endogenous control, *rpl13a*, by proteomic analysis jeopardizes to an extent our QPCR data. In closure, due to the inability of proteomic analysis to detect changes in expression in Gabra1, and to the limitations associated with our QPCR analysis, the proteomic analysis data presented here should be taken with caution.

CLOSING REMARKS AND FUTURE DIRECTIONS

During the initial stages of this research, limited data was available regarding the functional role of *GABRA1* in embryo brain development and confounding phenotypes were described across murine models of *GABRA1* deficiency. A zebrafish model was not available. Thus, we aimed to use morpholino technology to transiently knockdown *gabra1.* Concurrently with my ongoing research, the Sanger Institute (sa43718 allele) and Samarut and colleagues developed two independent zebrafish models that harbor mutations in *gabra1.* Importantly however, the sa43718 allele was not yet characterized, thus functional analysis of this mutant zebrafish line was part of the work here presented. Altogether, data obtained from these models contribute and support to the hypothesis that *GABRA1*-associated seizures have a developmental underlying component and that *GABRA1* plays an essential role in larval locomotion.

As part of this research, we identified and reported a novel *GABRA1* mutation (c.875C>T, p.Thre292Ile). In the end term, genetic screening has led to identifying many novel *GABRA1* genetic variants now known to contribute to the etiology of epilepsy, including the c.875C>T, p.Thre292Ile variant here reported. Identifying these variants is critical for pinpointing pathways that can be used as targets for developing novel therapeutics for patients with *GABRA1*-associated epilepsies. So far, the c.875C>T, p.Thre292Ile has been characterized *in vitro* (120). Importantly, Chen et al (2022) propose the use and combination of verapamil and diazepam for treatment of epilepsies associated with the loss of function c.875C>T, p.Thre292Ile variant. Nonetheless, further

investigation into the *in vivo* effects of this variant and its response to treatment is warranted.

So far, over 500 allelic variants have been reported in *GABRA1*, of which only 45 are categorized as pathogenic, and fewer have been characterized *in vivo*. No precise genotype:phenotype correlation exists between the reported variants, their location, and disease to date. Because different variants can result in different molecular responses inducing either loss- or gain- of $GABA_AR$ function (120), functional characterization of additional variants is critical.

Albeit most human *GABRA1* mutations are missense and present in a heterozygous state, our research aimed to investigate the functional role of *GABRA1* during development. To do so, we designed morpholinos to inhibit the translation of *gabra1* or mRNA splicing. Our first study showed knockdown of *gabra1*, where *gabra1* expression was reduced by 50%, likely resembling a heterozygous state. However, our knockdown model exhibited hypomotile phenotypes which do not recapitulate the generalized seizure phenotypes observed in patients. Moreover, behavioral analysis of the *gabra1* sa43718 mutant larvae, harboring a nonsense mutation in the GABA binding domain of *gabra1,* resulted in light-induced seizure-like phenotypes only in homozygous larvae. Similarly, Samarut and colleagues reported seizure-like phenotypes in homozygous *gabra1* mutants. This could indicate that that in fish, mutation of *gabra1* is haplosufficient, thus mutant phenotypes will be only exhibited in homozygous recessive mutants.

Importantly, human nonsense mutations in the extracellular domain of *GABRA1* have been reported (153), thus functional characterization of nonsense mutations further contribute to our understanding on the effects of these mutations to epileptogenesis. Additionally, the seizure-like phenotype observed in the *gabra1* nonsense mutant larvae was associated with decreased response to PTZ, a GABA antagonist, thus suggesting that channel functionality is impaired. Further work should investigate the electrophysiological effects of this allele, to determine whether $GABA_AR$ function is altered, thus contributing to the seizure-like phenotypes depicted by *gabra1* mutant larvae.

This work, to our knowledge, is the first to report a whole-brain proteomic analysis of a germline mutant of *gabra1*. Our proteomic findings are not completely consistent with the transcriptomic data previously reported in a germline mutant of *gabra1.* Classes of similar gene products are revealed but only 11 of the total identified proteins overlap with the mRNA profile provided by Samarut and colleagues. We provide further evidence to support the hypothesis that epilepsy has an underlying developmental component. The role of the proteins identified abnormally regulated in *gabra1* mutants should be further analyzed to understand their direct role in epilepsy development. Moreover, our proteomic analysis spotlights a potential molecular-blue print underlying epileptic phenotypes. However, it is yet to be investigated whether this molecular-blue print is true in patient-variants.

Dnm1b should be given special attention since both transcript and protein levels were differentially expressed in two independent *gabra1* loss-of-function zebrafish

models. In fish two orthologs of the mammalian *DNM1* have been identified, *dnm1a* and *dnm1b*. Researchers have attempted to characterize the expression patterns of *dnm1b*. However, it has only been detected through RT-PCR, without clear spatio-temporal signals through whole mount *in situ* hybridization analysis (133). Thus it is suggested that dnm1b transcript could expressed at low levels during embryonic development. Interestingly, downregulation of *dnm1b* (Dnm1b) was detected through transcriptomic and proteomic analysis in *gabra1* mutant brains. Thus, we still need to answer some remaining questions. What is the role of *dnm1b*? Does *dnm1b* interact with *gabra1*? If it does, how? And how does downregulation of *gabra1* alter the expression of *dnm1b*?

Collectively, our proteomic analysis indicates that presynaptic neurotransmitter release, vesicle transport, and overall synaptogenesis are disrupted in *gabra1*-deficient brains. Moreover, our data highlight an essential correlation between metabolism (cellular respiration) and epilepsy. Thus, suggesting that these mechanisms could be directly implicated in epileptogenesis early in development. In closure, our analysis validates the premise that mutation of *gabra1* results in developmental seizures and provides a blueprint of putative proteins which may mediate these phenotypes *in vivo* (Figure 4.2).

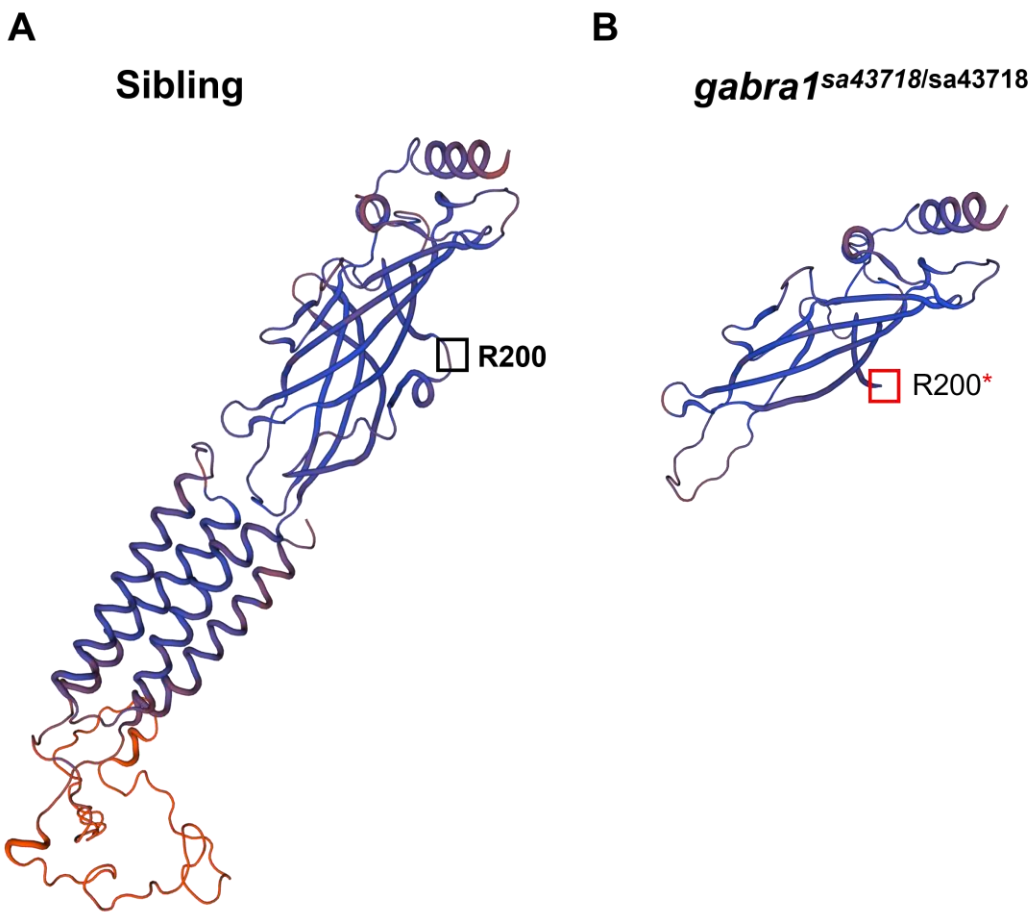

Figure 4.1. Predicted protein structure of the *gabra1*^{sa43718} allele.

Structural prediction of *gabra1* protein generated using SWISS-MODEL. Wildtype sibling (A) and homozygote (*gabra1*$^{sa43718/sa43718}$) (B) proteins are depicted.

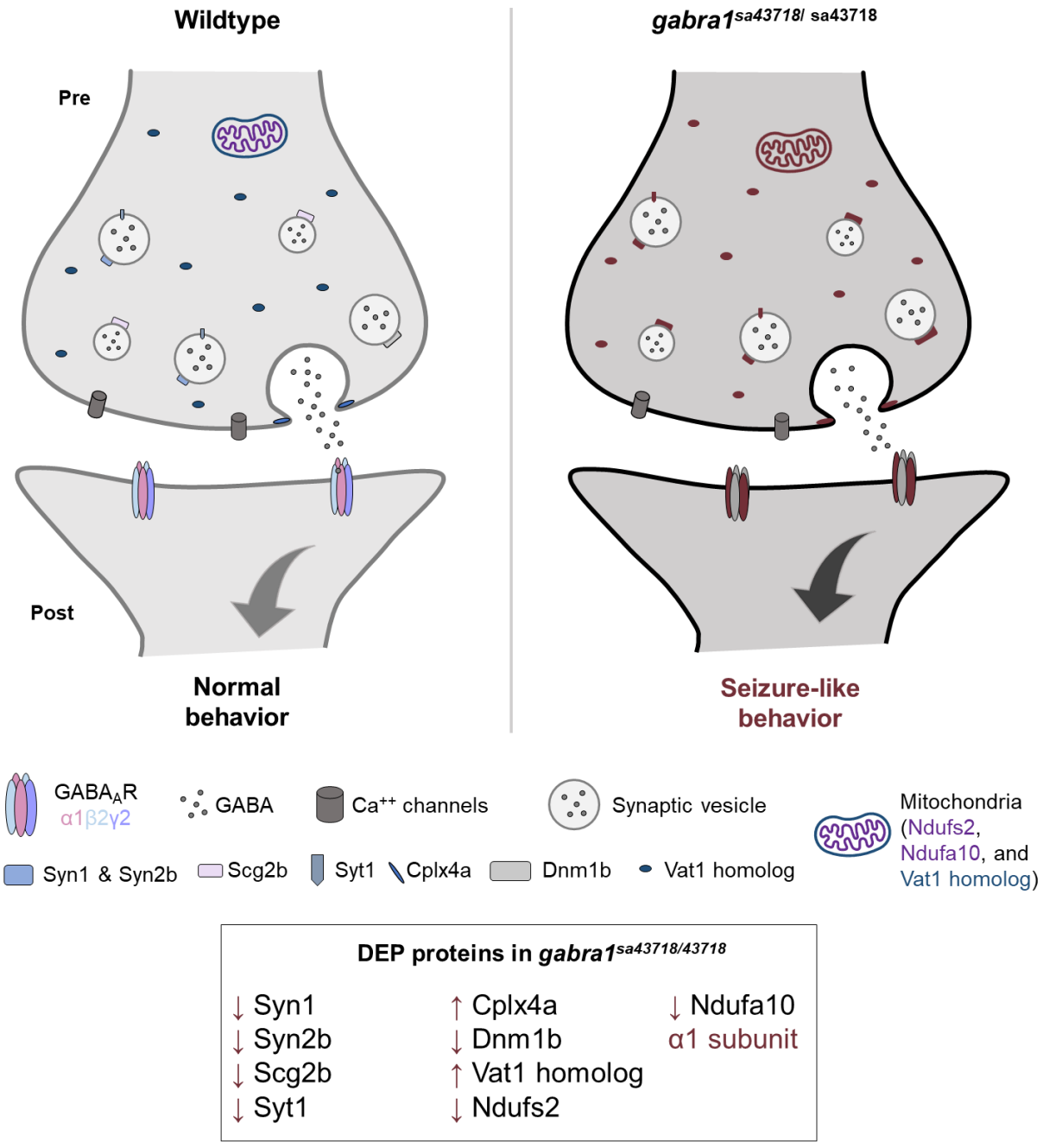

Figure 4.1. Proposed blueprint of putative DEP underlying seizures *in vivo*.

Schematic representation of the structural organization of a GABAergic synapse, showing differentially expressed proteins (DEP) that could potentially contribute to seizure-phenotype development in *gabra1* mutants. The scheme highlights DEP involved in

synaptogenesis, vesicle formation, release, and recycling. Differentially expressed proteins of interest in *gabra1*$^{sa43718/43718}$ mutant brains are in dark red color (right panel). The trend of regulation in mutant brains is indicated by an arrow up or down next to each protein name. Mutation of genes encoding for some of these proteins has been associated with epileptic syndromes in humans (human genes underlying epileptic syndromes: *DNM1*, *NDUFS2, NDUFA10, SYN1*, and *SYN2*). The panel on the left represents the wildtype synapse.

Pre: presynaptic, Post: postsynaptic, Syn1: synapsin-1, Syn2b: synapsin2b, Scg2b: secretogranin-2b, Syt1: synaptotagmin-1, Cplx4a: complexin-4a, Dnm1b: dynamin-1b, Vat-1 homolog: vesicle amine transport protein 1 homolog, Ndufs2*:* NADH:ubiquinone oxidoreductase core subunit S2, Ndufa10: NADH:ubiquinone oxidoreductase core subunit A10, proteins implicated in mitochondrial complex I.

Full list in of DEP in Supplemental Table 3.1.

References

1. Sigel E, Steinmann ME. Structure, function, and modulation of GABA(A) receptors. J Biol Chem. 2012 Nov 23;287(48):40224–31.

2. Ghit A, Assal D, Al-Shami AS, Hussein DEE. GABAA receptors: structure, function, pharmacology, and related disorders. J Genet Eng Biotechnol. 2021 Aug 21;19(1):123.

3. GABRA1 - Gamma-aminobutyric acid receptor subunit alpha-1 - Homo sapiens (Human) | UniProtKB | UniProt [Internet]. [cited 2023 Apr 20]. Available from: https://www.uniprot.org/uniprotkb/P14867/entry

4. Sieghart W, Fuchs K, Tretter V, Ebert V, Jechlinger M, Höger H, et al. Structure and subunit composition of GABAA receptors. Neurochem Int. 1999 May 1;34(5):379–85.

5. Ye GL, Baker KB, Mason SM, Zhang W, Kirkpatrick L, Lanthorn TH, et al. GABAA Receptor α1 Subunit (Gabra1) Knockout Mice: Review and New Results. In: Kalueff AV, Bergner CL, editors. Transgenic and Mutant Tools to Model Brain Disorders [Internet]. Totowa, NJ: Humana Press; 2010 [cited 2020 Apr 9]. p. 65–90. (Neuromethods). Available from: https://doi.org/10.1007/978-1-60761-474-6_4

6. Lynagh T, Pless SA. Principles of agonist recognition in Cys-loop receptors. Front Physiol [Internet]. 2014 [cited 2023 Jan 12];5. Available from: https://www.frontiersin.org/articles/10.3389/fphys.2014.00160

7. McKernan RM, Whiting PJ. Which GABAA-receptor subtypes really occur in the brain? Trends Neurosci. 1996 Apr 1;19(4):139–43.

8. Falco-Walter J. Epilepsy—Definition, Classification, Pathophysiology, and Epidemiology. Semin Neurol. 2020 Dec;40(06):617–23.

9. World Health Organization. Epilepsy [Internet]. [cited 2023 Jan 12]. Available from: https://www.who.int/news-room/fact-sheets/detail/epilepsy

10. Scheffer IE, Berkovic S, Capovilla G, Connolly MB, French J, Guilhoto L, et al. ILAE classification of the epilepsies: Position paper of the ILAE Commission for Classification and Terminology. Epilepsia. 2017;58(4):512–21.

11. Myers KA. Genetic Epilepsy Syndromes. Contin Lifelong Learn Neurol. 2022 Apr;28(2):339.

12. Macdonald RL, Gallagher MJ. The Genetic Epilepsies. In: Rosenberg's Molecular and Genetic Basis of Neurological and Psychiatric Disease [Internet]. Elsevier; 2015 [cited 2019 Feb 6]. p. 973–98. Available from: https://linkinghub.elsevier.com/retrieve/pii/B978012410529400084X

13. Cossette P, Liu L, Brisebois K, Dong H, Lortie A, Vanasse M, et al. Mutation of *GABRA1* in an autosomal dominant form of juvenile myoclonic epilepsy. Nat Genet. 2002 Jun;31(2):184–9.

14. Maljevic Snezana, Krampfl Klaus, Cobilanschi Joana, Tilgen Nikola, Beyer Susanne, Weber Yvonne G., et al. A mutation in the GABAA receptor α1-subunit is associated with absence epilepsy. Ann Neurol. 2006 May 22;59(6):983–7.

15. Epi4K Consortium, Epilepsy Phenome/Genome Project, Allen AS, Berkovic SF, Cossette P, Delanty N, et al. De novo mutations in epileptic encephalopathies. Nature. 2013 Sep 12;501(7466):217–21.

16. Johannesen K, Marini C, Pfeffer S, Møller RS, Dorn T, Niturad CE, et al. Phenotypic spectrum of GABRA1: From generalized epilepsies to severe epileptic encephalopathies. Neurology. 2016 13;87(11):1140–51.

17. Hernandez CC, XiangWei W, Hu N, Shen D, Shen W, Lagrange AH, et al. Altered inhibitory synapses in de novo GABRA5 and GABRA1 mutations associated with early onset epileptic encephalopathies. Brain J Neurol. 2019 Jul 1;142(7):1938–54.

18. Lohmann K, Klein C. Next Generation Sequencing and the Future of Genetic Diagnosis. Neurotherapeutics. 2014 Oct;11(4):699–707.

19. Farnaes L, Nahas SA, Chowdhury S, Nelson J, Batalov S, Dimmock DM, et al. Rapid whole-genome sequencing identifies a novelGABRA1variant associated with West syndrome. Cold Spring Harb Mol Case Stud. 2017 Sep;3(5).

20. 137160[MIM] - ClinVar - NCBI [Internet]. [cited 2023 Jan 19]. Available from: https://www.ncbi.nlm.nih.gov/clinvar

21. Krampfl K, Maljevic S, Cossette P, Ziegler E, Rouleau GA, Lerche H, et al. Molecular analysis of the A322D mutation in the GABA receptor alpha-subunit causing juvenile myoclonic epilepsy. Eur J Neurosci. 2005 Jul;22(1):10–20.

22. Löscher W. Critical review of current animal models of seizures and epilepsy used in the discovery and development of new antiepileptic drugs. Seizure. 2011 Jun 1;20(5):359–68.

23. Grone BP, Baraban SC. Animal models in epilepsy research: legacies and new directions. Nat Neurosci. 2015 Mar;18(3):339–43.

24. Dawson TM, Golde TE, Lagier-Tourenne C. Animal models of neurodegenerative diseases. Nat Neurosci. 2018 Oct;21(10):1370–9.

25. Piret SE, Thakker RV. Chapter 13 - Mouse Models: Approaches to Generating in vivo Models for Hereditary Disorders of Mineral and Skeletal Homeostasis. In: Thakker RV, Whyte MP, Eisman JA, Igarashi T, editors. Genetics of Bone Biology and Skeletal Disease [Internet]. San Diego: Academic Press; 2013 [cited 2023 Apr 15]. p. 181–204. Available from: https://www.sciencedirect.com/science/article/pii/B9780123878298000135

26. Guénet JL. The mouse genome. Genome Res. 2005 Dec 1;15(12):1729–40.

27. Keifer J, Summers CH. Putting the “Biology” Back into “Neurobiology”: The Strength of Diversity in Animal Model Systems for Neuroscience Research. Front Syst Neurosci [Internet]. 2016 [cited 2023 Apr 15];10. Available from: https://www.frontiersin.org/articles/10.3389/fnsys.2016.00069

28. Ayhan Y, McFarland R, Pletnikov MV. Animal models of gene-environment interaction in schizophrenia: a dimensional perspective. Prog Neurobiol. 2016 Jan;136:1–27.

29. Nestler EJ, Hyman SE. Animal Models of Neuropsychiatric Disorders. Nat Neurosci. 2010 Oct;13(10):1161–9.

30. Krüttner S, Falasconi A, Valbuena S, Galimberti I, Bouwmeester T, Arber S, et al. Absence of familiarity triggers hallmarks of autism in mouse model through aberrant tail-of-striatum and prelimbic cortex signaling. Neuron. 2022 May 4;110(9):1468-1482.e5.

31. Kralic JE, Korpi ER, O'Buckley TK, Homanics GE, Morrow AL. Molecular and Pharmacological Characterization of GABAA Receptor α1 Subunit Knockout Mice. J Pharmacol Exp Ther. 2002 Sep 1;302(3):1037–45.

32. Ogris W, Lehner R, Fuchs K, Furtmüller B, Höger H, Homanics GE, et al. Investigation of the abundance and subunit composition of GABAA receptor subtypes in the cerebellum of α1-subunit-deficient mice. J Neurochem. 2006;96(1):136–47.

33. Albuja AC, Khan GQ. Absence Seizure. In: StatPearls [Internet]. Treasure Island (FL): StatPearls Publishing; 2023 [cited 2023 May 23]. Available from: http://www.ncbi.nlm.nih.gov/books/NBK499867/

34. Landazuri P. Myoclonic Seizures☆. In: Reference Module in Biomedical Sciences [Internet]. Elsevier; 2014 [cited 2023 May 23]. Available from: https://www.sciencedirect.com/science/article/pii/B9780128012383051692

35. Arain FM, Boyd KL, Gallagher MJ. Decreased viability and absence-like epilepsy in mice lacking or deficient in the GABAA receptor α1 subunit. Epilepsia. 2012 Aug;53(8):e161-165.

36. Arain F, Zhou C, Ding L, Zaidi S, Gallagher MJ. The Developmental Evolution of the Seizure Phenotype and Cortical Inhibition in Mouse Models of Juvenile Myoclonic Epilepsy. Neurobiol Dis. 2015 Oct;82:164–75.

37. Kralic JE, Wheeler M, Renzi K, Ferguson C, O'Buckley TK, Grobin AC, et al. Deletion of GABAA Receptor α1 Subunit-containing Receptors Alters Responses to Ethanol and Other Anesthetics. J Pharmacol Exp Ther. 2003 May 1;305(2):600–7.

38. Zhou C, Huang Z, Ding L, Deel ME, Arain FM, Murray CR, et al. Altered cortical GABAA receptor composition, physiology, and endocytosis in a mouse model of a human genetic absence epilepsy syndrome. J Biol Chem. 2013 Jul 19;288(29):21458–72.

39. Engeszer RE, Patterson LB, Rao AA, Parichy DM. Zebrafish in The Wild: A Review of Natural History And New Notes from The Field. Zebrafish. 2007 Mar;4(1):21–40.

40. Spence R, Gerlach G, Lawrence C, Smith C. The behaviour and ecology of the zebrafish, Danio rerio. Biol Rev. 2007 Dec 17;83(1):13–34.

41. Kimmel CB, Ballard WW, Kimmel SR, Ullmann B, Schilling TF. Stages of embryonic development of the zebrafish. Dev Dyn. 1995;203(3):253–310.

42. Hunt A, Tracey A, Rapp A, Berger A, Ellington A, Kimberley A, et al. The zebrafish reference genome sequence and its relationship to the human genome. Nature. 2013 Apr;496(7446):498.

43. Reyes-Nava NG. Zebrafish: A Comprehensive Model to Understand the Mechanisms Underlying Neurodevelopmental Disorders. In: Costa, Andres., Villalba, Eugenio., editors. Horizons in Neuroscience Research. Nova Biomedical; 2018.

44. Varga M. the Node. 2016 [cited 2023 Apr 15]. The Doctor of Delayed Publications - the remarkable life of George Streisinger. Available from: https://thenode.biologists.com/doctor-delayed-publications-remarkable-life-george-streisinger/careers/

45. Geisler R, Rauch GJ, Geiger-Rudolph S, Albrecht A, van Bebber F, Berger A, et al. Large-scale mapping of mutations affecting zebrafish development. BMC Genomics. 2007 Jan 9;8(1):11.

46. Acevedo-Arozena A, Wells S, Potter P, Kelly M, Cox RD, Brown SDM. ENU mutagenesis, a way forward to understand gene function. Annu Rev Genomics Hum Genet. 2008;9:49–69.

47. Zebrafish Mutation Project - Wellcome Sanger Institute [Internet]. [cited 2023 Apr 15]. Available from: https://www.sanger.ac.uk/collaboration/zebrafish-mutation-project/

48. Blackburn PR, Campbell JM, Clark KJ, Ekker SC. The CRISPR System—Keeping Zebrafish Gene Targeting Fresh. Zebrafish. 2013 Mar;10(1):116–8.

49. Cresko WA, Yan YL, Baltrus DA, Amores A, Singer A, Rodríguez-Marí A, et al. Genome duplication, subfunction partitioning, and lineage divergence: Sox9 in stickleback and zebrafish. Dev Dyn. 2003;228(3):480–9.

50. Postlethwait JH, Woods IG, Ngo-Hazelett P, Yan YL, Kelly PD, Chu F, et al. Zebrafish Comparative Genomics and the Origins of Vertebrate Chromosomes. Genome Res. 2000 Dec 1;10(12):1890–902.

51. Basnet RM, Zizioli D, Taweedet S, Finazzi D, Memo M. Zebrafish Larvae as a Behavioral Model in Neuropharmacology. Biomedicines [Internet]. 2019 Mar 26 [cited 2020 May 31];7(1). Available from: https://www.ncbi.nlm.nih.gov/pmc/articles/PMC6465999/

52. Zebrabox for zebrafish embryos or larvae behavior analysis [Internet]. [cited 2023 Apr 21]. Available from: https://www.viewpoint.fr/product/zebrafish/fish-behavior-monitoring/zebrabox

53. Thornton C, Dickson KE, Carty DR, Ashpole NM, Willett KL. Cannabis constituents reduce seizure behavior in chemically-induced and scn1a-mutant zebrafish. Epilepsy Behav. 2020 Sep 1;110:107152.

54. Baraban SC, Taylor MR, Castro PA, Baier H. Pentylenetetrazole induced changes in zebrafish behavior, neural activity and c-fos expression. Neuroscience. 2005 Jan 1;131(3):759–68.

55. Afrikanova T, Serruys ASK, Buenafe OEM, Clinckers R, Smolders I, Witte PAM de, et al. Validation of the Zebrafish Pentylenetetrazol Seizure Model: Locomotor versus Electrographic Responses to Antiepileptic Drugs. PLOS ONE. 2013 Jan 14;8(1):e54166.

56. Cocco A, Rönnberg AMC, Jin Z, André GI, Vossen LE, Bhandage AK, et al. Characterization of the γ-aminobutyric acid signaling system in the zebrafish (Danio rerio Hamilton) central nervous system by reverse transcription-quantitative polymerase chain reaction. Neuroscience. 2017 Feb 20;343:300–21.

57. Samarut É, Swaminathan A, Riché R, Liao M, Hassan-Abdi R, Renault S, et al. γ-Aminobutyric acid receptor alpha 1 subunit loss of function causes genetic generalized epilepsy by impairing inhibitory network neurodevelopment. Epilepsia. 2018;59(11):2061–74.

58. Reyes-Nava NG, Yu HC, Coughlin CR II, Shaikh TH, Quintana AM. Abnormal expression of GABAA receptor subunits and hypomotility upon loss of gabra1 in zebrafish. Biol Open. 2020 Apr 13;9(4):bio051367.

59. Sadamitsu K, Shigemitsu L, Suzuki M, Ito D, Kashima M, Hirata H. Characterization of zebrafish GABAA receptor subunits. Sci Rep. 2021 Mar 18;11(1):6242.

60. Maillard PY, Baer S, Schaefer É, Desnous B, Villeneuve N, Lépine A, et al. Molecular and clinical descriptions of patients with GABAA receptor gene variants (GABRA1, GABRB2, GABRB3, GABRG2): A cohort study, review of literature, and genotype-phenotype correlation. Epilepsia. 2022 Oct;63(10):2519–33.

61. Carvill GL, Weckhuysen S, McMahon JM, Hartmann C, Møller RS, Hjalgrim H, et al. GABRA1 and STXBP1: Novel genetic causes of Dravet syndrome. Neurology. 2014 Apr 8;82(14):1245–53.

62. Kodera H, Ohba C, Kato M, Maeda T, Araki K, Tajima D, et al. De novo GABRA1 mutations in Ohtahara and West syndromes. Epilepsia. 2016 Apr;57(4):566–73.

63. ClinVar. National Center for Biotechnology Information [VCV001685835.1], [Internet]. [cited 2023 Apr 14]. Available from: https://www.ncbi.nlm.nih.gov/clinvar/variation/VCV001685835.1

64. Fokstuen S, Makrythanasis P, Hammar E, Guipponi M, Ranza E, Varvagiannis K, et al. Experience of a multidisciplinary task force with exome sequencing for Mendelian disorders. Hum Genomics. 2016 Jun 28;10:24.

65. Lachance-Touchette P, Brown P, Meloche C, Kinirons P, Lapointe L, Lacasse H, et al. Novel α1 and γ2 GABAA receptor subunit mutations in families with idiopathic generalized epilepsy. Eur J Neurosci. 2011 Jul;34(2):237–49.

66. Steudle F, Rehman S, Bampali K, Simeone X, Rona Z, Hauser E, et al. A novel de novo variant of GABRA1 causes increased sensitivity for GABA in vitro. Sci Rep. 2020 Feb 11;10(1):2379.

67. Boycott KM, Vanstone MR, Bulman DE, MacKenzie AE. Rare-disease genetics in the era of next-generation sequencing: discovery to translation. Nat Rev Genet. 2013 Oct;14(10):681–91.

68. Bick D, Jones M, Taylor SL, Taft RJ, Belmont J. Case for genome sequencing in infants and children with rare, undiagnosed or genetic diseases. J Med Genet. 2019 Apr 25;

69. Tetreault M, Bareke E, Nadaf J, Alirezaie N, Majewski J. Whole-exome sequencing as a diagnostic tool: current challenges and future opportunities. Expert Rev Mol Diagn. 2015 Jun;15(6):749–60.

70. Sawyer SL, Hartley T, Dyment DA, Beaulieu CL, Schwartzentruber J, Smith A, et al. Utility of whole-exome sequencing for those near the end of the diagnostic odyssey: time to address gaps in care. Clin Genet. 2015 Aug 18;

71. Koboldt DC, Steinberg KM, Larson DE, Wilson RK, Mardis ER. The next-generation sequencing revolution and its impact on genomics. Cell. 2013 Sep 26;155(1):27–38.

72. Danielsson K, Mun LJ, Lordemann A, Mao J, Lin CHJ. Next-generation sequencing applied to rare diseases genomics. Expert Rev Mol Diagn. 2014 May;14(4):469–87.

73. Gilissen C, Hoischen A, Brunner HG, Veltman JA. Unlocking Mendelian disease using exome sequencing. Genome Biol. 2011;12(9):228.

74. Gilissen C, Hoischen A, Brunner HG, Veltman JA. Disease gene identification strategies for exome sequencing. Eur J Hum Genet EJHG. 2012 May;20(5):490–7.

75. Macnamara EF, Schoch K, Kelley EG, Fieg E, Brokamp E, Undiagnosed Diseases Network, et al. Cases from the Undiagnosed Diseases Network: The continued value of counseling skills in a new genomic era. J Genet Couns. 2019 Apr;28(2):194–201.

76. Wangler MF, Yamamoto S, Chao HT, Posey JE, Westerfield M, Postlethwait J, et al. Model Organisms Facilitate Rare Disease Diagnosis and Therapeutic Research. Genetics. 2017 Sep;207(1):9–27.

77. Epi4K Consortium, Epilepsy Phenome/Genome Project, Allen AS, Berkovic SF, Cossette P, Delanty N, et al. De novo mutations in epileptic encephalopathies. Nature. 2013 Sep 12;501(7466):217–21.

78. Ackermann GE, Paw BH. Zebrafish: a genetic model for vertebrate organogenesis and human disorders. Front Biosci J Virtual Libr. 2003 Sep 1;8:d1227-1253.

79. Monesson-Olson B, McClain JJ, Case AE, Dorman HE, Turkewitz DR, Steiner AB, et al. Expression of the eight GABAA receptor α subunits in the developing zebrafish central nervous system. PloS One. 2018;13(4):e0196083.

80. Samarut É, Swaminathan A, Riché R, Liao M, Hassan-Abdi R, Renault S, et al. γ-Aminobutyric acid receptor alpha 1 subunit loss of function causes genetic generalized epilepsy by impairing inhibitory network neurodevelopment. Epilepsia. 2018 Nov;59(11):2061–74.

81. Maljevic Snezana, Krampfl Klaus, Cobilanschi Joana, Tilgen Nikola, Beyer Susanne, Weber Yvonne G., et al. A mutation in the GABAA receptor α1-subunit is associated with absence epilepsy. Ann Neurol. 2006 May 22;59(6):983–7.

82. Farnaes L, Nahas SA, Chowdhury S, Nelson J, Batalov S, Dimmock DM, et al. Rapid whole-genome sequencing identifies a novel GABRA1 variant associated with West syndrome. Cold Spring Harb Mol Case Stud. 2017 Sep;3(5).

83. Nolan D, Fink J. Chapter 30 - Genetics of epilepsy. In: Geschwind DH, Paulson HL, Klein C, editors. Handbook of Clinical Neurology [Internet]. Elsevier; 2018 [cited 2018

Mar 22]. p. 467–91. (Neurogenetics, Part II; vol. 148). Available from: http://www.sciencedirect.com/science/article/pii/B9780444640765000302

84. von Deimling M, Häsler R, Steinbach V, Holterhus PM, von Spiczak S, Stephani U, et al. Gene expression analysis in untreated absence epilepsy demonstrates an inconsistent pattern. Epilepsy Res. 2017 May 1;132:84–90.

85. Hernandez CC, Gurba KN, Hu N, Macdonald RL. The GABRA6 mutation, R46W, associated with childhood absence epilepsy, alters 6β22 and 6β2 GABA(A) receptor channel gating and expression. J Physiol. 2011 Dec 1;589(Pt 23):5857–78.

86. DeLorey TM, Handforth A, Anagnostaras SG, Homanics GE, Minassian BA, Asatourian A, et al. Mice lacking the beta3 subunit of the GABAA receptor have the epilepsy phenotype and many of the behavioral characteristics of Angelman syndrome. J Neurosci Off J Soc Neurosci. 1998 Oct 15;18(20):8505–14.

87. Hirose S. Mutant GABA(A) receptor subunits in genetic (idiopathic) epilepsy. Prog Brain Res. 2014;213:55–85.

88. Arain FM, Boyd KL, Gallagher MJ. Decreased viability and absence-like epilepsy in mice lacking or deficient in the GABAA receptor α1 subunit. Epilepsia. 2012 Aug;53(8):e161-165.

89. Huang RQ, Bell-Horner CL, Dibas MI, Covey DF, Drewe JA, Dillon GH. Pentylenetetrazole-Induced Inhibition of Recombinant γ-Aminobutyric Acid Type A (GABAA) Receptors: Mechanism and Site of Action. J Pharmacol Exp Ther. 2001 Sep 1;298(3):986–95.

90. Zhou C, Ding L, Deel ME, Ferrick EA, Emeson RB, Gallagher MJ. Altered Intrathalamic GABAA Neurotransmission in a Mouse Model of a Human Genetic Absence Epilepsy Syndrome. Neurobiol Dis. 2015 Jan;73:407–17.

91. Arain F, Zhou C, Ding L, Zaidi S, Gallagher MJ. The Developmental Evolution of the Seizure Phenotype and Cortical Inhibition in Mouse Models of Juvenile Myoclonic Epilepsy. Neurobiol Dis. 2015 Oct;82:164–75.

92. Li H, Durbin R. Fast and accurate short read alignment with Burrows-Wheeler transform. Bioinforma Oxf Engl. 2009 Jul 15;25(14):1754–60.

93. Li H, Handsaker B, Wysoker A, Fennell T, Ruan J, Homer N, et al. The Sequence Alignment/Map format and SAMtools. Bioinforma Oxf Engl. 2009 Aug 15;25(16):2078–9.

94. Goecks J, Nekrutenko A, Taylor J, The Galaxy Team. Galaxy: a comprehensive approach for supporting accessible, reproducible, and transparent computational research in the life sciences. Genome Biol. 2010 Aug 25;11(8):R86.

95. Thisse C, Thisse B. High-resolution in situ hybridization to whole-mount zebrafish embryos. Nat Protoc. 2008;3(1):59–69.

96. Peng X, Lin J, Zhu Y, Liu X, Zhang Y, Ji Y, et al. Anxiety-related behavioral responses of pentylenetetrazole-treated zebrafish larvae to light-dark transitions. Pharmacol Biochem Behav. 2016 Jun 1;145:55–65.

97. Jin M, He Q, Zhang S, Cui Y, Han L, Liu K. Gastrodin Suppresses Pentylenetetrazole-Induced Seizures Progression by Modulating Oxidative Stress in Zebrafish. Neurochem Res. 2018 Feb 7;1–14.

98. Macdonald RL, Gallagher MJ, Feng HJ, Kang J. GABAA receptor epilepsy mutations. Biochem Pharmacol. 2004 Oct;68(8):1497–506.

99. Reyes-Nava NG, Yu HC, Coughlin CR, Shaikh TH, Quintana AM. Abnormal expression of GABAA receptor subunits and hypomotility upon loss of gabra1 in zebrafish. Biol Open [Internet]. 2020 Apr 15 [cited 2020 Apr 14];9(4). Available from: https://bio.biologists.org/content/9/4/bio051367

100. Choi YJ, Lee SY, Yang KS, Park JY, Yoon SZ, Yoon SM. Polymorphism rs4263535 in GABRA1 intron 4 was related to deeper sedation by intravenous midazolam. J Int Med Res. 2015 Oct;43(5):686–98.

101. Kodera H, Ohba C, Kato M, Maeda T, Araki K, Tajima D, et al. De novo GABRA1 mutations in Ohtahara and West syndromes. Epilepsia. 2016 Apr;57(4):566–73.

102. Hirose S. Chapter 3 - Mutant GABAA receptor subunits in genetic (idiopathic) epilepsy. In: Steinlein OK, editor. Progress in Brain Research [Internet]. Elsevier; 2014 [cited 2018 Jul 30]. p. 55–85. (Genetics of Epilepsy; vol. 213). Available from: http://www.sciencedirect.com/science/article/pii/B978044463326200003X

103. Maillard PY, Baer S, Schaefer É, Desnous B, Villeneuve N, Lépine A, et al. Molecular and clinical descriptions of patients with GABAA receptor gene variants

(GABRA1, GABRB2, GABRB3, GABRG2): A cohort study, review of literature, and genotype–phenotype correlation. Epilepsia. 2022;63(10):2519–33.

104. Maljevic S, Møller RS, Reid CA, Pérez-Palma E, Lal D, May P, et al. Spectrum of GABAA receptor variants in epilepsy: Curr Opin Neurol. 2019 Apr;32(2):183–90.

105. Samarut É, Swaminathan A, Riché R, Liao M, Hassan-Abdi R, Renault S, et al. γ-Aminobutyric acid receptor alpha 1 subunit loss of function causes genetic generalized epilepsy by impairing inhibitory network neurodevelopment. Epilepsia. 2018 Nov 1;59(11):2061–74.

106. ZMP | Busch Lab [Internet]. [cited 2022 Oct 24]. Available from: https://zmp.buschlab.org/

107. Kalueff AV, Gebhardt M, Stewart AM, Cachat JM, Brimmer M, Chawla JS, et al. Towards a comprehensive catalog of zebrafish behavior 1.0 and beyond. Zebrafish. 2013 Mar;10(1):70–86.

108. Canzian J, Müller TE, Franscescon F, Michelotti P, Fontana BD, Costa FV, et al. Modeling psychiatric comorbid symptoms of epileptic seizures in zebrafish. J Psychiatr Res. 2019 Dec 1;119:14–22.

109. Yaksi E, Jamali A, Diaz Verdugo C, Jurisch-Yaksi N. Past, present and future of zebrafish in epilepsy research. FEBS J. 2021;288(24):7243–55.

110. Stewart AM, Desmond D, Kyzar E, Gaikwad S, Roth A, Riehl R, et al. Perspectives of zebrafish models of epilepsy: what, how and where next? Brain Res Bull. 2012 Feb 10;87(2–3):135–43.

111. Gawel K, Langlois M, Martins T, van der Ent W, Tiraboschi E, Jacmin M, et al. Seizing the moment: Zebrafish epilepsy models. Neurosci Biobehav Rev. 2020 Sep 1;116:1–20.

112. Baraban SC, Taylor MR, Castro PA, Baier H. Pentylenetetrazole induced changes in zebrafish behavior, neural activity and c-fos expression. Neuroscience. 2005 Jan 1;131(3):759–68.

113. Zhou C, Ding L, Deel ME, Ferrick EA, Emeson RB, Gallagher MJ. Altered Intrathalamic GABAA Neurotransmission in a Mouse Model of a Human Genetic Absence Epilepsy Syndrome. Neurobiol Dis. 2015 Jan;73:407–17.

114. Fassio A, Raimondi A, Lignani G, Benfenati F, Baldelli P. Synapsins: From synapse to network hyperexcitability and epilepsy. Semin Cell Dev Biol. 2011 Jun 1;22(4):408–15.

115. Garcia CC. Identification of a mutation in synapsin I, a synaptic vesicle protein, in a family with epilepsy. J Med Genet. 2004 Mar 1;41(3):183–6.

116. Giannandrea M, Guarnieri FC, Gehring NH, Monzani E, Benfenati F, Kulozik AE, et al. Nonsense-Mediated mRNA Decay and Loss-of-Function of the Protein Underlie the X-Linked Epilepsy Associated with the W356× Mutation in Synapsin I. PLOS ONE. 2013 Jun 20;8(6):e67724.

117. Barbieri R, Contestabile A, Ciardo MG, Forte N, Marte A, Baldelli P, et al. Synapsin I and Synapsin II regulate neurogenesis in the dentate gyrus of adult mice. Oncotarget. 2018 Apr 10;9(27):18760–74.

118. Lopriore P, Gomes F, Montano V, Siciliano G, Mancuso M. Mitochondrial Epilepsy, a Challenge for Neurologists. Int J Mol Sci. 2022 Oct 30;23(21):13216.

119. Schubert Baldo M, Vilarinho L. Molecular basis of Leigh syndrome: a current look. Orphanet J Rare Dis. 2020 Jan 29;15(1):31.

120. Chen W, Ge Y, Lu J, Melo J, So YW, Juneja R, et al. Distinct Functional Alterations and Therapeutic Options of Two Pathological De Novo Variants of the T292 Residue of GABRA1 Identified in Children with Epileptic Encephalopathy and Neurodevelopmental Disorders. Int J Mol Sci. 2022 Jan;23(5):2723.

121. Timme-Laragy AR, Karchner SI, Hahn ME. Gene knockdown by morpholino-modified oligonucleotides in the zebrafish model: applications for developmental toxicology. Methods Mol Biol Clifton NJ. 2012;889:51–71.

122. Wang X, Yu D, Wang H, Lei Z, Zhai Y, Sun M, et al. Rab3 and synaptotagmin proteins in the regulation of vesicle fusion and neurotransmitter release. Life Sci. 2022 Nov 15;309:120995.

123. Tao B, Hu H, Mitchell K, Chen J, Jia H, Zhu Z, et al. Secretogranin-II plays a critical role in zebrafish neurovascular modeling. J Mol Cell Biol. 2018 Oct 1;10(5):388–401.

124. Yang P, Wang K, Zhang C, Wang Z, Liu Q, Wang J, et al. Novel roles of VAT1 expression in the immunosuppressive action of diffuse gliomas. Cancer Immunol Immunother. 2021 Sep 1;70(9):2589–600.

125. Eura Y, Ishihara N, Oka T, Mihara K. Identification of a novel protein that regulates mitochondrial fusion by modulating mitofusin (Mfn) protein function. J Cell Sci. 2006 Dec 1;119(23):4913–25.

126. Kim SY, Mori T, Chek MF, Furuya S, Matsumoto K, Yajima T, et al. Structural insights into vesicle amine transport-1 (VAT-1) as a member of the NADPH-dependent quinone oxidoreductase family. Sci Rep. 2021 Jan 22;11(1):2120.

127. Cali E, Rocca C, Salpietro V, Houlden H. Epileptic Phenotypes Associated With SNAREs and Related Synaptic Vesicle Exocytosis Machinery. Front Neurol. 2022 Jan 13;12:806506.

128. Tang J. Complexins. In: Squire LR, editor. Encyclopedia of Neuroscience [Internet]. Oxford: Academic Press; 2009 [cited 2023 Apr 23]. p. 1–7. Available from: https://www.sciencedirect.com/science/article/pii/B9780080450469013723

129. Zanazzi G, Matthews G. Enrichment and differential targeting of complexins 3 and 4 in ribbon-containing sensory neurons during zebrafish development. Neural Develop. 2010 Sep 1;5:24.

130. Mirza FJ, Zahid S. The Role of Synapsins in Neurological Disorders. Neurosci Bull. 2017 Dec 27;34(2):349–58.

131. Fassio A, Esposito A, Kato M, Saitsu H, Mei D, Marini C, et al. De novo mutations of the ATP6V1A gene cause developmental encephalopathy with epilepsy. Brain. 2018 Jun;141(6):1703–18.

132. Asinof S, Mahaffey C, Beyer B, Frankel WN, Boumil R. Dynamin 1 isoform roles in a mouse model of severe childhood epileptic encephalopathy. Neurobiol Dis. 2016 Nov;95:1–11.

133. Bragato C, Pistocchi A, Bellipanni G, Confalonieri S, Balciunie J, Monastra FM, et al. Zebrafish dnm1a gene plays a role in the formation of axons and synapses in the nervous tissue. J Neurosci Res [Internet]. [cited 2023 May 28];n/a(n/a). Available from: https://onlinelibrary.wiley.com/doi/abs/10.1002/jnr.25197

134. Vogel C, Marcotte EM. Insights into the regulation of protein abundance from proteomic and transcriptomic analyses. Nat Rev Genet. 2012 Apr;13(4):227–32.

135. Abreu R de S, Penalva LO, Marcotte EM, Vogel C. Global signatures of protein and mRNA expression levels. Mol Biosyst. 2009 Nov 12;5(12):1512–26.

136. Koussounadis A, Langdon SP, Um IH, Harrison DJ, Smith VA. Relationship between differentially expressed mRNA and mRNA-protein correlations in a xenograft model system. Sci Rep. 2015 Jun 8;5(1):10775.

137. Zhang J, Gao YY, Huang YQ, Fan Q, Lu XT, Wang CK. Selection of housekeeping genes for quantitative gene expression analysis in yellow-feathered broilers. Ital J Anim Sci. 2018 Apr 3;17(2):540–6.

138. Choosing an Endogenous Control - US [Internet]. [cited 2023 May 29]. Available from: https://www.thermofisher.com/us/en/home/life-science/pcr/real-time-pcr/real-time-pcr-learning-center/gene-expression-analysis-real-time-pcr-information/choosing-endogenous-control-gene-expression-analysis-real-time-pcr.html

139. Turabelidze A, Guo S, DiPietro LA. Importance of Housekeeping gene selection for accurate RT-qPCR in a wound healing model. Wound Repair Regen Off Publ Wound Heal Soc Eur Tissue Repair Soc. 2010;18(5):460–6.

140. Vandesompele J, De Preter K, Pattyn F, Poppe B, Van Roy N, De Paepe A, et al. Accurate normalization of real-time quantitative RT-PCR data by geometric averaging of multiple internal control genes. Genome Biol. 2002;3(7):research0034.1-research0034.11.

141. Thellin O, Zorzi W, Lakaye B, De Borman B, Coumans B, Hennen G, et al. Housekeeping genes as internal standards: use and limits. J Biotechnol. 1999 Oct 8;75(2):291–5.

142. Castro VL, Reyes-Nava NG, Sanchez BB, Gonzalez CG, Paz D, Quintana AM. Activation of WNT signaling restores the facial deficits in a zebrafish with defects in cholesterol metabolism. genesis. 2020;58(12):e23397.

143. Castellanos BS, Reyes-Nava NG, Quintana AM. Knockdown of hspg2 is associated with abnormal mandibular joint formation and neural crest cell dysfunction in zebrafish. BMC Dev Biol. 2021 Mar 8;21(1):7.

144. Rassier GT, Silveira TLR, Remião MH, Daneluz LO, Martins AWS, Dellagostin EN, et al. Evaluation of qPCR reference genes in GH-overexpressing transgenic zebrafish (Danio rerio). Sci Rep. 2020 Jul 29;10(1):12692.

145. Casadei R, Pelleri MC, Vitale L, Facchin F, Lenzi L, Canaider S, et al. Identification of housekeeping genes suitable for gene expression analysis in the zebrafish. Gene Expr Patterns. 2011 Mar 1;11(3):271–6.

146. Nakayasu ES, Gritsenko M, Piehowski PD, Gao Y, Orton DJ, Schepmoes AA, et al. Tutorial: best practices and considerations for mass-spectrometry-based protein biomarker discovery and validation. Nat Protoc. 2021 Aug;16(8):3737–60.

147. Garbis S, Lubec G, Fountoulakis M. Limitations of current proteomics technologies. J Chromatogr A. 2005 Jun 3;1077(1):1–18.

148. Piehowski PD, Petyuk VA, Orton DJ, Xie F, Ramirez-Restrepo M, Engel A, et al. Sources of Technical Variability in Quantitative LC-MS Proteomics: Human Brain Tissue Sample Analysis. J Proteome Res. 2013 May 3;12(5):2128–37.

149. Sinha A, Mann M. A beginner's guide to mass spectrometry–based proteomics. The Biochemist. 2020 Sep 9;42(5):64–9.

150. Molloy MP, Brzezinski EE, Hang J, McDowell MT, VanBogelen RA. Overcoming technical variation and biological variation in quantitative proteomics. Proteomics. 2003 Oct;3(10):1912–9.

151. Tabb DL, Vega-Montoto L, Rudnick PA, Variyath AM, Ham AJL, Bunk DM, et al. Repeatability and Reproducibility in Proteomic Identifications by Liquid Chromatography—Tandem Mass Spectrometry. J Proteome Res. 2010 Feb 5;9(2):761.

152. Poulos RC, Hains PG, Shah R, Lucas N, Xavier D, Manda SS, et al. Strategies to enable large-scale proteomics for reproducible research. Nat Commun. 2020 Jul 30;11(1):3793.

153. gabra1[gene] - ClinVar - NCBI [Internet]. [cited 2023 Apr 14]. Available from: https://www.ncbi.nlm.nih.gov/clinvar/?term=gabra1%5Bgene%5D&redir=gene

Appendix

Below is a list of publications I have contributed as an author, including three first-author (two manuscripts and a book chapter) and six contributing author publications.

1. Reyes-Nava N. G., Perez I, Grajeda B, Estevao IL., Ellis C. C., Quintana A. M. (2023). Mutation of gabra1 is associated with hypermotility and abnormal expression of proteins critical for ion homeostasis and synaptic vesicle transport. bioRxiv [Preprint]. 2023 Jan 27:2023.01.27.525860. doi: 10.1101/2023.01.27.525860. PMID: 36747751; PMCID: PMC9900897. *Contributions: Animal husbandry and genotyping, performed behavioral and molecular experiments, assisted with data analysis, and contributed to writing of the manuscript.*
2. Perez I, Reyes-Nava N. G., Pinales B. E., and Quintana A. M. (2023) Function of znf143b during Craniofacial Development. **AJUR**. *Contributions: Performed microinjections, animal husbandry, assisted with data analysis, rescue experiments, training, and guidance on animal husbandry, microinjections, alcian-blue staining, and flow cytometry.*
3. Paz D, Pinales BE, Castellanos BS, Perez I, Gil CB, Jimenez Madrigal L, Reyes-Nava NG, Castro VL, Sloan JL, Quintana AM. (2023) Abnormal chondrocyte intercalation in a zebrafish model of *cblC* syndrome restored by an MMACHC cobalamin binding mutant. ***Differentiation.*** 131(1). Doi.org/10.1016/j.diff.2023.04.003. *Contributions: performed microinjections, genotyping and contributed to husbandry.*
4. Castellanos B. S., Reyes-Nava N. G., and Quintana A. M. (2021). Knockdown of *hspg2* is associated with abnormal mandibular joint formation and neural crest cell dysfunction in zebrafish. ***BMC Developmental Biology.*** (21)7. doi: 10.1186/s12861-021-00238-4. *Contributions: produced aspects of the manuscript figures.*
5. Reyes-Nava, N. G*., Yu, H. C., Coughlin, C.R. 2nd, Shaikh, T. H., Quintana, A. M. (2020). Abnormal expression of $GABA_A$ receptor subunits and hypomotility upon loss of *gabra1* in zebrafish. ***Biology Open***. 9(4): bio051367. *Contributions: performed behavioral and molecular experiments, in situ hybridization, all morpholino injections, and assisted with data analysis.*
6. Castro VL, Reyes-Nava N. G., Sanchez BB, Gonzalez CG, Paz D, Quintana AM. (2020). Activation of WNT signaling restores the facial deficits in a zebrafish with defects in cholesterol metabolism. ***Genesis.*** 58(12): e23397. doi: 10.1002/dvg.23397. *Contributions: husbandry, genotyping, produced aspects of the manuscript figures, and assisted with drug treatments.*
7. Castro, V. L., Reyes J. F., Reyes-Nava, N. G**.,** Paz, D., Quintana, A. M. (2020). *Hcfc1a* regulates neural precursor proliferation and *asxl1* expression in the developing brain. ***BMC Neurosci***. 21(1):27. doi: org/10.1186/s12868-020-00577-1. *Contributions: performed cell counts, imaging, and genotyping.*

8. Hernandez, J. A., Castro, V. L., Reyes-Nava, N. G**.,** Montes, L. P., & Quintana, A. M. (2019). Mutations in the zebrafish *hmgcs1* gene reveal a novel function for isoprenoids during red blood cell development. ***Blood advances***, *3*(8), 1244–1254. Doi:10.1182/bloodadvances.2018024539. *Contributions: performed genotyping and imaging.*
9. Reyes-Nava, N. G., Hernandez, J. A., Castro, V. L., Reyes, J. F., Castellanos, B. S., Quintana, A. (2018). Zebrafish: A comprehensive model to understand the mechanisms underlying neurodevelopmental disorders. In ***Horizons in Neuroscience Research*** (vol. 36). Hauppauge, NY: Nova Science Publishers. *Contributions: Wrote sections of the chapter and assisted with literature search.*

Vita

Nayeli G. Reyes-Nava is from Ciudad Juarez, a city on the US-Mexico border. Nayeli takes pride in being a first-generation student. She obtained her bachelor's degree in biology from the Autonomous University of Ciudad Juarez in 2015 and completed her undergraduate thesis in the Botany and Biodiversity laboratory under Dr. Helvia Pelayo's mentorship. Nayeli joined Dr. Quintana's research laboratory in the Biological Sciences Department at the University of Texas at El Paso as a Bridges to the Baccalaureate Research Fellow in the Summer of 2016 to pursue her graduate studies. She was admitted into the UTEP Biological Sciences Ph.D. program in Fall 2017.

Nayeli has been studying the alpha-1 subunit of the $GABA_A$ receptor and its role in development, behavior, and disease. Her research may provide critical insights into the mechanisms of epilepsy disorders. Nayeli has received several fellowships and awards during her graduate studies, including the RISE fellowship, the Keelung-Hong graduate research fellowship, and the UTEP graduate excellence fellowship. She has presented her findings at various regional and national meetings, received travel awards, and published her work. Nayeli has also served as a teaching assistant for Biology and Immunology and helped mentor undergraduate students in the Quintana lab.

Nayeli is proud to have been awarded the Provost's Early Career Postdoctoral Fellow in Molecular Biosciences at UT Austin. Starting in September 2023, she will continue her training as an independent scientist in the Wallingford and Marcotte laboratories. She is excited about having a career that is full of surprises and challenges.

Contact Information: reyesnnayeli@gmail.com